Contractional effects of mantle plumes on Earth, Mars, and Venus

Daniel Mège*

*Laboratoire de Tectonique, ESA CNRS 7072, Boîte 129, Université Pierre et Marie Curie,
4 Place Jussieu, 75252 Paris cedex 05, France*

Richard E. Ernst[†]

Geological Survey of Canada, 601 Booth Street, Ottawa, Ontario K1A 0E8, Canada

ABSTRACT

Contractional structures are associated with the mantle plumes of three of the terrestrial planets, Mars, Venus, and Earth. On Mars, the early Tharsis volcanic province, centered at the Syria Planum area, is of probable plume origin. It has associated contractional structures in the form of wrinkle ridges on terrains interpreted to be flood basalts in the area of regional uplift and a contractional peripheral belt bounding the southern part of the uplift. Both features are concentric about the plume center. On Venus, contractional tectonics associated with plumes have produced wrinkle ridges that are concentric about volcanic rises; radial, parallel, or anastomosing contractional ridges associated with crustal plateaus; and circumferential uplift features that characterize coronae. On Earth, wrinkle ridges are associated with the 17–14 Ma Columbia River flood-basalt province, whereas peripheral thrusting is associated with the 60 Ma North Atlantic volcanic province and is theorized for the 1267 Ma Mackenzie plume event. Archean greenstone belts of the Dharwar craton (India) exhibit dome-and-basin folding interpreted similarly to Venusian crustal plateaus. Folding and thrusting in the Archean Yilgarn craton (Australia) are consistent with either of the two latter mechanisms. On the basis of these terrestrial and extraterrestrial examples, we present a model relating the development of contractional structures to the depth of the ductile-to-brittle transition and the geothermal gradient in the crust. We also provide guidelines for using contractional structures to infer the location of paleo-mantle plumes.

INTRODUCTION

Although the modern concept of fixed plumes rising from Earth's deep mantle has been established for three decades (Morgan, 1971), the actual surface expression of hotspots is still partly unresolved. Mantle-plume effects have been assumed to be only extensional and related to crustal uplift above plumes, either in response to dynamic forces (Houseman and England, 1986; Griffiths and Campbell, 1991) or to remote forces exerted in the weakened crust (White and McKenzie, 1989). However, numerical and experimental models suggest that volcanic topography, whether dynamic or supported by the crust or lithosphere, exhibits stresses that are not everywhere tensile (Banerdt et al., 1992; McGovern and Solomon, 1993; Merle and Borgia, 1996). In addition, uplift in hotspot settings is typically rapidly followed by subsidence (e.g., Olson, 1994), which modifies the stress-magnitude ratio. From a field-observation point of view, compression has sometimes been reported in plume

environments, such as the northeastern North Atlantic volcanic province (Boldreel and Andersen, 1998; Vågnes et al., 1998) and the Columbia Plateau (e.g., Hooper and Conrey, 1989), but the documented compression has not usually been linked to plume tectonics. An exception is attribution of a concentric thrust belt at the edge of the late Archean Yilgarn craton in Australia to concentration of remote compressive stress in a crust weakened by a plume (Passchier, 1995).

The first section of this paper is devoted to case histories from Mars, Venus, and Earth. The extraterrestrial examples are important, because possible compressional effects of mantle plumes can be better understood where plate tectonics does not occur, i.e., on Mars and Venus. Examples are given from the Tharsis region of Mars and from volcanic rises, crustal plateaus, and coronae on Venus. Case studies from Earth deal with the Columbia Plateau's Yakima folds, the formation of which is interpreted to have been influenced by the arrival of the early Yellowstone hotspot (17–14 Ma), offshore anticlines in the eastern North Atlantic volcanic province (ca. 60 Ma) associated with the arrival of the Thulean plume, concentric thrust faulting around the possible Yilgarn hotspot (2.69–2.68 Ga) in Australia, and folding converging toward a suspected plume center at the 2.9–2.6 Ga Bababudan greenstone belt of the Dharwar craton. In addition, inferences from the giant 1.267 Ga Mackenzie radiating-dike swarm suggest that thrusting around the periphery of plume-generated uplifts may be common.

The second section discusses these observations and proposes tectonic processes explaining their formation. The third section presents a general, case-history-driven model of tectonic compression at mantle plumes on Earth, Mars, and Venus in relation to crustal rheology and geothermal gradient. We also discuss the reasons why contractional patterns have not been frequently reported at terrestrial hotspots. Finally, we propose a guide to using contractional features when seeking pre-Mesozoic mantle plumes.

The model in the present paper is thus complementary to models that emphasize only extensional aspects of lithospheric tectonics above plumes (e.g., White and McKenzie, 1989, 1995; Griffiths and Campbell, 1991; Hill, 1991; Saunders et al., 1992; Courtillot et al., 1999; Mège, this volume).

CASE STUDIES OF PLUME TECTONICS INVOLVING COMPRESSION

Syria Planum plume on Mars

The geologic evolution of the Tharsis volcanic region on Mars (Fig. 1A) has been the topic of several regional studies (Hartmann, 1973; Frey, 1979; Sleep and Phillips, 1979, 1985; Plescia and Saunders, 1982; Banerdt et al., 1982, 1992; Scott and Tanaka, 1986; Scott and Dohm, 1990; Phillips et al., 1990; Tanaka et al., 1991; Mège and Masson, 1996; Mège, this volume) and innumerable works devoted to local aspects (see references in the papers listed here). These papers have highlighted

the complexity of this area, part of which is due to the duration of Tharsis volcanic and tectonic activity. The earliest events may be as old as the time of formation of the heavily cratered highlands (Tanaka, 1986), which would mean that the Tharsis tectonic activity may have begun before the oldest known rocks on Earth were formed (ca. 4.0 Ga).

The origin of Tharsis has been attributed to the impingement of a mantle plume on the bottom of the lithosphere. Recurrent volcanic and tectonic activity resulted in an uplift 5000 km in diameter, hosting giant shield volcanoes and encompassing most of the large tectonic structures of the planet (Fig. 1B). After an initial extensional tectonic event produced grabens radiating from the Thaumasia Plateau (Frey, 1979), volcanic and tectonic activity moved to the Syria Planum volcanic center. The Tharsis shield volcanoes formed later and were associated with a renewal of tectonic activity (Plescia and Saunders, 1982; Mège and Masson, 1996).

The companion paper (Mège, this volume) points out characteristics common to plume tectonics on Mars and Earth: (1) early thermal uplift followed by thermal subsidence after the plume has arrived at the base of the mechanical lithosphere, (2) rapid eruption of basaltic traps, (3) intrusion of a radiating-dike swarm and associated magmatic underplating at the onset of plume activity, followed by a long-lasting period of more differentiated magmatism, (4) failed passive rifting, and (5) development of a strong positive gravity anomaly produced by the intruded and underplated magmas. In this paper, we discuss contractional structures associated with the Syria Planum mantle plume.

Wrinkle ridges. The Syria Planum stage of volcanic activity formed the so-called "ridged plains" (Fig. 2) that correspond to the most voluminous flood lavas erupted at this time, probably during a short time span (Hiller et al., 1982) during the Hesperian system (3.8–1.8 Ga, Tanaka, 1986). The ridged plains, which are currently isostatically compensated at shallow depth (Frey et al., 1996), display periodically spaced (~30 km, Watters, 1991; Watters and Schultz, 1995), concentric wrinkle ridges (Figs. 1B, 3) (Mège and Masson, 1996; Watters, 1991; Schultz and Watters, 1995). Although many models of wrinkle-ridge origin have been published (see Watters, 1988, for a review), there is now agreement that wrinkle-ridge formation in-
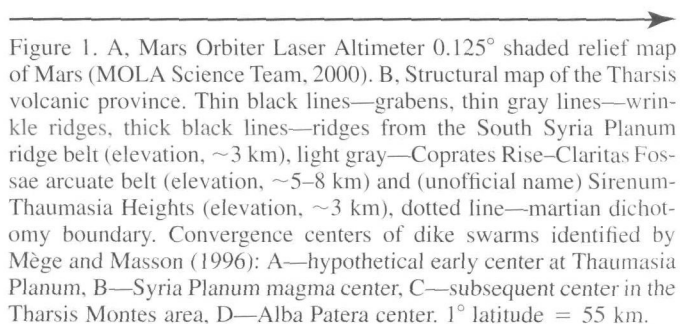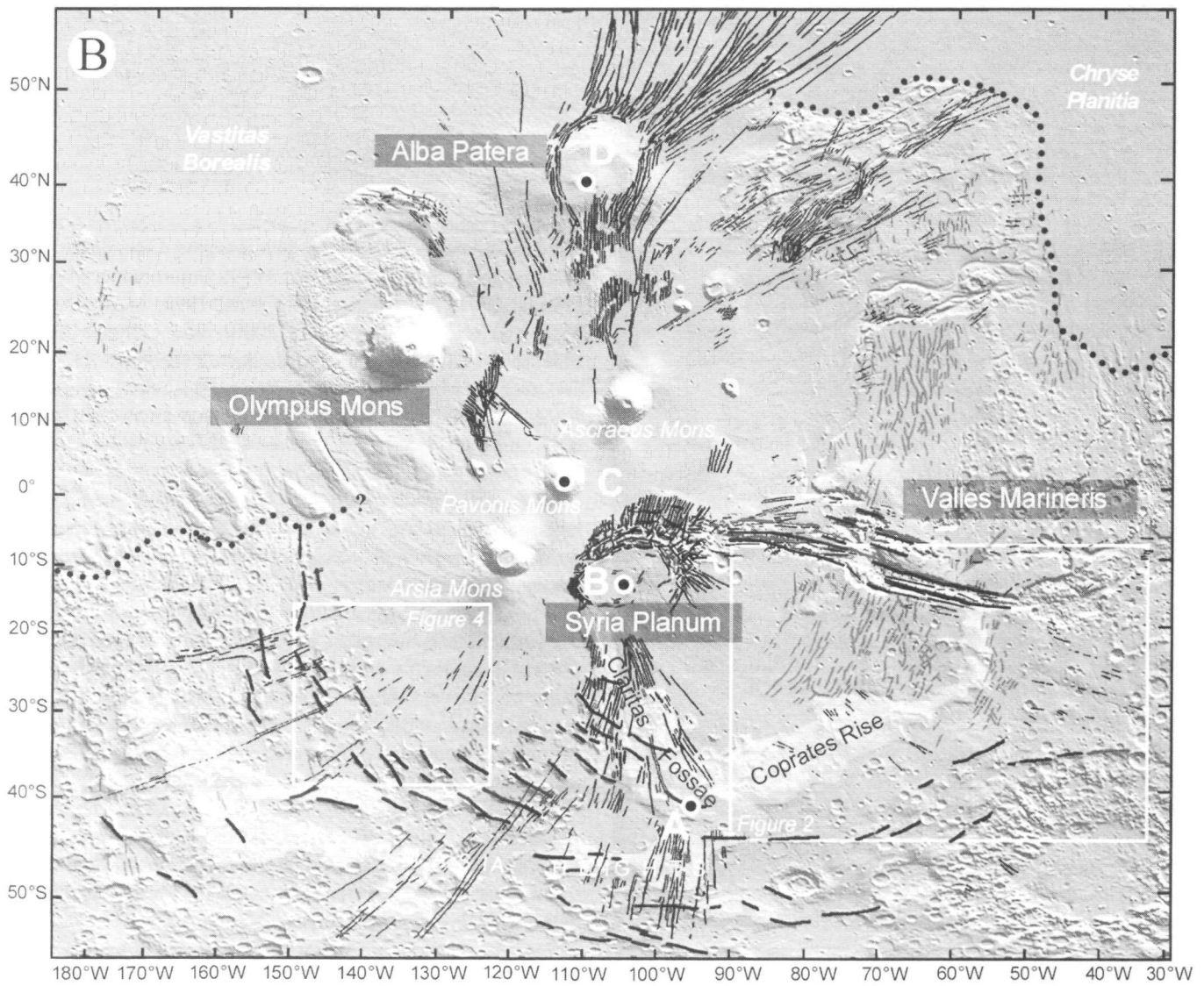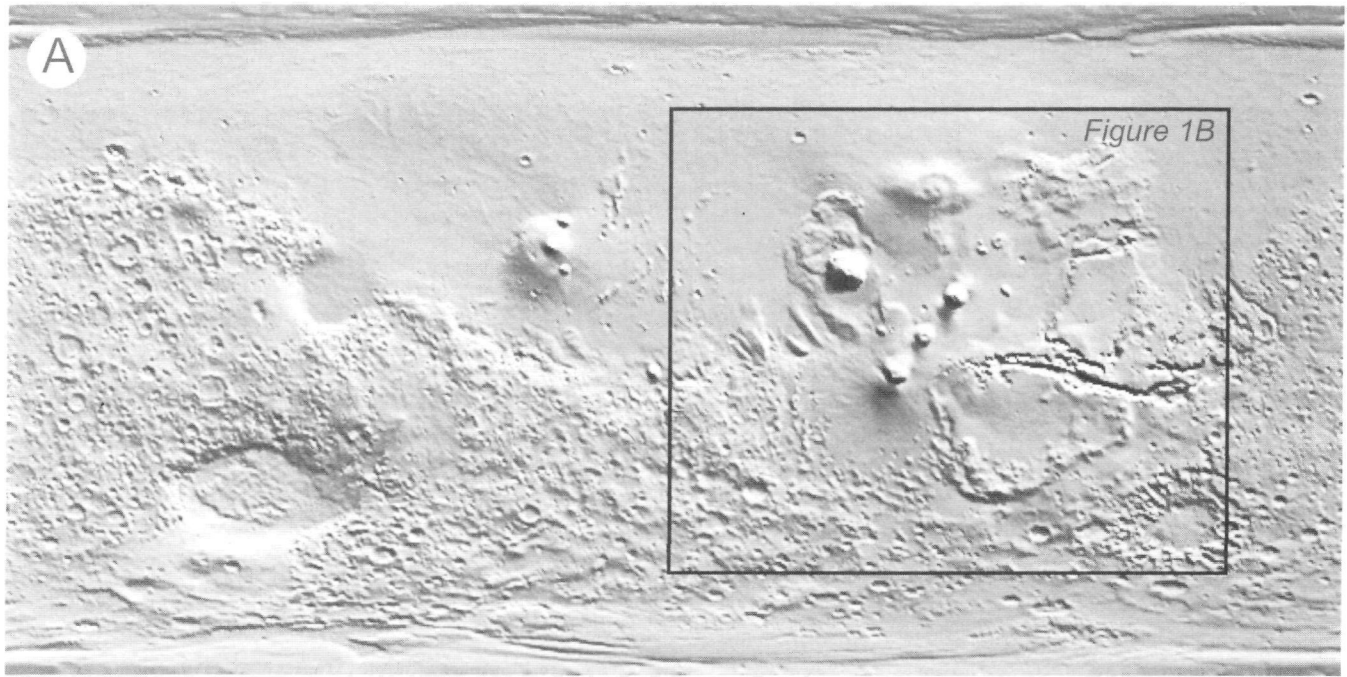
Figure 1. A, Mars Orbiter Laser Altimeter 0.125° shaded relief map of Mars (MOLA Science Team, 2000). B, Structural map of the Tharsis volcanic province. Thin black lines—grabens, thin gray lines—wrinkle ridges, thick black lines—ridges from the South Syria Planum ridge belt (elevation, ~3 km), light gray—Coprates Rise–Claritas Fossae arcuate belt (elevation, ~5–8 km) and (unofficial name) Sirenum-Thaumasia Heights (elevation, ~3 km), dotted line—martian dichotomy boundary. Convergence centers of dike swarms identified by Mège and Masson (1996): A—hypothetical early center at Thaumasia Planum, B—Syria Planum magma center, C—subsequent center in the Tharsis Montes area, D—Alba Patera center. 1° latitude = 55 km.

Figure 1B

A

B

50°N

Vastitas Borealis

Alba Patera   D

40°N

Chryse Planitia

30°N

20°N

Olympus Mons

10°N

Ascraeus Mons

0°

Pavonis Mons   C

10°S

Valles Marineris

Arsia Mons

Figure 4

B

Syria Planum

20°S

30°S

Claritas Fossae

Coprates Rise

40°S

A   Figure 2

50°S

180°W 170°W 160°W 150°W 140°W 130°W 120°W 110°W 100°W 90°W 80°W 70°W 60°W 50°W 40°W 30°W
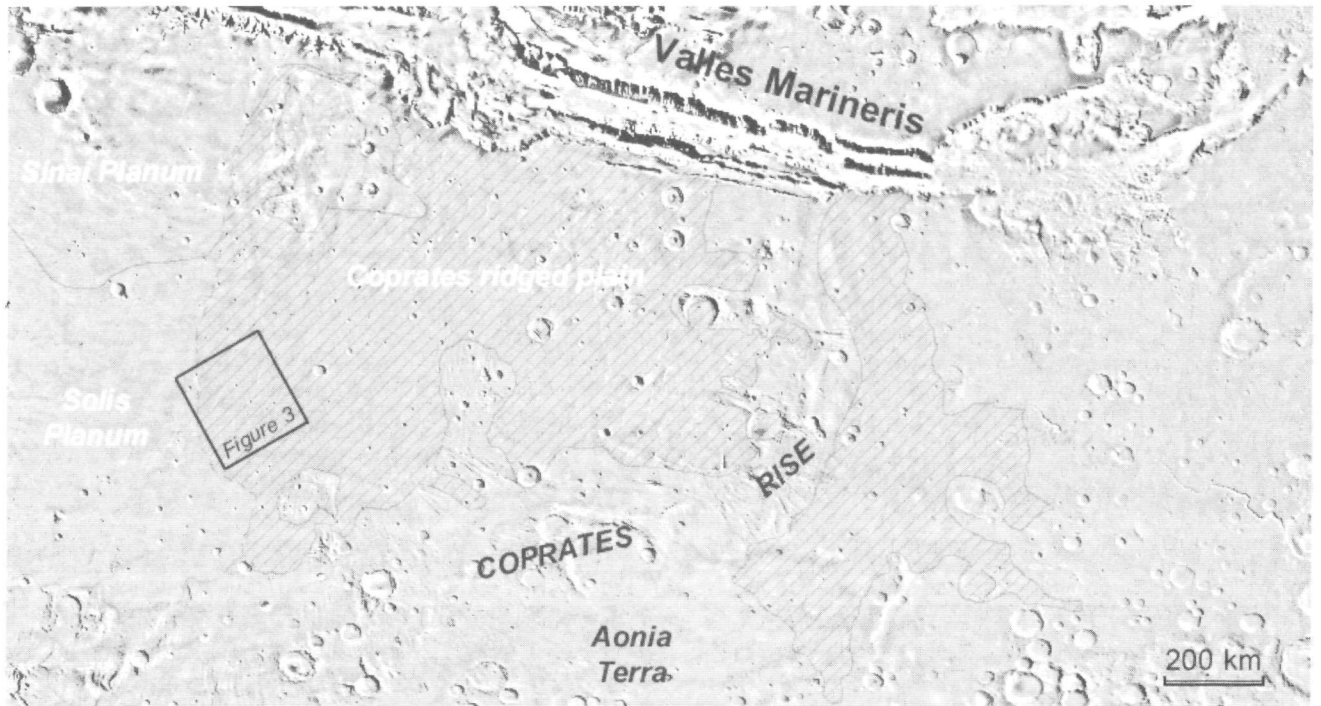
D. Mège and R.E. Ernst

Figure 2. The Coprates area. The early Hesperian Coprates ridged plain (diagonal lines, from Scott and Tanaka, 1986) is composed of lava flows associated with the Syria Planum magma center. Solis Planum (middle Hesperian) and Sinai Planum (Hesperian) are subsequent lava flows associated with the same magma center, and they partly mantle the Coprates lava flows. From Mars Digital Image Mosaic, U.S. Geological Survey.
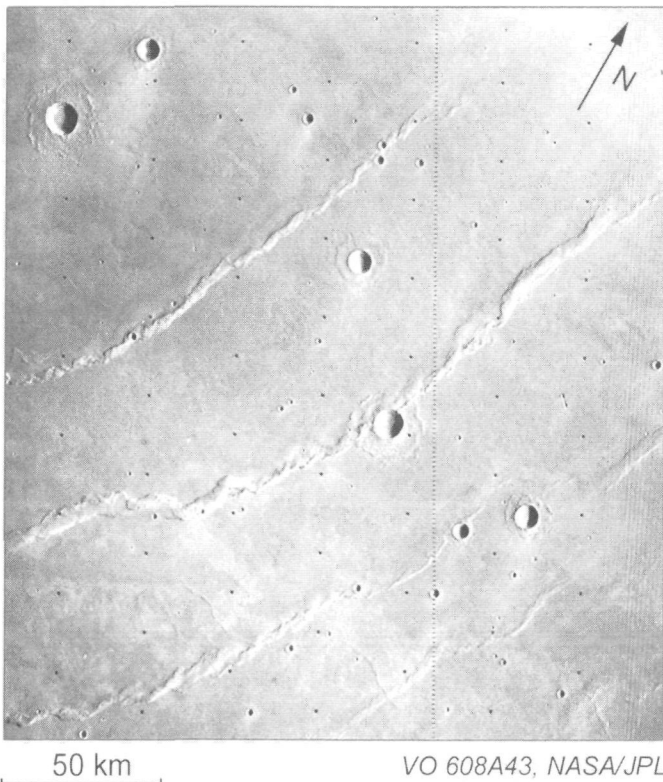

50 km   VO 608A43, NASA/JPL

Figure 3. Close-up of wrinkle ridges in the Coprates ridged plain. Location in Figure 2.

volved folding and thrusting (Plescia and Golombek, 1986; Watters, 1988; Suppe and Narr, 1989; Golombek et al., 1991; Plescia, 1991; Allemand and Thomas, 1992; Mangold, 1997; Mège and Reidel, 2000; Schultz, 2000), more or less at the same time as lava-flood emplacement during the early Hesperian (Watters and Maxwell, 1983; Watters, 1993; see Mangold et al., 1999, for an alternative view). Thrusts have been interpreted to be either emerging (Plescia and Golombek, 1986; Watters, 1988) or blind (Schultz, 2000). Thrusting is associated with coeval strike-slip faults (Schultz, 1989). No general agreement has been found on the deep-crustal structure of planetary wrinkle ridges, which have been interpreted as either thin-skinned features (Suppe and Narr, 1989; Allemand and Thomas, 1992; Watters, 1988; Mangold, 1997; Watters and Robinson, 1997) or thick-skinned features (Zuber and Aist, 1990; Golombek et al., 1991, 2000; Zuber, 1995). Principal-stress trajectories deduced from the analysis of the geometry of contemporaneous dikes show that mean ridge orientation is perpendicular to the maximum-principal-stress trajectory (Mège and Masson, 1996).

South Syria Planum ridge belt. At Tharsis, contractional features larger than the wrinkle ridges and having different structure are also observed at the southern periphery of the uplifted area, in the form of tens of large ridges (Figs. 1B, 4) defining the south Tharsis ridge belt (Schultz and Tanaka, 1994). Most of this ridge system is composed of structures falling within the category of high-relief ridges as defined by Wat-
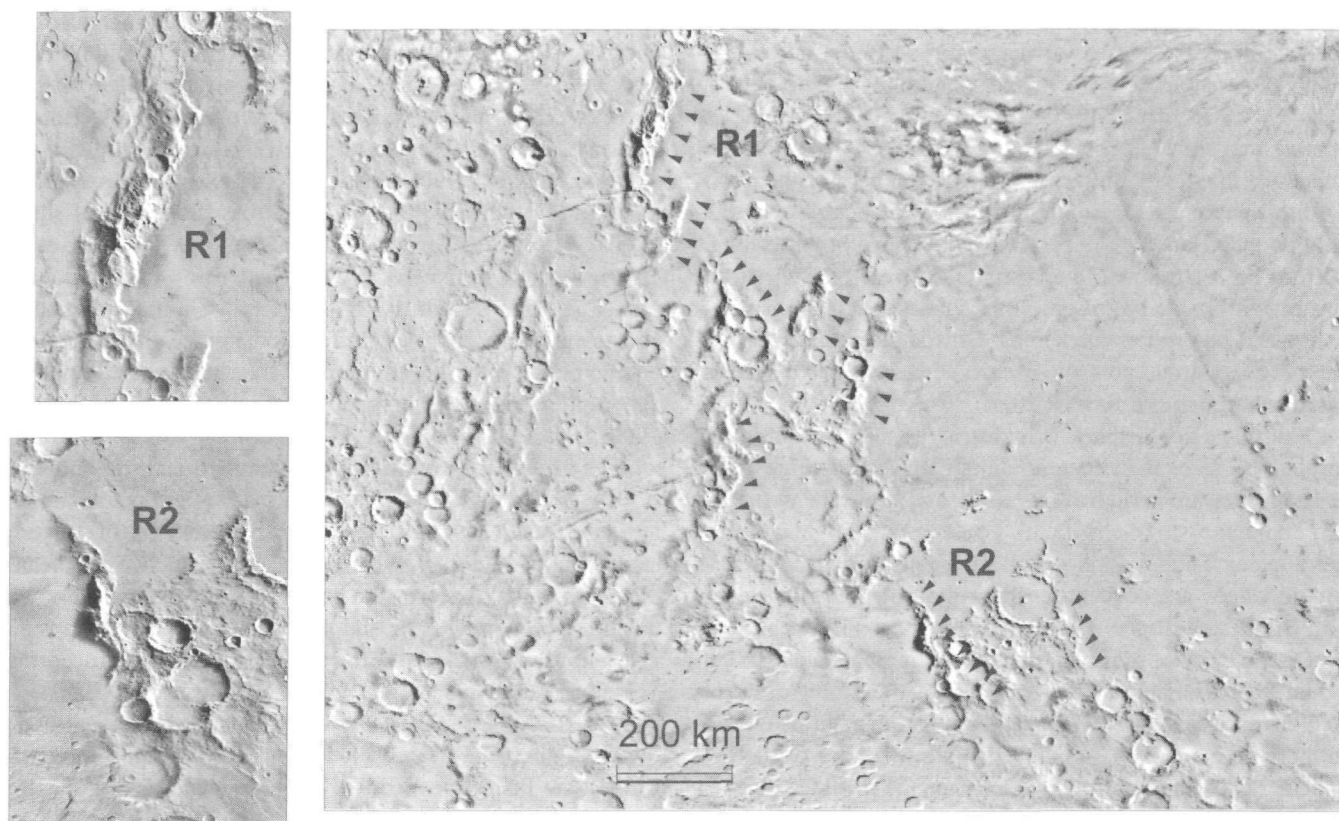
Figure 4. Western part of the South Syria Planum ridge belt. Arrows on the right image locate the main ridges in the area. Images on the left are close-ups of ridges R1 and R2. Location shown in Figure 1B. Background images from Mars Digital Image Mosaic, U.S. Geological Survey.

ters (1993). Most ridges are concentric about the Syria Planum magma center. Embayment of some ridges by Hesperian lava flows demonstrates that development of the contractional belt was initiated during Noachian, probably late Noachian, time, i.e., by the onset of Tharsis plume volcanic activity and before wrinkle-ridge formation (Tanaka and Schultz, 1991; Schultz and Tanaka, 1994). New topography data that are currently being acquired by the Mars Orbiter Laser Altimeter (MOLA) on board *Mars Global Surveyor* confirm that one ridge from the south Tharsis ridge belt, the Coprates Rise, is much broader (200 km) than the usual ridges (tens of kilometers). This MOLA data suggest that the Coprates Rise and several other ridges that are not concentric about Syria Planum define a coherent semicircular pattern bounding the depressed Syria Planum-related basaltic plains to the south (from the northern Coprates Rise in the east to the Claritas Fossae area in the west) (Fig. 1B). The south Tharsis ridge belt may thus be divided into a semicircular belt concentric about Syria Planum, which we call the south Syria Planum ridge belt, and a semicircular belt centered on the Syria Planum basaltic plains, that we will call the Coprates Rise-Claritas Fossae arcuate belt. Thus, two separate events producing tectonic compression may have existed at the south Tharsis ridge belt. Clearly, the Coprates Rise–Claritas Fossae

arcuate belt is morphologically distinct from the south Syria Planum ridge belt (Fig. 1), and the formation of the former should call for a different mechanism of deformation. Geologic analysis has revealed that the Coprates Rise-Claritas Fossae arcuate belt is composite and structurally highly complex and that its formation was polyphase (Masson, 1980; Tanaka and Davis, 1988; Underwood, 1992; Schultz and Tanaka, 1994).

The south Syria Planum ridge belt geometry suggests that its formation should have been influenced by processes centered at Syria Planum. Mège and Masson (1996) and Mège (1999a) proposed that it formed as a result of gravitational spreading of the Syria Planum topography, which had been uplifted during plume arrival.

Volcanic rises on Venus

The surface of Venus is composed of 80% volcanic plains, volcanic rises, and crustal plateaus (Head et al., 1992; Solomon et al., 1992; Stofan et al., 1995).

Volcanic rises are broad, circular uplifts 1000–2400 km in diameter displaying shield volcanoes and extensive volcanic flooding (Bindschadler et al., 1992a). Dynamic uplift due to mantle upwelling, supposed to have played a role in commonly

observed extensional tectonism ("rifting") at volcanic rises, is thought to predate a stage of magmatic accretion and under-plating responsible for permanent topographic support (Stofan et al., 1995; McGill, 1998). Crustal plateaus (discussed subsequently) and volcanic rises have been interpreted as consequences of mantle plumes impinging on the base of the Venusian lithosphere at two different stages of planetary evolution (Phillips and Hansen, 1998). The change in plume-tectonics style has been attributed to a change in convective style in the mantle (Phillips and Hansen, 1998) due to secular planetary cooling and lithosphere thickening. Crustal plateaus formed before this change, and volcanic rises, together with coronae (discussed subsequently), formed after.

Volcanic rises display wrinkle ridges that are similar in morphology, size, and structure to martian wrinkle ridges. Like the latter, they are periodically spaced, and some are associated with conjugate strike-slip faults (Watters, 1992). At volcanic rises such as Themis Regio (Fig. 5), western Eistla, and Bell, wrinkle ridges are concentric about the volcanic rise centers (e.g., Bilotti and Suppe, 1999).

On the basis of hypsometric and stratigraphic analysis carried out by Rosenblatt et al. (1997, 1998), the timing of events at volcanic rises is (1) uplift of the topographic surface due to the thermal anomaly of a plume rising to the base of the lithosphere, (2) fissure-controlled volcanism, (3) wrinkle-ridge formation, and (4) central magmatism (e.g., at Gula and Sif Montes). Central volcanism occurred after fissure-type eruptions, in accordance with the suggestion that central volcanism was delayed on Venus compared to Earth and Mars because of high atmospheric pressure (Head and Wilson, 1992). On Venus, wrinkle-ridge formation has been explained by volcanic topographic loading (Basilevsky, 1994) and subsidence (Rosenblatt et al., 1998). In detail, two wrinkle-ridge sets, one local and one regional, have been identified at volcanic rises (Rosenblatt et al., 1998; Bilotti and Suppe, 1999). The local wrinkle-ridge set is closer to the volcanic rise center and, therefore, stands at higher elevation than the regional ridge set. The regional ridges have been interpreted as a possible consequence of downward-flowing currents associated with the periphery of the mantle plume (Rosenblatt et al., 1998). This interpretation is supported by the correlation between the lowest ridged plains and regional negative gravity anomalies (Sandwell et al., 1997; Bilotti and Suppe, 1999), which suggests strong coupling between tectonic deformation mechanisms in the lava plains and the mantle processes (Rosenblatt et al., 1998). Therefore, subsidence due to both topographic loading and sinking currents may have played a role in wrinkle-ridge formation in a hotspot setting on Venus.

Crustal plateaus on Venus

Crustal plateaus (a term that includes some of the largest *tessera* inliers on Venus), such as eastern Ovda Regio and Tellus Regio, are some of the most deformed and oldest terrains observed on the surface of Venus (e.g., Basilevsky et al., 1999).

They are quasi-circular, intensely deformed regions having a thick, isostatically compensated crust (Herrick and Phillips, 1992). Preliminary SAR (Synthetic Aperture Radar) analysis lent support to plateau formation via sinking (Bindschadler et al., 1992a, 1992b; Gilmore et al., 1997). However, this model fails to explain several geologic observations, such as a shallow ductile-to-brittle transition (DBT) across thousands of square kilometers deduced from structural analysis (Hansen et al., 1999), early widespread pervasive extension and volcanism, minor shortening recorded by gentle folds, and accompanying volcanism. A magmatic-accretion model in which a local, deep-mantle plume impinges on globally thin lithosphere appears to better satisfy each of these observations (Ghent and Hansen, 1999; Hansen et al., 1999). For a contrary assessment of the relative ages of the extensional and contractional structures, see Ivanov and Head (2000). The deformation and magmatic history of crustal plateaus is exemplified by the results of structural analysis at eastern Ovda Regio. The same sequence of volcano-plutonic events appear to be equally valid, although less well documented, for other crustal plateaus on Venus (Phillips and Hansen, 1998), including, for instance, southwestern Fortuna Tessera (Hansen and Willis, 1998) and Tellus Regio (Banks and Hansen, 1999). Four types of structures have been identified at Ovda Regio (Fig. 6A): (1) The earliest tectonic structures formed are linear, steep-sided, flat-bottomed, tension fractures or grabens ("ribbons") arranged in radial patterns. Ribbon wavelength suggests that they formed in a thin brittle layer, 1–2 km thick, overlying a ductile layer (Hansen and Willis, 1998; Ghent and Hansen, 1999). (2) Subsequent broader-scale folding at plateau margins denotes a drastic change in tectonic regime. However, as fold strikes are perpendicular to ribbon strikes, the stress trajectories did not change appreciably; only the stress magnitudes need to have varied. Fold wavelength suggests that this change also corresponds to brittle-crust thickening to 2.5–10 km. (3) Anastomosing and closely spaced folds, interpreted as interference folds, are observed at the center of the plateau. No crosscutting relationships with other plateau structures could be found, so that temporal relationships could not be established. (4) The fourth series of structures are grabens parallel to, and superimposed on, ribbons. They preferentially formed across the anticlines and widen toward the crests. They probably formed after folding and are therefore expected to be consequences of folding. Complications are revealed at Tellus Regio where an additional series of contractional structures are observed.

The current elevation of crustal plateaus, together with current estimates for crustal thickness, requires a mechanism for permanent uplift, which most likely originates from magma accumulation within or beneath the crust. At least two major periods of volcanic activity are observed at crustal plateaus. Eruption of mafic lava flows that embay folds occurred during the late stages of plateau evolution (Banks and Hansen, 1999). In addition, the absence of heavily deformed craters on crustal plateaus suggests that surface rejuvenation occurred before, or
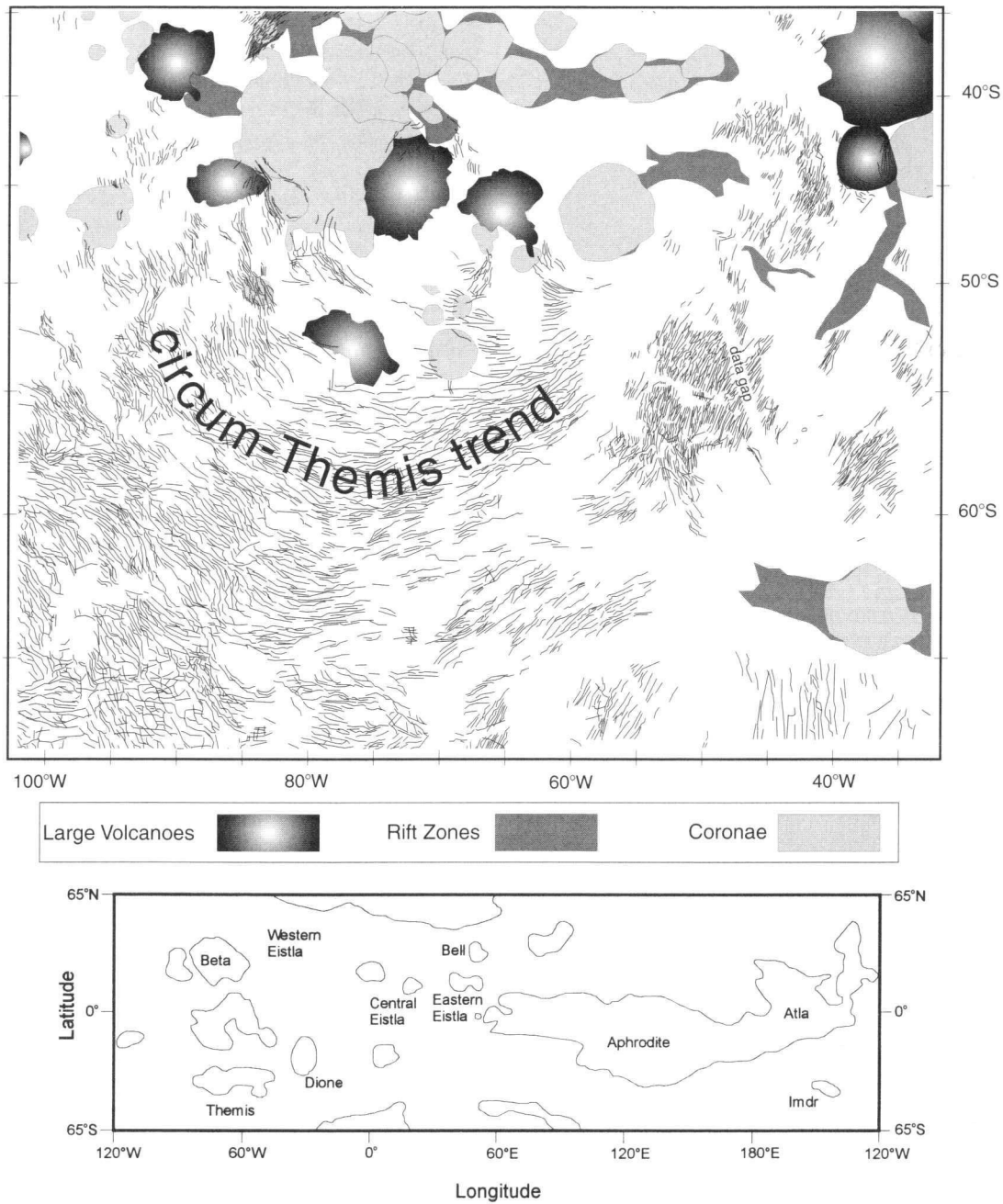
Figure 5. Concentric pattern of wrinkle ridges associated with the volcanic rise at Themis Regio, Venus, modified after Bilotti and Suppe (1999). Location map for volcanic rises modified from Stofan et al. (1992).

during, the formation of ribbon fractures and folds and thus reset the crater record clock to zero. Such a process requires an especially high heat flow that could permit crustal melting up to a very shallow level in the crust—maybe even to the topographic surface (Ghent and Hansen, 1999). Such conditions suggest the generation of a huge magma volume early in the tectonic evolution of crustal plateaus. Senske and Plaut (2000) have recently confirmed this view and identified layered volcanic materials at Tellus Regio, perhaps akin to flood basalts, that were subsequently deformed during the crustal plateau-forming events.

According to Ghent and Hansen (1999), mantle-plume impingement on the base of a thin lithosphere induces topographic uplift, magmatic underplating, and intrusion and extrusion of
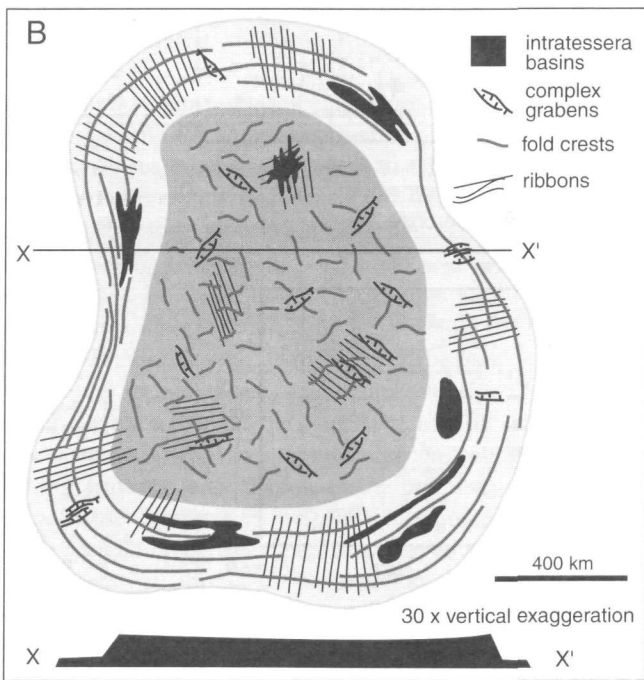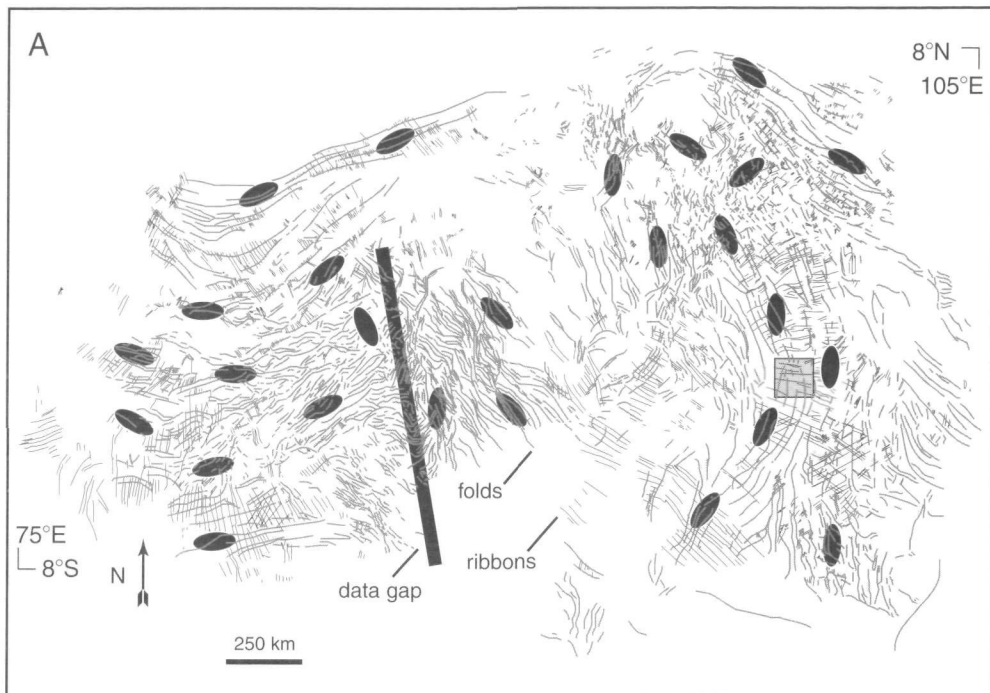
Figure 6. A, Structural map of eastern Ovda Regio, Venus (after Ghent and Hansen, 1999). The sequence of tectonic structure development is as follows: 1—"ribbon"; fractures (thin black lines), 2—marginal and anastomosing folds (thick gray lines), and 3—grabens at fold crests (not shown at this scale). The strain ellipses suggest radial and concentric arrangement of structural patterns and denote local influence on structure development. The anastomosing fold area is expected to represent areas of maximum subsidence. The shaded box toward the right locates the area shown in Figure 18C. B, Structural model of typical Venusian crustal plateau. After Hansen et al. (1999).

magmas. Combination of uplift and magma cooling from the surface downward would have resulted in pervasive lithosphere fracturing and ribbon formation. Further lava cooling and waning of dynamic support would have induced topographic subsidence. Subsidence would have resulted in the concentric fold-

ing at the plateau margins, perpendicular to the ribbons, and interference folding in the plateau interior (Fig. 6B). Brittle crust would thicken via folding, and later extension would be a consequence of gravitational relaxation of the overthickened fold crests.

Coronae and corona-type structures on Venus

Coronae are ovoid structures a few hundred to 2000 km in diameter forming clusters and chains on Venusian lava plains (Head et al., 1992). Their central topography varies from bulge-shaped to plateau-like to depressed. Depressed coronae (Fig. 7) display a peripheral topographic annulus with circumferential extensional fractures, sometimes associated with contractional ridges (Janes et al., 1992; Stofan et al., 1992). Although several interpretations for the origin of coronae have been proposed, such as response to circular subduction process (Sandwell and Schubert, 1992) or lithosphere delamination and sinking of dense lithosphere through the mantle (Stofan and Head, 1990), most authors attribute corona formation to mantle plumes or diapirs (Janes et al., 1992; Squyres et al., 1992b; Stofan et al., 1992; Magee-Roberts and Head, 1993; Koch and Manga, 1996; Jaeger, 2000). Janes et al. (1992) proposed that coronae result from mantle diapirs less than ~100 km in diameter rising from the mantle. Stofan et al. (1992) suggested that corona-related volcanism is either small scale or of short duration, in contrast to volcanic rises. Consistent with this interpretation, Phillips and Hansen (1998) proposed that corona-related volcanism would originate from convective patterns in the mantle, whereas volcanic rises would result from deeply rooted mantle plumes. Corona evolution is thought to start with diapir impingement on the bottom of the Venusian lithosphere, leading to lithosphere uplift and thinning (Janes et al., 1992; Squyres et al., 1992b; Stofan et al., 1992; McGovern and Solomon, 1998). Coronae are commonly associated with the emplacement of giant radiating systems of grabens, thought to overlie subsurface mafic dikes (e.g., Grosfils and Head, 1994), and, less commonly, circumferential graben systems also possibly marking subsurface dikes (Ernst and Buchan, 1998). After dike emplacement, diapirs would then spread and flatten at the base of the lithosphere at the same time as dynamic support is waning. Volcanism and shallow intrusions in the crust would then induce gravitational relaxation of topography that would explain the plateau-like and depressed morphologies (Janes et al., 1992). On the basis of numerical experiments of diapir ascent, Koch and Manga (1996) suggested that the diapir spreading is centered at the level of neutral buoyancy and that the style of corona topography depends on that depth. The shallower this level, the higher the expected bulge, whereas the deeper this level, the deeper the central depression and the wider the peripheral annulus.

Although corona-annulus formation is predicted by single-stage elastic modeling of corona gravitational relaxation, such models do not predict a compressive state of stress (Janes et al., 1992). However, in agreement with geophysical modeling of corona topography (Smrekar and Stofan, 1997) and experimental modeling of corona evolution in response to a deflating diapir (Krassilnikov, 2000), multiple stages of volcanic loading and subsequent gravitational relaxation were shown to be able

Figure 7. Compressional features associated with the northeast part of Sith corona (10.2°S, 176.5°E). After Stofan et al. (1992).

to produce a contractional annulus if the elastic lithosphere thickness is small or null (McGovern and Solomon, 1998).

Yellowstone plume and Columbia Plateau, western North America

The cause of Columbia River flood-basalt volcanism in western North America since ca. 17 Ma has been controversial. Both backarc spreading (e.g., Carlson and Hart, 1987) and melting associated with the Yellowstone mantle plume (Zoback and Thompson, 1978; Duncan, 1982; Pierce and Morgan, 1992; Geist and Richards, 1993; Zoback et al., 1994; Camp, 1995) were advocated as possible sources. More recent geochemical results have unambiguously shown that the Columbia River Basalt Group has a mantle-plume signature (Hooper and Hawkesworth, 1993; Hooper, 1997; Takahashi et al., 1998). Structures akin to wrinkle ridges, e.g., the Yakima folds (also called Yakima ridges) are associated in time with this flood-basalt event (Figs. 8–10).

The Yakima folds are a series of regularly spaced (~20 km, Watters, 1989; Schultz and Watters, 1995) thrust-faulted anticlines in the western Columbia Plateau (Reidel, 1984; Price and Watkinson, 1989; Reidel et al., 1989a; Tolan and Reidel, 1989; Watters, 1989). The folds are evidence of contractional deformation in the Columbia River basalt flows both throughout the period of volcanic activity (Camp and Hooper, 1981) and still ongoing (Malone, 1978; Campbell and Bentley, 1981; Reidel et al., 1994; West et al., 1996). The peak of Yakima ridge growth corresponds to the onset of Yellowstone hotspot volcanic activity, and the ridge-growth rate was closely dependent on the rate of Columbia River basalt magma supply (Rei-

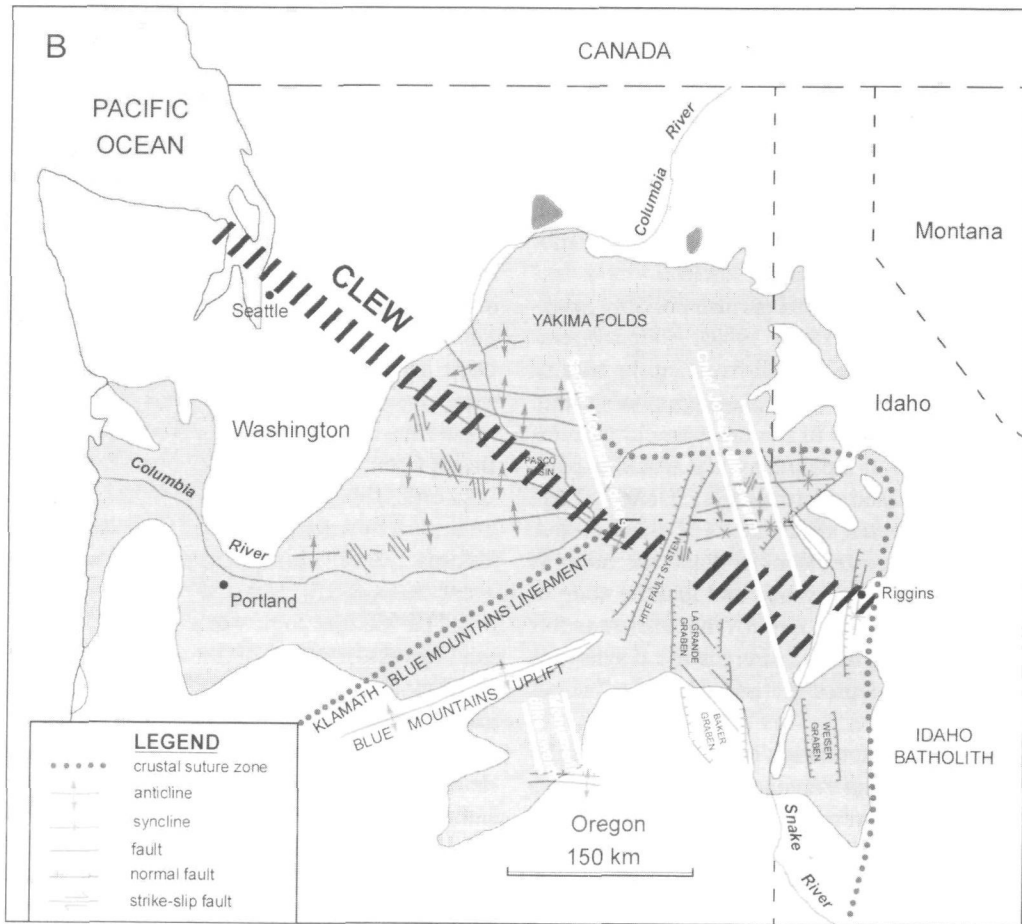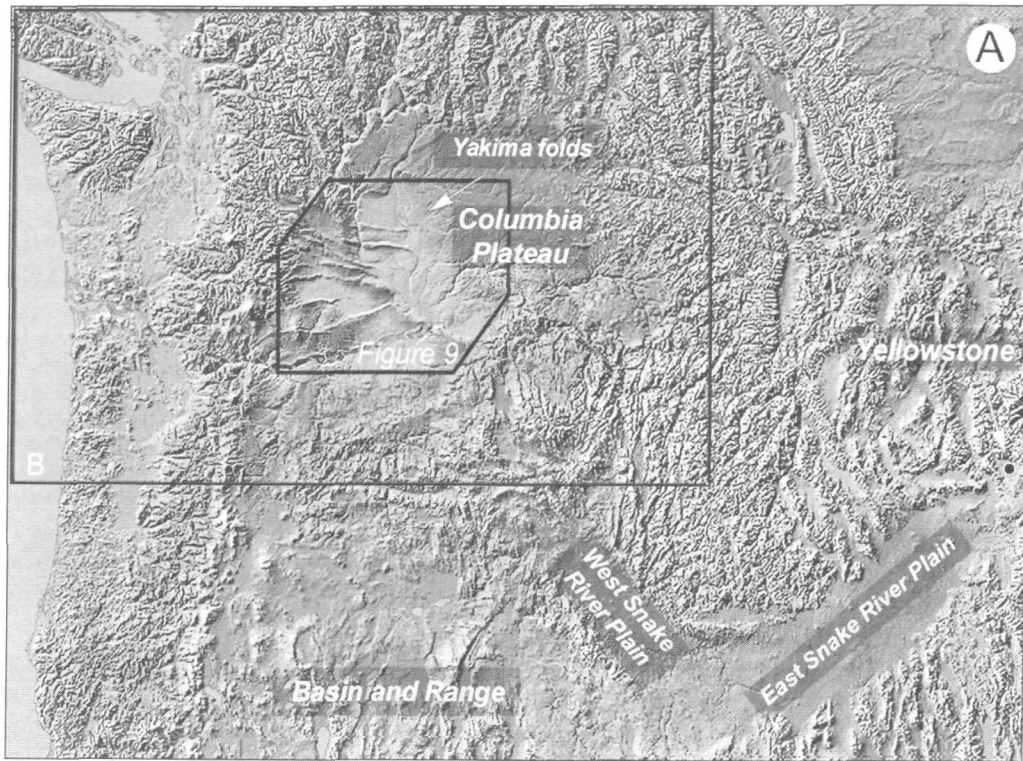Figure 8. A, Tectonic setting of the Columbia Plateau (digital elevation model, from Thelin and Pike, 1991). B, Main structural patterns at the Columbia Plateau (modified after Hooper and Conrey, 1989). CLEW—Cle Elum–Wallula topographic lineament.
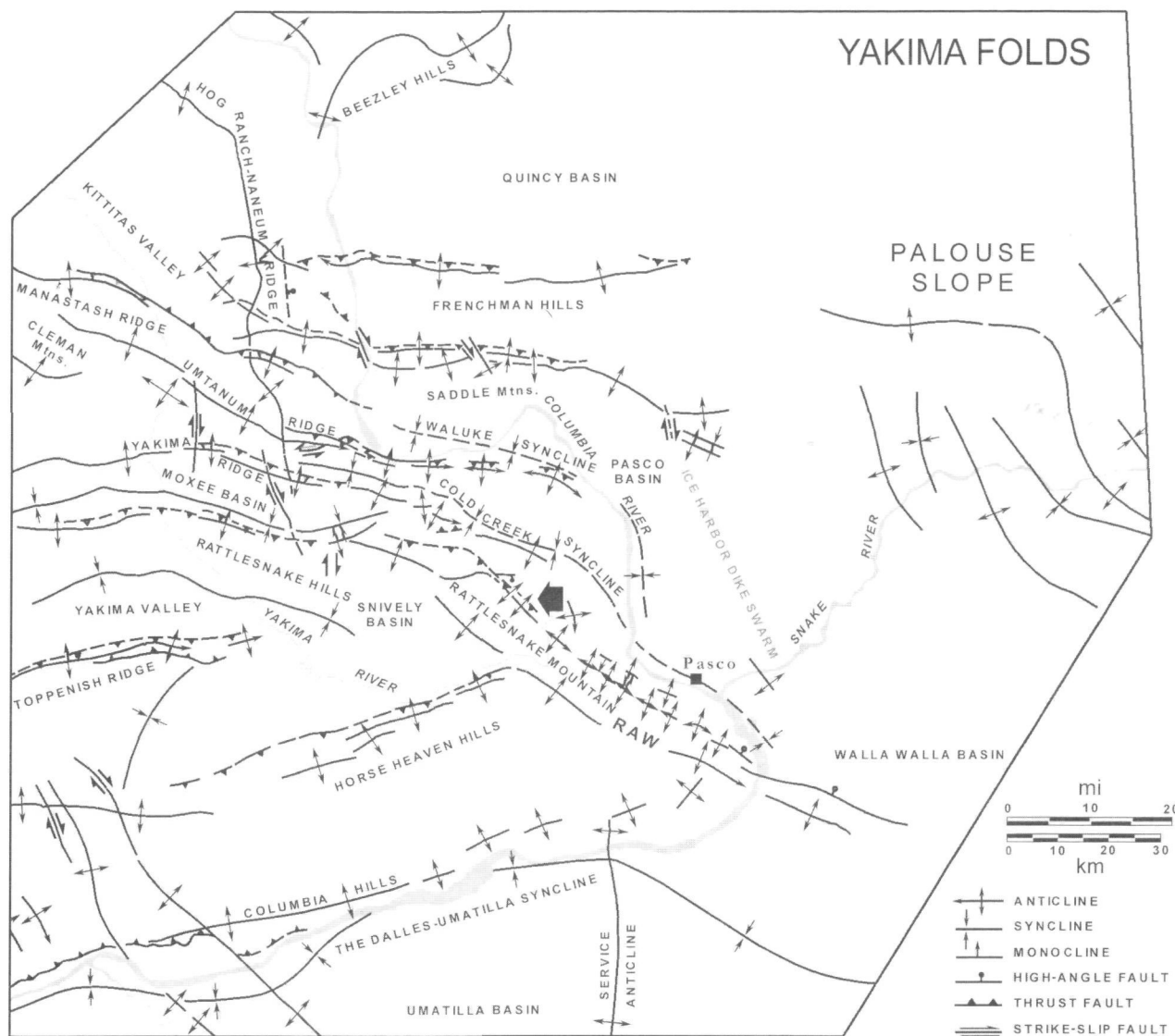
Figure 9. Structural map of the western Columbia Plateau (for location, see Fig. 8). Modified after Reidel et al. (1989a). The black arrow locates the photograph in Figure 10. RAW—Rattlesnake–Wallula Alignment.

del, 1984; Reidel et al., 1989a). Seismic, borehole, and magnetotelluric data from the Columbia Plateau have shown that the Yakima ridges are thin skinned (e.g., (Catchings and Mooney, 1988; Reidel et al., 1989a; Jarchow et al., 1994; Lutter et al., 1994). The Yakima ridges are associated with conjugate strike-slip faults coeval with ridge development (Hooper and Conrey, 1989; Reidel et al., 1984; Tolan and Reidel, 1989). More details on ridge structure can be found in Bentley (1977), Reidel (1984), Hagood (1986); Price and Watkinson (1989), Reidel et al. (1989a, 1994), Lutter et al. (1994), and Mège and Reidel (2000).

The bulk of the Yakima folds is oriented roughly east-west (Figs. 9 and 11). However, in detail, three domains can be distinguished on the basis of ridge orientation (Watters, 1989). The mean ridge-segment orientation northeast of the Cle Elum–Wal-

lula topographic lineament (CLEW, Fig. 8B is N100°E; it is N135°E within the lineament, and N79°E southeast of the lineament. Various arguments suggest that the Cle Elum–Wallula topographic lineament has been a dextral shear zone since eruption of the Columbia River Basalt Group, although the amount, timing, and geographical distribution of displacement are controversial (Hooper and Conrey, 1989; Mann and Meyer, 1993; Reidel and Tolan, 1994). It is clear, however, that the Cle Elum–Wallula topographic lineament affected the orientation of some of the Yakima ridges. Furthermore, the Hog Ranch–Naneum ridge, which is oblique to the other ridges of the Yakima fold-and-thrust belt (Fig. 9), was shown to continue at depth beneath the 3–6-km-thick lava pile. Analysis of well logs shows that this structure bounded an early Tertiary basin before lava flooding (Campbell, 1989) and therefore is atypical of the other
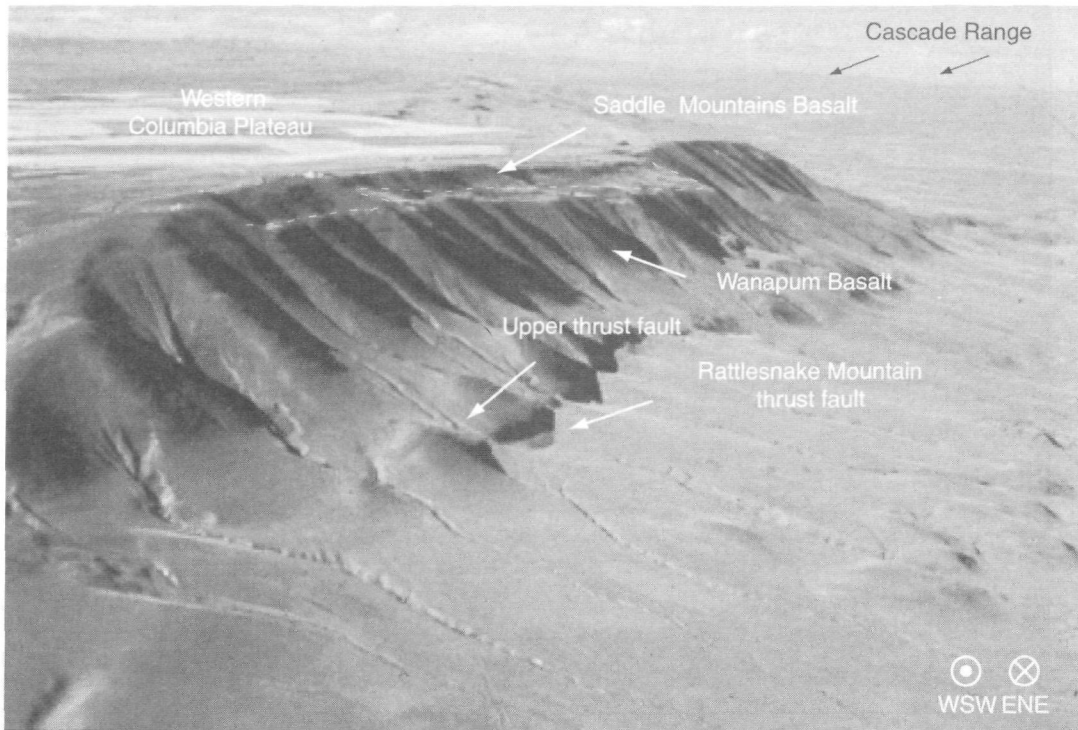
Figure 10. Rattlesnake Mountain, Columbia Plateau. Photograph courtesy of S.P. Reidel.

ridges. Apart from the above anomalies, the majority of Yakima ridges have consistent, roughly parallel trends.

Most strain at the Yakima ridges was produced at 17–15 Ma, contemporaneous with the emplacement of dike swarms that fan north-northwest on the plateau (e.g., Tolan et al., 1989; Ernst and Buchan, 1997). The dikes underwent no, or only minor, postemplacement rotation (Martin, 1984; S.P. Reidel, 1999, written communication; Hagstrum et al. 1999; Ernst and Buchan, this volume, Chapter 12). Southward they converge on a center about which the Yakima ridges form a circumferential arc (Fig. 11). This center is located in the McDermitt volcanic field, which was the center of the Yellowstone plume activity at 17 Ma. The orthogonal orientation of dikes and ridges (e.g., Hooper and Conrey, 1989), as well as focal mechanisms (Suppe et al., 1975; Zoback, 1992), show that the ridges formed, and are still, perpendicular to the maximum-principal-stress trajectory. The permutation in principal-stress trajectories required to explain simultaneous ridge formation at the surface and dike emplacement at depth has been explained by a mere increase of lithostatic pressure with depth while maintaining constant horizontal principal stresses (Hooper and Conrey, 1989; Hooper, 1997).

The source of compressive stress at the Columbia Plateau is still controversial. Little appears to have changed since Beck (1978) noted that "few tectonic models for the evolution of the Pacific Northwest treat specifically with the Columbia Plateau in any detail. In many the region is either not mentioned at all,

or is treated as a minor embarrassment to be dismissed as painlessly as possible." Suppe et al. (1975) and Beck (1978) first suggested that the tectonics of the plateau may be a consequence of the Yellowstone mantle plume. We note that the orientation of both ridges and dikes is consistent with axially symmetric principal-stress trajectories that would have resulted from the Yellowstone plume center's position at 16.1 Ma, which coincides with the location of the McDermitt caldera (Fig. 11). This interpretation is not compromised by paleomagnetic studies showing that the ridges were rotated clockwise 20°–30° after 12 Ma (Reidel et al., 1984; Sheriff, 1984), because the rotations only accommodate local shears at fold hinges during ridge growth (Reidel et al., 1984). Alternative hypotheses include (1) formation of the Yakima fold-and-thrust belt in relation to oblique subduction of the Juan de Fuca plate (e.g., Atwater, 1970; Reidel et al., 1989a; Burchfiel et al., 1992), to which is superposed Basin and Range extension (Hooper and Conrey, 1989), or (2) westward gravitational sliding of the Basin and Range above the hot and buoyant mantle (Hemphill-Haley and Humphreys, 1997; Shen-Tu et al., 1999) toward the subducting, shallow-dipping Pacific plate, in conjunction with the coastal ranges sliding along the San Andreas fault system toward a more steeply dipping Juan de Fuca plate. The latter kinematic scenario has been advocated as the boundary motion driving the formation of the Yakima ridges (E.D. Humphreys, cited by Kerr, 1997).
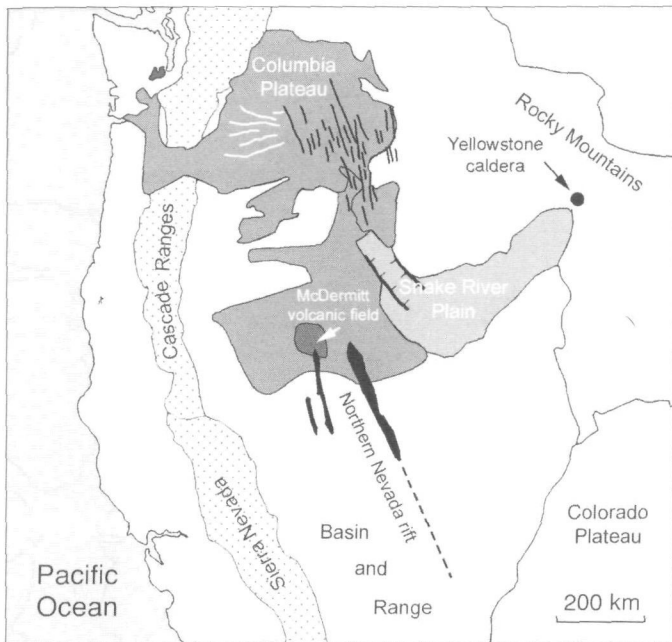
Figure 11. Tectonic and magmatic features associated with the early Yellowstone plume. The McDermitt volcanic field marks the location of plume impact. Dark gray—McDermitt volcanic field, medium gray—Columbia River Basalt Group (to the north) and other tholeiitic basalts of similar age (to the south), light gray—Snake River Plain volcanism, black—Northern Nevada Rift, dotted pattern—coastal ranges, dark lines—dike trends, white lines—Yakima ridge trends, lines with hachures—western Snake River Plain graben. Modified after Zoback et al. (1994) and Cummings et al. (2000).

North Atlantic volcanic province, northwestern Europe

Some 20 faulted anticlines have been observed in the North Atlantic volcanic province on seismic profiles at the northwestern European margin (Fig. 12), most of them at the Faeroe-Rockall Plateau, (Boldreel and Andersen, 1993, 1998; Brodie and White, 1995; Vågnes et al., 1998). The anticlines were initiated above sea level during late Paleocene–early Eocene time, after Paleocene flood-basalt outpouring associated with the arrival of the Thulean plume, and result from inversion of Mesozoic structures. The geodynamic framework of this region at that time makes this compressional event striking. Evolution of the area since the Paleocene–Eocene is marked by arrival of the Thulean plume (White and McKenzie 1989) and North Atlantic opening, so that major contractional structures are unexpected. Evidence of Eocene compression has also been found on land by Geoffroy et al. (1993, 1994) in the Faeroe Islands. Anticline orientations offshore follow two preferential trends. Nine trend northwest, denoting northeast-southwest compressive stress, consistent with the northeast-southwest stress orientations found in the Faeroe Islands (Geoffroy et al., 1993, 1994). The other anticlines have various orientations. Comparison with plate reconstruction, Tertiary flood-basalt province geography (White and McKenzie, 1989), and location of the

hotspot center during the Paleocene (Lawver and Müller, 1994) shows that the overall pattern of the anticlines, most of which formed above the edge of the initial plume-derived thermal anomaly if its extent was as suggested by White (1992), can alternatively be interpreted as broadly concentric about the Thulean plume at the time of its arrival (Fig. 12). Local deviation from the concentric pattern may be due to the influence of the orientation of the Mesozoic faults that guided the anticlinal trends. The growth rate of the offshore anticlines has been found to have been constant from the Eocene until the present (Vågnes et al., 1998) and therefore requires a stable and long-lasting stress source.

Hypotheses for explaining Eocene compression in the Faeroe Islands include transform-zone stresses caused by the Aegir and Reykjanes spreading ridges (Geoffroy et al., 1993; Boldreel and Andersen 1998) and separation of a Greenland plate between the North Atlantic and Labrador Sea (Geoffroy et al., 1993). Compression offshore has also been suggested to result from the Alpine orogeny, with a contribution from ridge-push forces (Boldreel and Andersen, 1998; Vågnes et al., 1998). However, these interpretations fail to explain the concentric orientation of the majority of anticlines about the Thulean plume. A recent hypothesis suggests that the anticline pattern at the North Atlantic volcanic province might have resulted from gravitational spreading of the plume topographic swell (Bourgeois, 2000; O. Bourgeois, 2000, personal communication).

Yilgarn craton, Australia

Myers and Swagers (1997) have described the geologic units of the Yilgarn craton, and a summary of its evolution can be found in Passchier (1998). The craton amalgamated from several terranes mainly between 2.7 and 2.6 Ga. It then joined with the Pilbara craton during the Capricorn orogen in 2.0–1.6 Ga. The Capricorn orogen displays evidence of formation of an asymmetric contractional belt and a foreland basin in which relics of ophiolites have been found, suggesting a cycle including collision and subduction. This collisional-zone geodynamic style contrasts with the style that prevailed during the earlier Archean amalgamation, which was dominated by outpouring of massive mafic magmas and intrusion of granites, associated with extensional and contractional tectonics. Archean tectonic activity has been attributed to one or several possible mantle plumes (Passchier, 1995), an hypothesis initially suggested by Campbell and Hill (1988). Geologic analysis of one of the terranes, the East Yilgarn terrane (Kalgoorlie terrane in Myers and Swagers, 1997, and the Eastern Goldfields terrane in Passchier, 1998) led to a plume-tectonics model of terrane evolution (Passchier, 1995). Plume impingement on the lithosphere would have resulted in flood-lava outpouring associated with extension above the plume at ca. 2.69–2.68 Ga, contemporaneous with concentric thrusting at the edge of the inferred hotspot (Fig. 13). Extension was polydirectional and has been interpreted to have been produced by the plume's en-

Figure 12. Early Tertiary anticlines observed on the northwestern European shelf plotted on a plate-reconstruction map for the time just after the onset of North Atlantic oceanic spreading (base map after White and McKenzie, 1989) and Paleocene and Eocene locations of the plume center according to two plume-track models (Lawver and Müller, 1994, and White and McKenzie, 1989). Small dark circles: location of the Thulean plume center at 60 Ma (late Paleocene) and 50 Ma (early Eocene–middle Eocene), after Lawver and Müller (1994). Gray circle—extent of the initial thermal anomaly using Lawver and Müller's model. Small dashed circle: location of the plume center at magnetic anomaly 23 (Paleocene-Eocene boundary) after White and McKenzie (1989). Large dashed circle: extent of the initial thermal anomaly in White and McKenzie's model. In both models, the size of the thermal anomaly is after White (1992). Dark lined areas—extrusive volcanic rocks. Light lined areas—extent of Tertiary igneous activity (after White and McKenzie, 1989). Continuous anticline axes and thrust symbols—anticlines and thrust faults, after Boldreel and Andersen (1993, 1998); dotted anticline axes—additional anticlines, after Vågnes et al. (1998); thick dashed anticline axis (south of England)—additional anticline, after Brodie and White (1995). Anticline orientation is attributed to the influence of both the location of the Thulean plume center and the orientation of earlier (Mesozoic) faults, resulting in partially concentric patterns at the edge of the spreading thermal anomaly due to the plume.
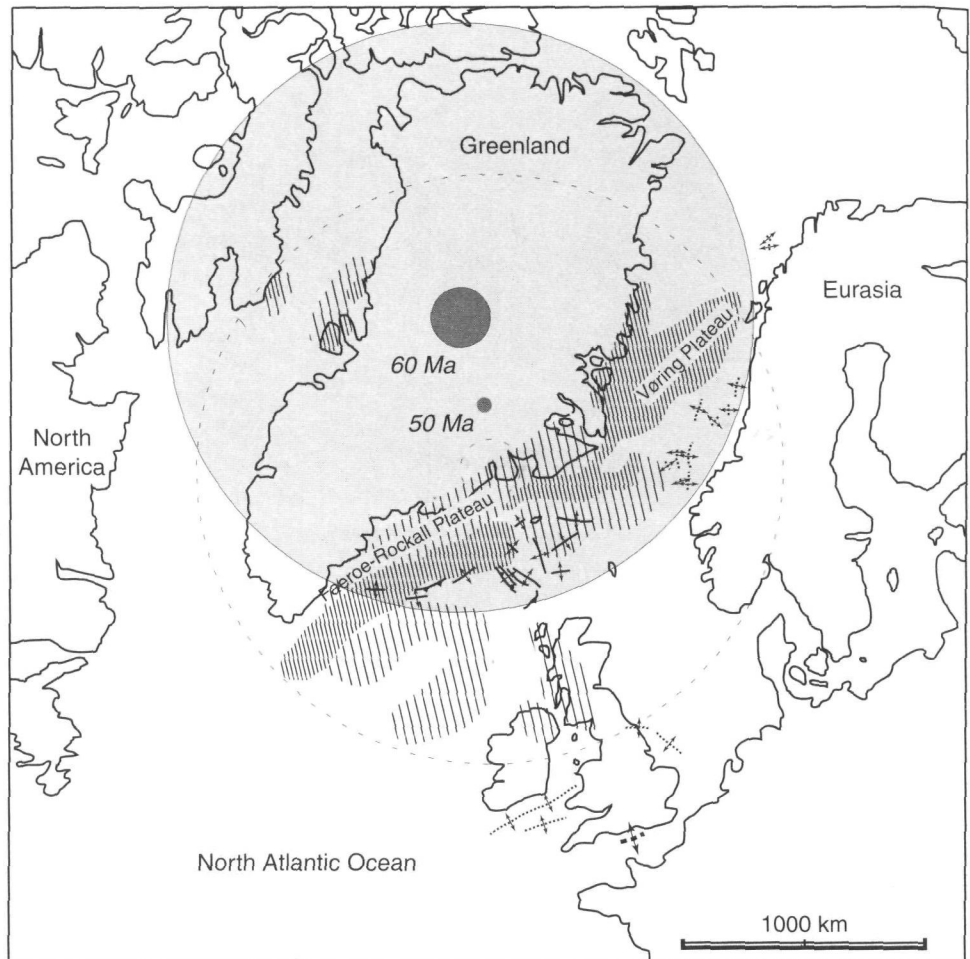
tering the uplifted crust above the plume conduit, whereas coeval compression has been interpreted as the result of strain concentration at the edge of the crustal domain weakened by the plume in a compressional tectonic regime (Passchier, 1995).

Dharwar craton, India

The late Archean Dharwar craton (India) is composed of greenstone belts cropping out over large surface areas. It displays dome-and-basin structure associated with shear zones. Dome-and-basin folding at the Dharwar is contemporaneous with high-temperature, low-pressure metamorphism (Moyen, 2000). Oblique convergence has been suggested to explain these structures (Chadwick et al., 2000). However, although oblique convergence may explain the shear zones, it fails to explain detailed structural observations within greenstone belts of the Dharwar craton. Analysis of macro- and microstructures

(stretching lineations, cleavage and foliation planes, folds, and crenulation lineations), as well as scaled experimental modeling, has led Chardon (1997) and Chardon et al. (1998) to refine earlier Archean dome-and-basin models based on vertical tectonism (Gorman et al., 1978; Bouhallier et al., 1995; Choukroune et al., 1995, 1997; Chardon et al., 1996). Fold and microfold axes are observed throughout the Dharwar greenstone belts (Fig. 14A). The outer axes define a concentric pattern. Closer to the belt center, sinuous fold axes suggest unstable stress trajectories. Fold and microfold axes then gradually converge and plunge toward a central area (Chardon et al., 1998) that is interpreted to mark the center of maximum subsidence.

The structural data reported herein, as well as scaled experimental modeling (Dixon and Summers, 1983; Chardon, 1997) and geochemical data (Moyen et al., 1997; Jayananda et al., 2000), argue in favor of an evolution model in which impingement of a mantle plume on the base of the lithosphere was
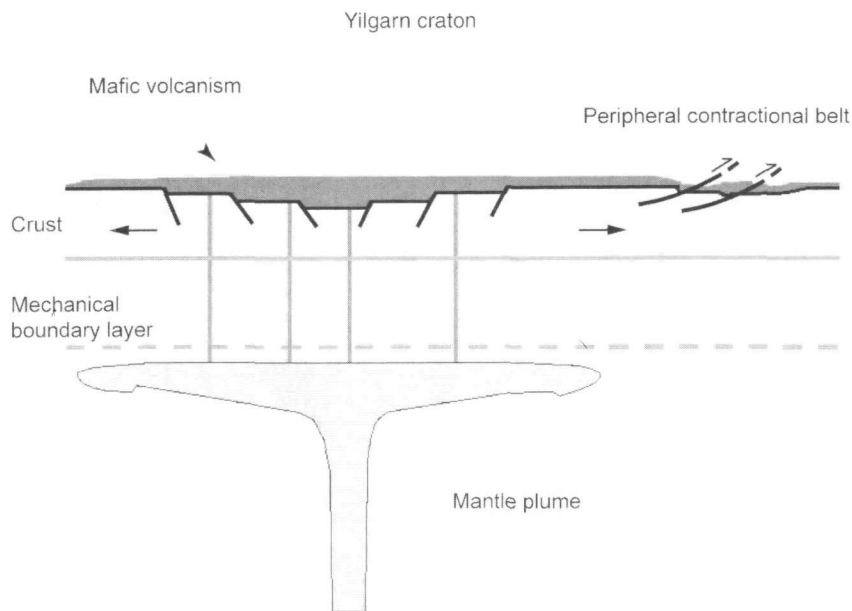
Figure 13. Mechanism of peripheral-belt formation at the possible Yilgarn hotspot by circumferential thrusting occurring at the same time as rifting, after Passchier (1995). Thrusting has been explained either by remote compression at the craton edge simultaneous with extension induced above the plume center (Passchier, 1995) or by gravitational spreading occurring at the same time as passive rifting (Mège, 1999a).

followed by eruption of dense volcanic rocks on a lighter continental gneissic crust. Rayleigh-Taylor instability would have resulted in centripetal sinking of the volcanic load into the crust (Fig. 14B), i.e., sagduction (negative diapirism). Intense shear deformation between the sinking volume and the stable crust is accommodated by inward-dipping décollements (Chardon et al., 1998).

Contractional belts associated with giant radiating-dike swarms

A line of argument based on injection patterns of radiating-dike swarms suggests that peripheral zones of compression may be commonly associated with plume-generated uplift. The 1.267 Ga Mackenzie swarm of the Canadian Shield extends over 100° of arc and reaches 2500 km from the plume center determined by the convergence of the swarm (Fig. 15).

By using a trap-door model for uplift, Baragar et al. (1996) calculated the amount of uplift required by the crustal extension due to Mackenzie dikes. Calculations were performed along two arcs, each spanning 30° at the 400 km and 900 km distances from the plume center (Fig. 15). Aggregate dike thickness (number of dikes times average thickness of 30 m) were calculated for the arcs as 3.06 km along 180 km of arc at the 400 km distance and as 1.65 km along 392 km of arc at the 900 km distance. If it is assumed that the dilatancies along the arcs at the two distances (400 km and 900 km) resulted from the same trap-door uplift, then the length of the base (center of uplift to hinge line) can be calculated. Two end-member scenarios were considered: (1) the intrusion density of the dikes measured along each arc was representative of the intrusion density around the entire circumference of the plume center and (2) only the dikes within the arc contributed to uplift. For the two

scenarios, the base-line lengths were 1529 km and 1485 km; the amounts of uplift based on the 400 km distance were 124.0 km and 69.1 km, respectively, and the amounts of uplift based on the 900 km distance were 32.5 km and 17.5 km, respectively.

An alternative calculation involved a spherical cap instead of a trap-door model (Şengör, this volume). The dilatancies based on the 900 km distance were used to calculate the areal expansion above the plume due to cumulative dike injection (approximated by total dilatancy times 900 km); this calculation was done for both scenarios (see previous description), and the numbers were used to calculate uplift by using a spherical-cap model. The estimates of (spherical cap) uplift ranged from 3.7 to 54 km [$h = (\delta A \times a)/(\pi r^2)$, where h is uplift measured at the center, δA is the change in area due to dike injection, a is Earth's radius, and r is distance to edge of spherical cap]. The true estimate of uplift will probably lie between the estimates from the trap-door and spherical-cap models. In any case, uplift values calculated by both methods for reasonable parameters are unrealistically large. Baragar et al. (1996) suggested the following explanations for unrealistic uplift estimates. If domal uplift proceeded concentrically outward from its apex in the form of a relatively steep-fronted wave, then the density of dikes could be greatly increased over that which could be achieved by simple uplift. Another proposal was that uplift was imposed on a preexisting east-west extensional stress field, and the resulting stress created a zone of concentrated extension passing through the apex of the dome and through the area measured (Baragar et al., 1996).

The unreasonable magnitude of uplift could also be eliminated by using a variation of the steep-fronted wave model in which the uplifted lithosphere was allowed to spread outward off the domal uplift during or after dike injection, but before thermal decay of the uplift. Our model is similar to that proposed
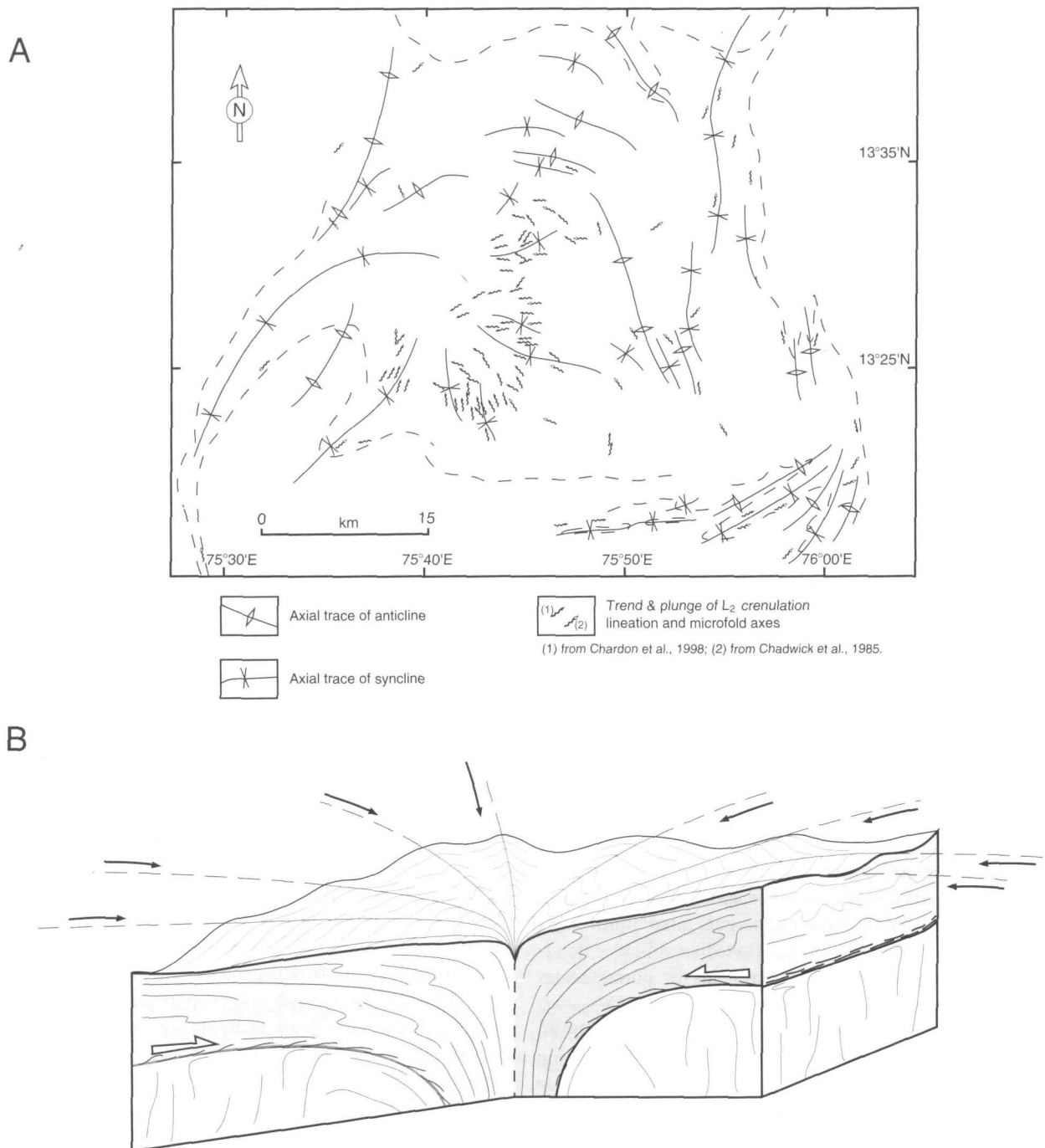
Figure 14. Structural patterns and tectonic interpretation of the Bababudan greenstone belt, one of the Dharwar craton greenstone belts, India (Chardon et al., 1998). A, Structural lineation map. B, Interpretation in terms of gravitational (Rayleigh-Taylor) instability inducing dense volcanic-load sinking into crustal basement. The ductile-to-brittle transition is located either within the volcanic load or at the surface.

for long-wavelength domal uplifts on Venus by McKenzie (1994). In McKenzie's model, domal uplift results in crustal "flow" down the flanks of the uplift and results in both rifting at the uplift center and thrusting around the uplift periphery.

An upper limit for the amount of outward spreading above the Mackenzie plume can be deduced by assuming that all dike-induced crustal extension is accommodated by outward spreading of crust from the plume center (Fig. 15). Estimates of this extension are equivalent to the values given in Baragar et al. (1996) for the radial difference between dike-intruded (uplifted)

Figure 15. Gravity spreading off topographic uplifts. A, The 1270 Ma Mackenzie dike swarm of the Canadian Shield (Baragar et al., 1996). Focal point of 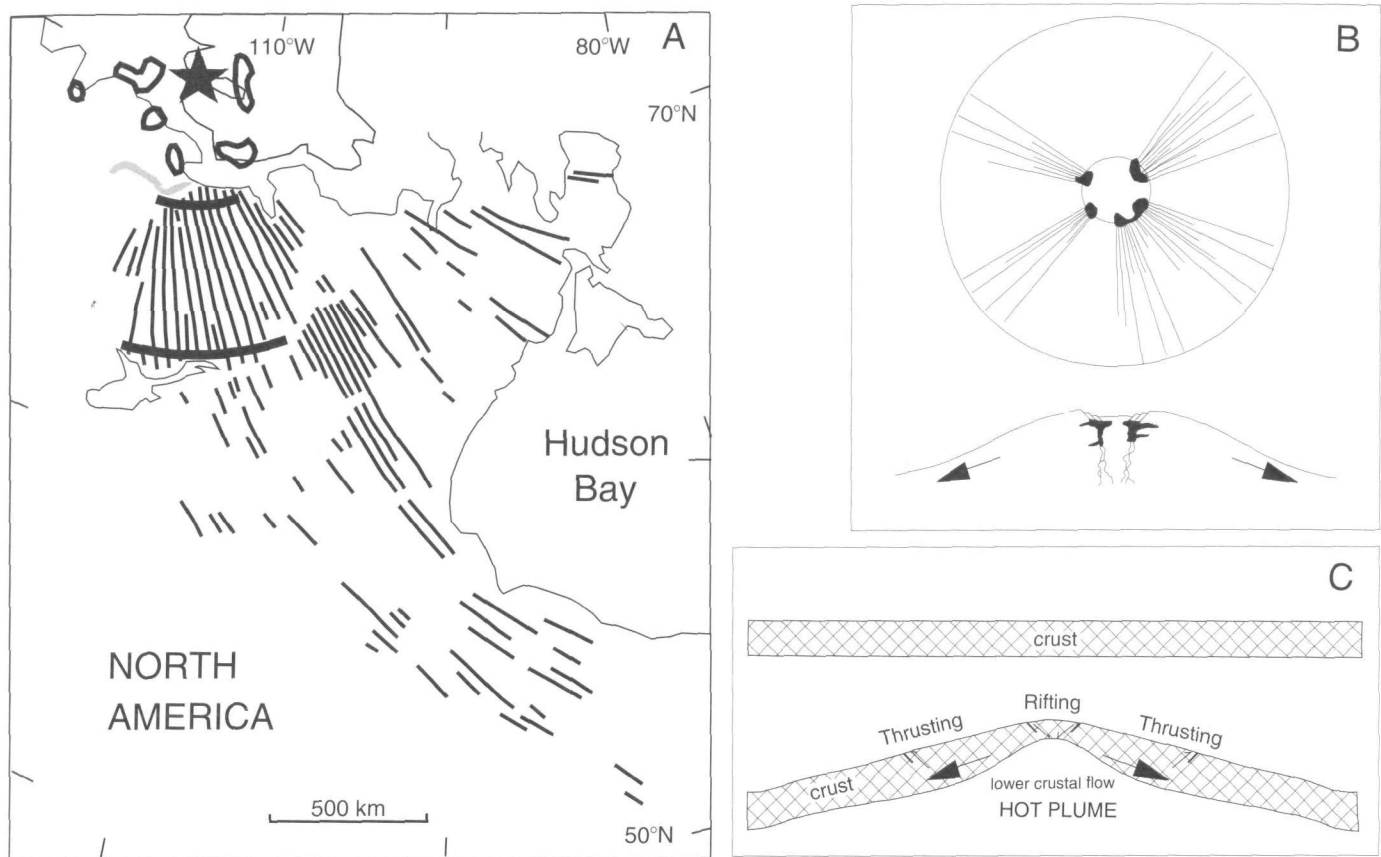swarm (star) is interpreted to locate the plume center and is surrounded by a ring of magma chambers identified by gravity anomalies (outlined areas). Additional gravity anomaly marks the Darnley Bay intrusion, which may be younger (westernmost anomaly). Gray pattern locates coeval Coppermine volcanic rocks. Traverses at 400 and 900 km from plume center (bold arcs) used to calculate crustal dilation due to dike injection. B, Model for plume-generated uplift (note vertical exaggeration), emplacement of magma chambers along periphery of apical graben, and intrusion of dike subswarms emplaced laterally from these magma chambers (Baragar et al., 1996). The magnitude of crustal dilation indicated by emplacement of the Mackenzie dike swarm (determined at 400 and 900 km distances) requires unrealistic domal uplift (see text) and, therefore, implies crustal spreading off the uplift. C, Model for crustal spreading associated with Beta Regio and other plume-generated volcanic centers on Venus showing postulated formation of central graben and peripheral thrusts (after McKenzie, 1994).

and dike-free (pre-uplifted). According to the two end-member scenarios (as previously outlined) the amount of outward spreading, therefore, ranges from 0.49 to 6.80 (calculated at the 400 km distance), and from 0.26 to 3.79 (calculated at the 900 km distance). Interpreted as measuring movement outward off the domal uplift, this process has two consequences, formation of a central apical graben and peripheral shortening.

An apical graben has been recognized in the central region above the Mackenzie plume (Fig. 15) from a ring of gravity anomalies that partially surround the focal point of the Mackenzie dike swarm. These anomalies are interpreted to locate mafic intrusions emplaced along border faults of the apical graben. The apical graben has a radius of ~200 km. Assuming that the broad apical graben is caused by the outward spreading determined on the flanks of the uplift, we can use the flank estimates (previously given) to calculate geometric parameters associated with the apical graben. On the basis of the flank

estimates of outward spreading (maximum, 6.8 km), the apical graben should have a maximum collapse volume of ~2200 km^3 ($\pi \times 6.8^2 \times 15$); this calculation assumes crustal involvement to depths of 15 km (corresponding to the approximate depth of the ductile-to-brittle transition). If assumed to be accommodated by a down-dropped block 200 km in radius, then the throw on the border faults of the apical graben should range up to ~20 m [$2200/(\pi \times 200^2)$].

Radial spreading of crust off a mantle plume must terminate. The most logical place would be as a series of thrust faults at the margin of the uplift (at ~1500 km away from the Mackenzie plume center on the basis of the hinge-model calculation of Baragar et al., 1996). The estimated amount of shortening ranges up to ~6.8 km (see previous analysis). The predicted shortening has not been observed, but would be very difficult to identify in complexly deformed rocks in this part of the Canadian Shield. Note that Şengör (this volume) and McKenzie

(1994) considered peripheral thrusting to be rare on Earth because extension should be accommodated at plate boundaries rather than in a intraplate setting. This obstacle is overcome by the mechanism of gravitational spreading discussed in a subsequent section.

Many other radiating swarms on Earth, Venus, and Mars have dike spacings and thicknesses similar to those of the Mackenzie swarm; therefore, we would expect that the same analysis would apply. Crustal spreading off the domal uplift with associated formation of an apical graben and a contractional peripheral belt could therefore be common occurrences above plumes associated with giant radiating-dike swarms.

ORIGIN OF COMPRESSION

Classification of deformation styles

The examples presented herein emphasize that at least three separate styles of contractional deformation exist in association with mantle plumes: concentric wrinkle ridges, contractional peripheral belts, and dome-and-basin structures. Each is discussed in turn.

Wrinkle ridges are observed at Syria Planum on Mars, around some volcanic rises on Venus, and on the Columbia Plateau on Earth. Structural similarities between wrinkle ridges on Mars and the Yakima fold-and-thrust belt of the Columbia Plateau, some of which were first pointed out by Plescia and Golombek (1986) and Watters (1988, 1992), include (1) formation in stratified basaltic-type lava floods, consistent with inferences from mechanical modeling that layering plays a key role in the mechanics of ridge development (Schultz, 2000); (2) ridge length on the order of 100 km (Yakima ridges: 97 km, Mège and Reidel, 2000; Coprates ridged plain on Mars: 101 km, Mège, 1999b); (3) periodic spacing, 20–30 km (Watters, 1991; Schultz and Watters, 1995); (4) association with conjugate strike-slip faults coeval with ridge development; and (5) concentric distribution about major volcanic centers in the absence of other stress sources (ridges trend perpendicular to the maximum-compressive-stress trajectory). Many Venusian wrinkle ridges share these characteristics as well (Bilotti and Suppe, 1999).

Formation of a contractional peripheral belt is another kind of compressional tectonic style above mantle plumes. The south Syria Planum ridge belt on Mars is the prototype example. Possible analogues may be observed associated with the North Atlantic volcanic province and coronae on Venus and are implied by the analysis of the dilatancy due to emplacement of the Mackenzie dike swarm. From seismic data at the North Atlantic volcanic province and numerical modeling of coronae and the south Syria Planum belt ridges, compressive stress appears to be accommodated by folding, thrusting, or a combination of these mechanisms. The Yilgarn craton is a possible additional example. However, field outcrops in this latter case are too sparse to discriminate between the peripheral-contractional-belt

deformation style and the dome-and-basin deformational style.

Contractional tectonics at Venusian crustal plateaus and dome-and-basin folding at the Dharwar craton are examples of pervasive contractional deformation above a mantle plume. Fold orientation may be radial, concentric, or oblique about the supposed plume center, depending on its proximity. Anastomosing fold axes and sinuous geometry of many long fold axes denote unstable stress trajectories at a local scale.

Mechanisms of wrinkle-ridge formation

Although we discuss wrinkle ridges observed around major magmatic centers that are linked with mantle plumes or diapirs, it must be noted that wrinkle ridges are also observed in other (nonplume) settings on Mars and Venus, as well as on Mercury and the Moon. Those ridges are usually associated with basaltic infilling of impact basins. Mascon (mass concentration) tectonics (Melosh, 1978) elegantly explains wrinkle-ridge formation on the Moon in such settings and might explain the formation of some wrinkle ridges observed in impact craters and impact basins on Mars and Venus (Watters, 1993).

Stress sources for wrinkle-ridge formation around major magmatic centers include (1) global planetary cooling, (2) plate-boundary processes, (3) surface loading by the lava pile and associated gravitational spreading, (4) thermal subsidence following initial plume-related topographic uplift, and (5) subsidence due to surface loading by flood basalts and deep-crustal loading by dense underplated magmas. We explore each of these stress sources and show that the first three mechanisms are likely less important than the two others.

Planetary cooling. It has been proposed that global planetary cooling is the main origin for buckling of wrinkle-ridged units on Mars (Schubert et al., 1992; Mangold et al., 1999). However, global planetary cooling cannot by itself explain preferential wrinkle-ridge orientation in the Tharsis hemisphere of Mars, at volcanic rises on Venus, nor at the Yakima folds on Earth. Moreover, wrinkle-ridge formation simultaneous with widespread extension on Mars, is hard to reconcile with the net decrease in planetary radius that is predicted from planetary cooling.

Plate-boundary processes on Earth: Effect of subduction. Several works have emphasized the role of subduction-related stress on Yakima ridge formation (e.g., Reidel et al., 1989a; Burchfiel et al., 1992; Saltus, 1993). Although we agree that subduction may have played a role, several reasons lead us to refute subduction as the primary source of stress:

1. The observed correlation between the rate of ridge growth and the rate of basalt outpouring implies that ridge growth occurred through successive stages lasting years or tens of years (Self et al., 1997), a time scale that cannot be correlated with variations in subduction rate.

2. There is no continuity between the stress state at the Yakima fold-and-thrust belt and the Cascade Ranges. The stress state at the Cascades is currently compressional, strike slip, or

extensional (Zoback et al., 1990), while it is uniformly compressional at the Columbia Plateau. GPS (Global Positioning System) measurements and thermal modeling at the Cascadia subduction zone suggest that upper-lithosphere and subducting-slab coupling decreases across the continental margin from strong in the west (stick-slip), to transitional, to weak (free sliding) in the east (Savage et al., 1991; Dragert et al., 1994; Dragert and Hyndman, 1995). Thus, we suggest that the complex state of stress at the Coastal Ranges may result from the subducting slab and its variation in geometry (Crosson and Owens, 1987), while another stress source prevails at the Columbia Plateau.

3. The stress state at the Columbia Plateau is atypical of subduction-related stress on land in most settings, as previously pointed out by Catchings and Mooney (1988). More details regarding the subduction issue are given in Appendix 1.

Plate-boundary processes on Earth: Effect of intraplate extension. Influence of Basin and Range extension since Miocene time over a large part of the Columbia Plateau is demonstrated by significant extension associated with strike-slip faulting and dike emplacement consistent with the Basin and Range extension direction. However, none of these features is observed on the western part of the Columbia Plateau. Hooper and Conrey (1989) emphasized that the same orientation of principal stresses over the whole Columbia Plateau can explain the orientation of grabens, strike-skip faults, and ridges. They attributed ridge growth after Columbia River basalt outpouring to the continuation of earlier strain patterns. However, the east-west extension at that time deduced from graben orientation suggests that should earlier east-trending structures have been initiated before eruption of the Columbia River Basalt Group and continued deforming during Basin and Range extension, they would have moved in a strike-slip sense, with a minor component of shortening, rather than by accommodating pure shortening, as observed (see Reidel et al., 1984, for a further discussion on the role of strike-slip faulting at the Yakima ridges).

The hypothesis that Basin and Range extension in eastern Washington and Oregon and western Idaho is driven by gravitational sliding of the topography and that Yakima ridge formation is a consequence of subsequent Coastal Range motion (E.D. Humphreys, cited by Kerr, 1997; see first section) faces the same problems as interpreting the mechanism of ridge formation as due to subduction-related stress. In particular, the current ≤20° slab dip angle for the Juan de Fuca plate beneath the North American coast (Crosson and Owens, 1987; Hyndman et al., 1990; Hyndman and Wang, 1995) would probably impede the Coastal Ranges from sliding. Publication of a more extensive description of this model is needed before it can be assessed.

Plate-tectonics processes on Venus and Mars. Although plate-tectonics activity has been hypothesized on Venus, e.g., for explaining formation of coronae (Sandwell and Schubert, 1992), most current models of Venus evolution are in general inconsistent with such mechanisms. For example, widespread wrinkle-ridge formation (Bilotti and Suppe, 1999) is inconsistent with the plate-tectonics requirement that strain focuses at plate boundaries. Tectonic activity on Venus is thought to mainly result from vertical movements associated with mantle upwelling and/or downwelling (Bindschadler et al., 1992a; Gilmore et al., 1997; Phillips and Hansen, 1998; Ghent and Hansen, 1999; Rosenblatt et al., 1998), although the existence of rifts is evidence of limited lateral crustal movements.

Interpretation of possible shorelines in the martian lowlands (Parker et al., 1993) has focused interest on plate-tectonics hypotheses on Mars, resulting in a plate-tectonics scenario by Sleep (1994). Recent detection of magnetic anomalies in the southern highlands (Acuña et al., 1999), some of which form linear patterns, has also been used as evidence of plate tectonics (Connerney et al., 1999). Many geologic observations, however, are not consistent with these hypotheses (e.g., Pruis and Tanaka, 1995, and references therein; Smrekar and Raymond, 1999). Most recent interpretations of the martian magnetic anomalies suggest alternative hypotheses of origin such as magma accretion in a tensional tectonic regime (Grimm, 2000), early vigorous first-order convection in the martian mantle before dynamo shut-off (Kletetschka et al., 2000), gravity destabilization of mafic materials accreted to the crust (Mège et al., 2000), magnetic eolian deposits (Ruzicka, 2000), polar wandering (Sprenke and Baker, 2000); and dike emplacement (Wilson and Head, 2000; Nimmo, 2000). Although the existence of standing bodies of water is supported by a number of observational elements (e.g., Scott and Tanaka, 1986; Head et al., 1998, 2000), strong observational arguments against such existence have also been put forward (Malin and Edgett, 1999), and correlation with oceanic processes in the terrestrial sense has not been reported. Plate-boundary processes are thus unlikely to have influenced wrinkle-ridge formation on Venus and Mars.

Gravitational spreading. Gravitational spreading is discussed in more detail in the section on contractional peripheral belts. The problem with applying gravitational spreading to the formation of wrinkle ridges is that many examples exist where ridges having nonrandom orientation are not associated with significant topographic slopes. Examples include the most distal wrinkle ridges associated with the Tharsis volcanic area on Mars, wrinkle ridges in horizontal lava plains on Venus (such as Lavinia Planitia), wrinkle ridges in mascons on the Moon and other planetary bodies, and wrinkle ridges in the Caloris basin of Mercury. The role of compressive gravitational-spreading stress in wrinkle-ridge formation appears, therefore, not to be decisive.

Subsidence in relation to a mantle plume. Noting that the Yakima ridges formed exclusively on the most subsiding part of the Columbia Plateau (Tolan et al., 1989; Reidel et al., 1989a, 1989b) and that the rate of ridge growth very clearly correlates with the rate of plateau subsidence (Reidel et al., 1989a), it is likely that a genetic link exists between subsidence and ridge

formation. Subsidence at the Columbia Plateau and Cascade Range started contemporaneously with an Eocene rifting event, i.e., before eruption of the Columbia River Basalt Group (e.g., Reidel et al., 1994). Subsidence waned during the Oligocene. At the Columbia Plateau, subsidence resumed when the basalt flows erupted, while it continued waning in the Cascades during the Miocene, suggesting that subsidence of the Columbia Plateau mainly resumed in response to another mechanism separate from that affecting the Cascades. Other difficulties encountered by subduction-induced subsidence were already discussed in the section on plate-boundary processes. Consequently, we suggest that subsidence after basalt eruption was primarily induced by the Yellowstone hotspot, with a possible, secondary influence of subduction. Figure 16 suggests how subduction-related stress could provide part of the deviatoric stress required for the formation of the ridges, whereas the dominant control on ridge orientation is due to the Yellowstone hotspot-related stresses.

Subsidence can be found in virtually all plume-tectonics models published to date as a feature of hotspot evolution occurring after early thermal uplift. Rosenblatt et al. (1998) suggested that subsidence is one of the driving mechanisms for wrinkle-ridge formation on Venus. On Mars, ridged-plain compensation at shallow depth (Frey et al., 1996) is evidence of ridged-plain subsidence. Subsidence of horizontal topography is expected to produce a topographic depression. An example of such a depression may be the Coprates Planum ridged plain, the center of which is depressed by some 2 km compared to the surrounding regions (Fig. 1A). Subsidence would be expected to have modified any slope associated with initial uplift, but would not be expected to induce inversion of slope orientation

(e.g., Olson, 1994). For this reason, subsidence may not be easily recognized in the topographic data or by geomorphologic analysis.

Wrinkle-ridge formation by subsidence tends to favor a thin-skinned mechanism of deformation, as the lower part of the downwarping brittle crust should be in an extensional regime below a mid-depth neutral plane. Seismic data at the Yakima fold-and-thrust belt is in agreement with this inference. As discussed subsequently, subsidence may result both from waning of the thermal anomaly after the initial, plume-related, topographic uplift and from surface loading by flood basalts.

Thermal subsidence. After thermal topographic uplift, hotspot topography depends on the balance between magma production and thermal cooling. The thermal anomaly of the hot blob is on the order of 100–350 °C in typical terrestrial plumes and produces initial topographic uplift as the blob ahead of the plume conduit approaches the lithosphere. Thermal cooling occurs almost as soon as the blob has begun spreading out and tends to lower the topography created earlier above the plume. The maximum subsidence expected from this mechanism alone is expected to be above the center of the plume. However, as most of the magma is generated above the plume conduit, the elevation of the uplifted hotspot center tends to remain much the same following the plume impact, while the surrounding uplifted areas tend to subside (Olson, 1994). Although the area above the plume center becomes isostatically supported, the dynamic support is subtracted from the surrounding areas. Olson's (1994) numerical models of a stationary plume 350 °C hotter than the surrounding mantle suggest that in terrestrial conditions, the surface elevation of the area surrounding the plume conduit may increase for some 15 m.y. after plume ini-

Figure 16. Hypothetical mechanism of Yakima fold-and-thrust belt formation by superimposition of Yellowstone-related radial compressive stress on subduction-related compressive stress, based on analogy with Martian and Venusian wrinkle ridges in hotspot settings, the geometry of which is thought to reflect radial compression about mantle plumes. Coupling between subducting and overlying plates (light gray) would produce roughly east-west σ_1 trajectory, north-south σ_2, and vertical σ_3. The high topography of the early Yellowstone hotspot, south of the Columbia Plateau, would increase the roughly north-south–oriented hotspot-related radial stress. The north-south principal-stress trajectory would eventually increase to σ_1 and switch with the east-west principal-stress trajectory (intermediate gray), so that the total stress field (dark gray) would favor the formation of roughly east-trending contractional structures.
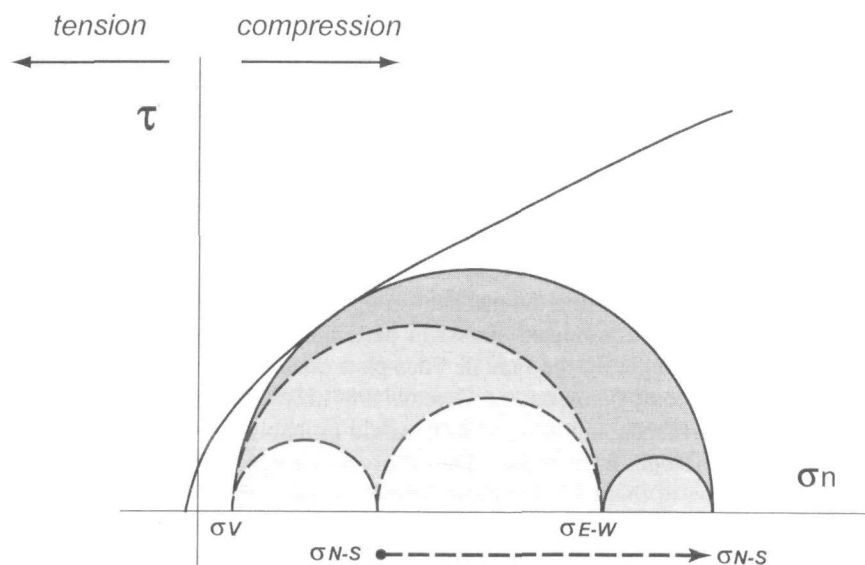
tiation in the mantle and then decrease until the plume activity ceases. After 15 m.y., continued subsidence occurs in proximity to the plume center, while minor uplift is still ongoing farther away from the plume center. Then, subsidence gradually propagates laterally outward, and after a few tens of millions of years, most of the uplift has waned, except above the plume center.

This pattern of dynamic uplift, central magmatic underplating, and subsidence in surrounding areas is in agreement with geologic observations at the Thulean plume during the Paleocene and Eocene (Nadin et al., 1995). At the Yakima folds it explains field relationships demonstrating that some ridges were initiated before flood-lava eruption (Hooper and Conrey, 1989; Reidel et al., 1989a). It is may also be a good approximation of wrinkle-ridge formation at Syria Planum on Mars and at volcanic rises on Venus. Olson's (1994) calculations were carried out for Earth, and so the time scale and uplift amplitude may not be applicable to extraterrestrial cases, but the succession and geographic zoning of events are expected to have been similar.

Subsidence in response to volcanic loading. Mascon subsidence, which is a mechanism for ridge formation on a horizontal surface, predicts that some flood-lava areas undergo compression while other areas undergo strike-slip faulting or enter a tensional regime (Melosh, 1978). Slightly different is the case of the wrinkle-ridged areas that were previously thermally uplifted, because in that case subsidence back to horizontal may result in a net decrease in topographic elevation. Both strike-slip faulting and contractional features are expected, in agreement with observations at, e.g., Coprates Planum on Mars and the Yakima fold-and-thrust belt.

Figure 17 shows the required size of the lava-flood province in order to induce Coprates ridged plain (Fig. 17, A and B) and Yakima fold-and-thrust belt (Fig. 17, C and D) subsidence according to elastic theory. Subsidence due to lava loading occurs if the loaded area, of wavelength λ, is greater than (Turcotte and Schubert, 1982)

$$\lambda_{min} = 2\pi \ (D/\rho_c g)^{1/4} \qquad (1)$$

where D is the plate flexural rigidity, ρ_c is crust density, and g is acceleration due to gravity. Flexural rigidity decreases with the third power of the decrease in plate elastic thickness h and also depends on its Young's modulus E and Poisson's ratio v:

$$D = Eh^3/12(1 - v^2). \qquad (2)$$

No plate deflection occurs if $\lambda < \lambda_{min}$, whereas isostatic compensation is achieved if $\lambda \gg \lambda_{min}$. Current elastic lithosphere thickness at the Coprates ridged plain has been estimated from gravity and topography to be on the order of 35 km (Zuber et al., 2000). Although this value is not directly related to elastic thickness during wrinkle-ridge formation, it gives an idea of its maximum value. The heat flow during the Syria Planum flood-

basalt event is likely to have been higher, resulting in thinner elastic lithosphere. Figure 17A clearly shows that subsidence of the Coprates ridged plain is expected for a broad range of elastic thickness.
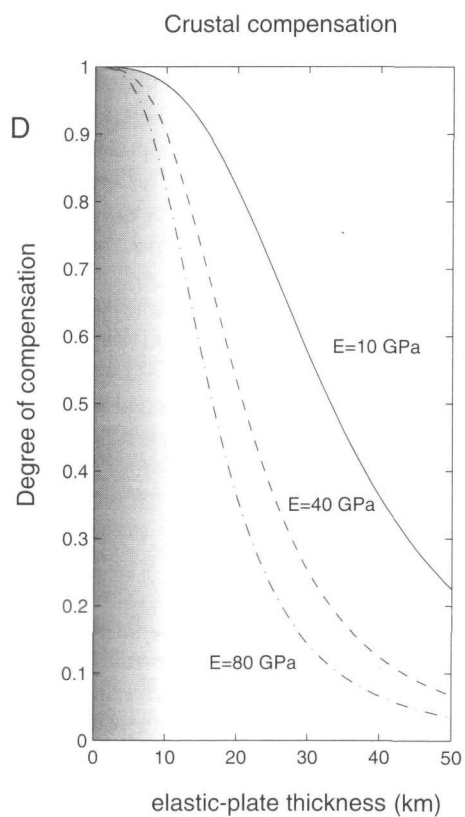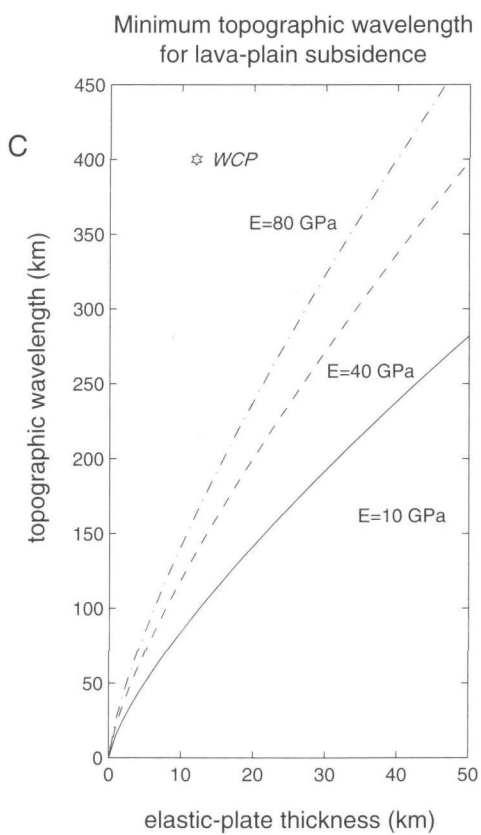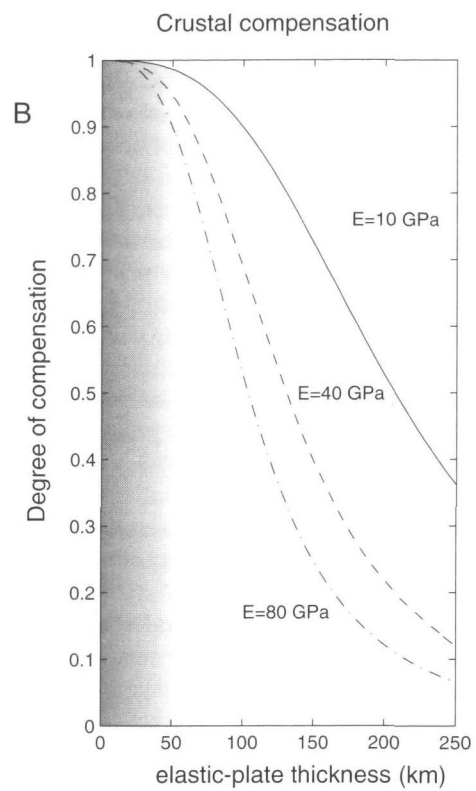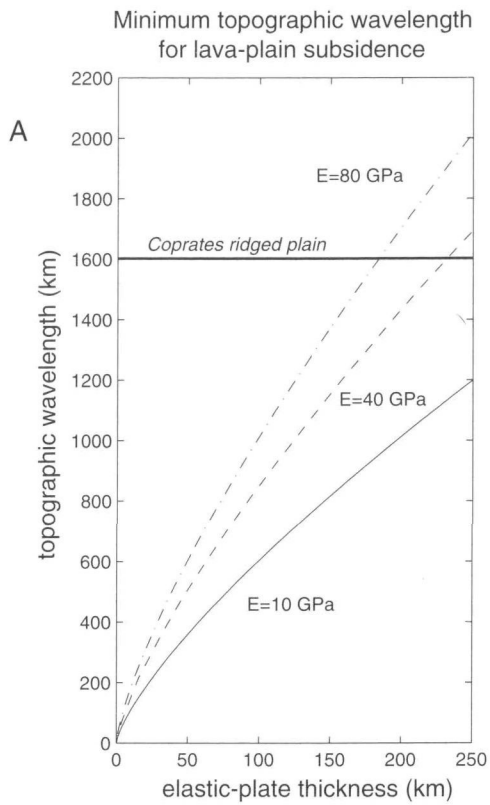
The degree of topography compensation C is given by (Turcotte and Schubert, 1982)

$$C = (\rho_m - \rho_c)/[\rho_m - \rho_c + (D/g)(2\pi/\lambda)^4], \qquad (3)$$

where ρ_m is mantle density. Clearly, C is very close to 1 for the Coprates ridged plain for crustal thicknesses on the order of tens of kilometers, which means that loading subsidence is isostatic (Fig. 17B), as previously suggested by Frey et al. (1996). We conclude that lava loading must have induced immediate isostatic compensation and subsidence.

Figure 17, C and D, shows that lava loading by the Columbia River Basalt Group can explain most (all?) of the isostatic state of the Columbia Plateau for a similar range of brittle-crust thickness, in agreement with the existing correlation between eruption rate, subsidence rate, and ridge growth. Only a very limited contribution of subsidence due to an additional mechanism, for instance in relation to other geodynamic events in the Pacific Northwest region, is necessary for explaining the full isostatic state of the western Columbia Plateau.

Subsidence in response to deep-crustal loading. Density anomalies within or just beneath the lithosphere (Fleitout and Froidevaux, 1982) are considered by Zoback (1992) as second-order stress sources on Earth. Magmatic underplating at aborted rifts associated with mantle plumes provides major density anomalies that may reorient stress patterns and control seismic slip (Assumpção, 1992; VanDecar et al., 1995; Zoback and Richardson, 1996). Numerical elastic modeling of stress-pattern modification at volcanic rifts due to underplated magmas by Zoback and Richardson (1996) for various lithospheric rheologies shows that underplating drastically increases horizontal compressive stress at shallower depths both above the underplated area and in the areas of the crust adjacent to it. Depending on the rheology of the lithosphere chosen, the state of stress in the shallow-crustal areas at a greater distance from the underplated region may still be in compression or may actually be in minor tension when the edges of the numerical model are stress free. Surface compression due to dense crustal loading at mantle plumes is expected to enhance compression because of thermal subsidence subsequent to plume arrival, as well as subsidence induced by surface loading by flood basalt. Results of seismic studies show that a 4–17-km-thick, high-density material (seismic velocity of 7.5 km·s^{-1}), probably due to magmatic underplating, exists beneath the western Columbia Plateau between the lower crust and upper mantle (Catchings and Mooney, 1988). Seismic velocities beneath the Columbia Plateau (Catchings and Mooney, 1988) suggest that no eruptive activity was associated with Eocene rifting beneath the Yakima fold-and-thrust belt. Therefore, we interpret the underplated magmatic material to be likely the deep counterpart of the Co-

Minimum topographic wavelength
for lava-plain subsidence

A

Crustal compensation

B

Minimum topographic wavelength
for lava-plain subsidence

C

Crustal compensation

D

lumbia River Basalt Group. Eocene crustal thinning, which probably did not have time to re-equilibrate before Columbia River Basalt Group eruption (White and McKenzie, 1995), may have played a key role in trapping magma at depth (i.e., through the effects of a *thinspot* as defined by Thompson and Gibson, 1991) and forming a dense pillow that would have generated compressive stress in the Columbia River basalts. Surface contraction would be expected right above the Eocene rift and also in adjacent areas, i.e., exactly where the Yakima fold-and-thrust belt is located. Despite the lack of data on crustal structure at extraterrestrial mantle plumes, it is possible that the same mechanism was also involved in wrinkle-ridge formation on other planets.

Mechanism of contractional peripheral-belt formation

Despite differing settings, a common characteristic of circumferential ridge belts is that they have been explained by gravitational spreading of mantle-plume swells (Mège and Masson, 1996; Bourgeois, 2000; McGovern and Solomon, 1998; Smrekar and Stofan, 1997). Gravitational spreading is observed on a smaller scale on many volcanic edifices (Borgia, 1994; Van Wyk de Vries et al., 2000) and results in circumferential contractional structures that have been modeled as fault-propagation anticlines verging away from the volcanoes. It is interesting that the scale of these structures is highly variable (Borgia et al., 1990). Fold depths range from hundreds of meters (e.g., the central Costa Rica volcanic range), to kilometers (as at Etna and Kilauea), to involving the whole brittle-crust thickness (as at Olympus Mons on Mars). The latter two ex-

amples represent the transition in scale between a volcano and a mantle plume. Another study investigating the case for plume-scale contractional structures resulting from gravitational spreading is also underway (Borgia et al., 2000).

Gravitational spreading is well documented for the south Syria Planum ridge belt on Mars and for coronae on Venus. The case for the North Atlantic volcanic province anticlines and Yilgarn thrusts on Earth need additional discussion. In the North Atlantic volcanic province, gravitational stress resulted from topographic uplift subsequent to partial melting associated with the combination of mantle decompression during North Atlantic opening and emplacement of the Thulean hotspot thermal anomaly. White (1992) suggested that initial vertical uplift at the Thulean plume, 100–300 °C hotter than normal mantle (lower bound by White et al., 1997; upper bound by Bijwaard and Spakman, 1999), may have been as high as 2 km, with a swell diameter as large as 2000–2200 km, creating a considerable gravitational potential whose structural effect would have been formation of anticlines at the edge of the uplift.

Although the timing of arrival of the Thulean plume remains controversial, it does not affect the hypothesis of anticlinal formation in response to gravitational relaxation of Thulean plume topography. If plume arrival was in the Tertiary, the gravitational potential was the result of both the high thermal anomaly in the hot blob (*plume head* observed in experimental models, e.g., Richards et al., 1989) and decompression melting during North Atlantic rifting (White and McKenzie, 1989). Alternatively, if the plume is 100–130 m.y. old, as suggested by Lawver and Müller (1994), plume impingement on the lithosphere would have produced a first swell in northern Canada. Subsequent Paleocene rifting would have produced a second swell centered at the eastern Greenland margin that helped generate the Tertiary flood basalts and provided the gravitational potential that allowed the formation of the anticlinal belt.

At the Yilgarn craton, the peripheral thrusts have been suggested to form as a consequence of the regional stress field (Passchier, 1995). Gravitational spreading is an alternative that is consistent with early thrusting during the plume history and with contemporaneous circumferential compression and polydirectional extension in the uplifted area. However, field outcrops at the Yilgarn craton are too discontinuous to permit definitive conclusions. Field observations are also consistent with interpretation of contractional structures as a consequence of negative Rayleigh-Taylor instability (discussed later).

The dynamic topographic relief that initially creates gravitational stress at hotspots builds up before lava-flood outpouring (Olson, 1994; Menzies et al., 1997). The results of analogue experiments show that contractional peripheral-belt formation peaks as soon as topographic uplift occurs. Therefore, peripheral belts are expected to form even before wrinkle ridges form, in agreement with observations at Syria Planum, where stratigraphic relationships show that most of the ridge belt is probably Noachian in age and thus is older than the early Hesperian wrinkle-ridged plains (Schultz and Tanaka, 1994) which de-

---

Figure 17. Subsidence on (A and B) Coprates ridged plain and (C and D) western Columbia Plateau in response to loading as a function of elastic-plate thickness and Young's modulus. For this analysis, Poisson's ratio = 0.25, crustal density = 2800 kg·m^{-3}, and mantle density = 3300 kg·m^{-3}. The dependence of the results on density and Poisson's ratio is very small. A, Minimum topographic wavelength for subsidence, Coprates ridged plain. The thick line indicates the Coprates wavelength and shows that subsidence is expected for a wide range of crustal thicknesses. The area of the Coprates ridged plain is 1400 km × 800 km; the periodic load = 800 km (corresponding to half the wavelength λ in equation 1; the other half-wavelength is assumed to be the permanently uplifted region). B, Degree of compensation, Coprates ridged plain. Full compensation can be attained at shallow depth (shaded), in agreement with gravity-data analysis by Frey et al. (1996). C, Minimum topographic wavelength for subsidence on the western Columbia Plateau (WCP). Topographic wavelength is 400 km, i.e., twice the Columbia Plateau diameter, and elastic plate thickness is assumed to correspond to the brittle crust thickness, which is taken to be 12 km before lava flooding. For such values, the Columbia Plateau is predicted to subside whatever the elastic plate strength. D, Degree of crustal compensation, western Columbia Plateau. The shaded area indicates the elastic plate thickness domain where full or very high compensation is obtained whatever the chosen plate strength.

A Experimental modeling

B Bababudan greenstone belt, Dharwar craton

Maximum
subsidence

1

2

3

15 km

C Eastern Ovda Regio, Venus

50 km

PRE-SAGDUCTION STRUCTURES (VENUS)

Ribbon fractures

SAGDUCTION STRUCTURES

Sagduction center
(on Venus: outside the mapped area)

Contraction
- syncline axis
- anticline axis

Extension
syncontraction
a: fracture
b: ductile shear with normal sense
c: oblique slip (Dharwar)

Extension
postcontraction
crestal fracture (a) or normal fault (b)

DHARWAR: REGIONAL-SCALE STRUCTURES

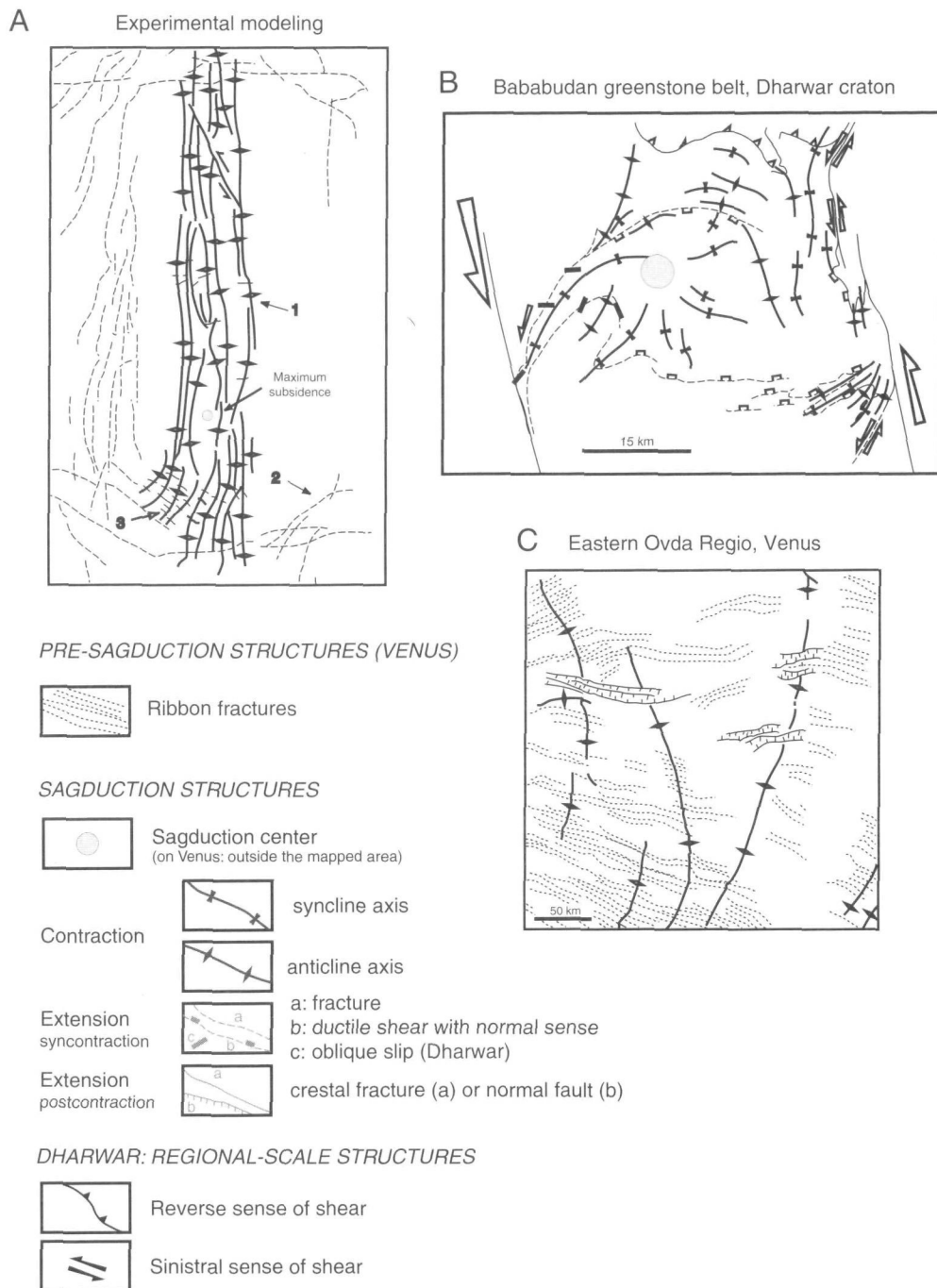Reverse sense of shear

Sinistral sense of shear

Figure 18. Structural interpretation of experimental model of topographic subsidence due to negative Rayleigh-Taylor instability (Dixon and Summers, 1983). This model is interpreted as an analogue of subsidence due to basaltic overplating on a crust of lower density and is compared to structural patterns at the Bababudan greenstone belt, Dharwar craton, and the eastern Ovda Regio, Venus. A, Late evolutionary stage of experimental model of dense upper crust sinking into less dense lower crust (interpreted from Dixon and Summers, 1983). The dense material has been intentionally thickened along a line in order to produce line subsidence. Small circle locates the area where maximum subsidence has been obtained. Solid lines—folds, dashed lines—extensional structures. Strain during sagduction is accommodated by (1) folding parallel to the central subsidence line and radial folding and perpendicular fracturing relative to the area of maximum subsidence, (2) fracturing parallel to the central subsidence line, and (3) fracturing at fold hinges perpendicular to fold axis. B, Internal strain pattern at the Bababudan greenstone belt, after Chardon et al. (1998). C, Interpretation of *Magellan* synthetic aperture radar image of part of eastern Ovda Regio (location in Fig. 6A), modified after Ghent and Hansen (1999).

veloped during later subsidence (see earlier wrinkle-ridge discussion). Initiation of the Faeroe-Rockall Plateau anticlines during the Paleocene is also evidence that they are early features in the hotspot history. The results of the study of the Mackenzie dike swarm discussed previously suggest that the magnitude of peripheral-belt shortening could be as much as 7 km.

Dome-and-basin folding

Similarities between the structural patterns of the Dharwar greenstone belts and Venusian crustal plateaus argue in favor of a common mechanism of origin, which in both cases has been suggested to be crustal-scale Rayleigh-Taylor instability associated with a mantle plume (Bouhallier et al., 1995; Choukroune et al., 1995, 1997; Chardon et al., 1998; Ghent and Hansen, 1999; Hansen et al., 1999). Outcrop conditions at the Yilgarn craton shown to be consistent with peripheral-belt formation are also consistent with this interpretation. Rayleigh-Taylor instability was first demonstrated to explain some greenstone-belt structural patterns by Gorman et al. (1978) and has since been supported for some belts by geochemical data and detailed structural observations arguing in favor of a plume origin (Reymer and Schubert, 1986; Storey et al., 1991; Davies, 1993; Bouhallier et al., 1995; Choukroune et al., 1995, 1997; Abbott, 1996; Kent et al., 1996; Saunders et al., 1996; Arndt et al., 1997; Barley et al., 1997, 1998; Chardon et al., 1998; Jayananda et al., 2000). Although the role of mantle plumes in greenstone-belt formation since at least the mid-Archean is receiving increasing attention, Dixon and Summers (1983) and Hamilton (1998) emphasized that probably not all the greenstone belts can be explained by a single mechanism. Other mechanisms akin to plate tectonics probably played a role in some cases (e.g., Chardon, 1997; de Witt, 1998; Barley et al., 1998; Chadwick et al., 2000).

Scaled experimental models of Rayleigh-Taylor instability by Dixon and Summers (1983) allow evaluation of the crustal-scale structural style and sequence at the surface during the sinking of a dense load. Figure 18A shows the main results of the experiment reported by Dixon and Summers (1983). The first tectonic structures formed are folds at the center of the box. Their geometry is variable and depends on mechanical heterogeneities in the crust. For instance, previous volcanic fissures would provide linear heterogeneities that would guide the folds' orientation and determine the locus and geometry of the area of maximum strain and subsidence. The locus of the area of maximum subsidence is also dependent on load shape and on the horizontal size of the load compared to the size of the anomalously heated crust (Chardon, 1997). Central folding is followed by outer folding radially about the area of maximum subsidence and development of concentric extensional fractures. Hinge-perpendicular grabens then form at the crest of the outer folds.

Fold and fracture patterns in these experiments are fully consistent with observations at the Dharwar greenstone belts

where detailed structural mapping has been carried out (Fig. 18B). The tectonic style and the sequence of structural development also resemble those observed at Venusian crustal plateaus (Fig. 18C). Fold patterns and crestal grabens are correctly predicted by the experimental models. The main difference is the absence of ribbons in the models. The reason is that the Dixon and Summers' (1983) models are isothermal whereas ribbons at crustal plateaus are interpreted to result from plume-driven uplift. Ribbons are thus not expected to form in isothermal models. In addition to the folds and grabens already reported herein, the models by Dixon and Summers (1983) predict formation of extensional fractures near the experiment-box boundaries at the same time as folding. We interpret those fractures as mechanically equivalent to the shear zones observed at the edge of some greenstone belts (Fig. 14). Shear zones accommodate the movement between the subsiding load and the stable basement if basement-load decoupling is strong, whereas the fractures observed at the surface of the models accommodate the same movement if basement-load coupling is stronger.

DISCUSSION

Examples of plumes that appear not to have induced compression are frequent, and we suggest that these examples are in part due to rheologic requirements. In this section, we investigate the rheologic requirements for the formation of wrinkle ridges, a contractional peripheral belt, and domes and basins; from these requirements we propose a model relating these structures to crustal rheology and geothermal gradient. Then we propose guidelines to retrieve evidence of past mantle plumes from the observation of contractional structures.

Crustal rheology for wrinkle-ridge formation by subsidence

Crustal thickness. For a load of given dimensions, the capability of subsiding is mainly a function of crustal thickness (equation 2), which therefore provides one of the strongest constraints for wrinkle-ridge formation. Previous crustal heating by a mantle plume increases the ductile-crust thickness at the expense of the brittle-crust thickness and thus strongly favors subsidence during subsequent flood-basalt loading. Formation of Yakima ridges on only a part of the Columbia Plateau illustrates how crustal thickness affects wrinkle-ridge development during subsidence. The Columbia River Basalt Group erupted on a mosaic of three terranes (Reidel et al., 1994; Hooper, 1997) that accommodated subsidence in different ways. The most subsiding part of the Columbia Plateau, which contains all the ridges, corresponds to what we call here the western terrane. Three factors favored ridge formation on that terrane: (1) it is oceanic, hence the crust is intrinsically thin; (2) it was additionally thinned (and kept thin) during the earlier Eocene rifting event; and (3) existence of sedimentary layers between the crystalline basement and the lava flows of the western terrane decreased

effective brittle-crust thickness (Pollard and Johnson, 1973) and decoupled the Columbia River Basalt Group from the crystalline basement, allowing accommodation of different tectonic styles in both units. By comparison, the northeastern terrane (1) has a thick—thus rigid—cratonic basement, which may explain why subsidence was only accommodated by limited tilting to the west; (2) does not contain any soft layer between the basement and the Columbia River Basalt Group, so that both units may have been mechanically coupled and formed a rigid plate unable to deform in a thin-skinned style; and (3) was partly in a limited extensional regime during the period of Yakima fold-and-thrust belt development owing to Basin and Range extension. At the third terrane, the Blue Mountains terrane, a few gentle east-trending folds are observed but accommodate very small strain (Reidel et al., 1989a). Similar to the western terrane, the Blue Mountains terrane has an oceanic crust, and we suggest that it would perhaps have been suitable for ridge formation if it had not been so close to the area affected by Basin and Range tectonics, which has mainly induced extension since 15 Ma.

The crustal thickness constraint may also explain why no wrinkle ridges are associated with the Tharsis volcanic activity subsequent to Syria Planum events, such as the volcanic activity centered at Tharsis Montes. Although absolute ages are subject to large uncertainty (e.g., Tanaka, 1986), volcanic activity at Tharsis Montes may be 1 b.y. younger than the Syria Planum events. The absence of wrinkle ridges may thus be due to vertical crustal growth caused by Syria Planum-related magmatic underplating and volcanism and associated increasing brittle-crust thickness with secular planetary cooling.

Competent layer thickness. If considered elastic, subsidence-producing compression at the surface should induce extension at greater depth below a neutral plane. The thickness of the competent layer at the surface undergoing compression can be estimated from periodic spacing of wrinkle ridges on planetary surfaces (Watters, 1989, 1991) by using empirical fold-wavelength to layer-thickness ratios of 3–6 to 1 (Ghent and Hansen, 1999, and references therein). Mean ridge spacing at the Columbia Plateau is 20 km (Watters, 1989), suggesting that the thickness of the folded brittle layer should have been on the order of 3–7 km during flood-basalt emplacement. Because most of the Columbia River Basalt Group volume erupted in ~1.5 m.y. and ridge growth followed lava-flow emplacement with a delay that did not exceed a few hundred thousand years (Reidel et al., 1989a), ridge spacing was mainly established at 15.5 Ma (Swanson et al., 1981; Hooper and Conrey, 1989), after most of the Columbia River basalts were erupted (Reidel et al., 1989b). Basalt thickness increases from 3 to 6 km toward the Pasco basin (Fig. 9), which is in very good agreement with the thickness of the empirically determined deformed layer. By using similar reasoning, the 30 km mean ridge spacing in the Tharsis region (Watters, 1991) suggests that the part of the crust affected by the wrinkle ridges should be on the order of 5–10 km thick. This value is in agreement with evidence of layered

deposits at least 8 km thick displayed on the Valles Marineris walls (McEwen et al., 1999). Therefore, wrinkle-ridge spacing may give a clue to total basaltic-flow thickness and places constraints on the rheology of the upper part of the brittle crust. If the elastic approximation is valid, the tensile state of stress in the lower half of the brittle crust would favor (but by no means fully explain) the emplacement of nonfeeder dikes simultaneously with wrinkle-ridge formation (Watters and Maxwell, 1983).

Stratification of the ridged layer. Stratification has been shown to be a prerequisite for wrinkle ridges to develop (Schultz, 2000), which may explain development of wrinkle ridges in suspected thick sequences of mafic lavas and also in layered sediments (Plescia and Golombek, 1986). However, the ridges reported in layered sediments that are akin to the wrinkle ridges discussed in the present paper are smaller by at least two orders of magnitude and would accommodate negligible strain at hotspot scale. Moreover, no folded and thrust-faulted structures have been detected on seismic profiles in the Columbia Plateau layered sediments that were deposited during Eocene subsidence. Therefore, given a lack of other documented examples, flood basalts appear to be the only materials in which wrinkle ridges form and thus accommodate significant compression in a hotspot setting.

Flood-basalt décollement. Interpretation of a décollement between the flood basalts and the underlying rocks along which wrinkle ridges terminate at depth has been advocated both at the Columbia Plateau (Lutter et al., 1994) and the Syria Planum ridged plains (Allemand and Thomas, 1992; Thomas and Allemand, 1993; Mangold, 1997). However, seismic profiles across the Columbia Plateau have not imaged any décollement level below the Columbia River Basalt Group (Catchings and Mooney, 1988; Jarchow et al., 1994). On Mars, the décollement would coincide with the interface between the flood lavas and a megaregolith containing liquid water or permafrost. A megaregolith containing volatiles within the brittle crust would play an important role in décollement nucleation and slip because of the competency contrast the megaregolith would generate at shallow-crustal depths and its influence on crustal rheology and wrinkle-ridge formation by decreasing the crustal strength between the flood basalts and the supposedly denser crust underneath. Evidence for volatiles in the basement some time during the geologic history of ridged plains such as Coprates and Lunae Planum is supported by the presence of lobate ejecta craters in these regions (Battistini, 1984; Squyres et al., 1992a; Costard, 1993). However, several lines of evidence argue against a strong influence of a megaregolith on wrinkle-ridge formation and even question the existence of a megaregolith. (1) Permafrost has a very small volatile content (Battistini, 1984; Costard, 1990, 1993), maybe too small to localize a décollement. (2) The walls of the Valles Marineris graben system provide a deep (~8 km) cross section through a crust capped by a ridged unit. High-resolution images of Valles Marineris provided by the *Mars Global Surveyor* spacecraft

show that the walls display monotonic layered strata down to the base of the trough system. From detailed structural and geomorphologic analysis of the Valles Marineris walls (Peulvast and Masson, 1993; Mège, 1994; Peulvast et al., 1999), preliminary interpretation of the Mars Global Surveyor images (McEwen et al., 1999), and the analysis of ridge spacing already discussed, the Valles Marineris walls do not display any evidence of vertical variations in rock mechanical properties over the ~8 km depth. (3) This result is confirmed by analysis of landslides in Valles Marineris. Most landslides display characteristic features of rotational slides, which require that a strength contrast exists in the basement at the contact between the stable and unstable levels (Dikau et al., 1996). Landslides usually affect the entire height of the Valles Marineris walls, implying that the depth of the first major rheologic contrast in the crust should be close to the current trough floor and that the depth of the putative megaregolith must be deeper than ~8 km, i.e., probably too deep to serve as a décollement level for wrinkle ridges, but consistent with the estimate of 5–10 km for the depth to the bottom of the wrinkle ridges based on ridge spacing as discussed previously. (4) Little influence of a megaregolith in wrinkle-ridge formation is also supported by wrinkle-ridge development in dry crusts on Venus, the Moon, and Mercury. Therefore, unlike other authors (Allemand and Thomas, 1992; Thomas and Allemand, 1993; Mangold, 1997), we consider upper-crustal rheologic decoupling unnecessary to form wrinkle ridges.

Crustal rheology for peripheral-belt formation by gravitational spreading

Initiation of the South Syria Planum ridge belt contemporaneously with the onset of Syria Planum mantle-plume activity suggests an overall lithosphere structure similar to that existing during the period of wrinkle-ridge formation around Syria Planum. At Venusian coronae annuli, existence of a ductile level at shallow depth is also supported by high heat flow, suggested by thin (maybe zero thickness) elastic lithosphere.

At the Faeroe-Rockall Plateau, the anticlinal belt is observed to have developed in a thinned continental crust (White and McKenzie, 1989) to which dense materials have been magmatically underplated. Constraints from seismic velocities suggest that the upper continental crust (as defined by 2.8–4.54 km·s^{-1} velocities in Fig. 9 of White and McKenzie, 1989) is not more than 7 km thick, which is less than half the thickness of the lower continental crust (6.55 km·s^{-1}) plus underplated rocks (7.15 km·s^{-1}). In contrast, the upper crust of the continental shelf east of the Vøring Plateau is 11 km thick (up to 6.0 km·s^{-1}, Fig. 9 of White and McKenzie, 1989), and the lower crust, composed of basement materials (6–7 km·s^{-1}) and underplated rocks (7–~7.5 km·s^{-1}), is only half as thick (White and McKenzie, 1989). We suggest that this difference in upper- and lower-crust thickness is one of the main reasons why the Faeroe-Rockall Plateau displays contractional structures, whereas no such feature has been reported east of the Vøring Plateau. These observations are in agreement with rheologic requirements for gravitational spreading resulting from geologic, numerical, and experimental models.

Observations at terrestrial volcanoes (Borgia et al., 1992; Merle and Borgia, 1996) and numerical models of volcanic spreading suggest that the load must be decoupled from the basement to allow circumferential contraction around the load (McGovern and Solomon, 1993, 1998). Scaled experiments using analogue materials in which a brittle (Mohr-Coulomb) conical edifice overlies a crust divided into a brittle layer and an underlying ductile (Newtonian) layer show that the deformation style is determined by the ratio of brittle-layer thickness to ductile-layer thickness B/D (Merle and Borgia, 1996). The driving mechanism for the development of contractional structures around the volcanic topography is creep in the ductile layer. A contractional peripheral belt forms if the ductile-crust thickness is at least equal to the brittle-crust thickness ($B/D = 1$), in which case a single, wide, fault-propagation anticline verging away from the cone right at the edge of the topographic bulge is observed to form. Decreasing B/D results in the formation of several circumferential contractional annuli, gradually developing outward while the maximum elevation of the load decreases and its diameter increases. For instance, $B/D = 0.2$ results in ridges located at 10 different radii from the volcanic edifice. Decreasing B/D also modifies ridge structure, wavelength, and spacing; thrusting is hindered whereas folding becomes the main deformation style and fold wavelength and spacing increase from the edge of the uplifted crust outward. As an example, at Syria Planum, the number of parallel ridges at the edge of the uplift varies from one (southeast) to five (west) and most frequently is two or three, which suggests that $0.2 < B/D < 1$. Topography at the south Tharsis ridge belt has been modeled by blind thrusting and associated folding (Schultz and Tanaka, 1994), which is in accordance with the results obtained by experimental models. At the North Atlantic volcanic province, distinct contractional annuli have not be identified, possibly because the location of anticlines may have been primarily guided by Mesozoic structures. The range of distances between the early plume center and the anticlines in Figure 12 suggests either that B/D should have been low enough to allow the formation of several annuli or that topographic building was achieved in more than one stage.

In experiments in which the volcano is located close to a rigid boundary (the box boundary in experimental analogues), no peripheral annulus forms in the buttressed direction. Variations in crustal properties such as rigidity may thus provide an explanation for peripheral belts only partially circumscribing topographic uplifts. For instance, the martian dichotomy boundary, which may be a lithospheric rheologic boundary (e.g., McGill and Squyres, 1991; Breuer et al., 1993), may have impeded ridge-belt formation beyond the boundary north of the Syria Planum swell. Other explanations for the local absence of a peripheral belt around parts of hotspot swells include thin or
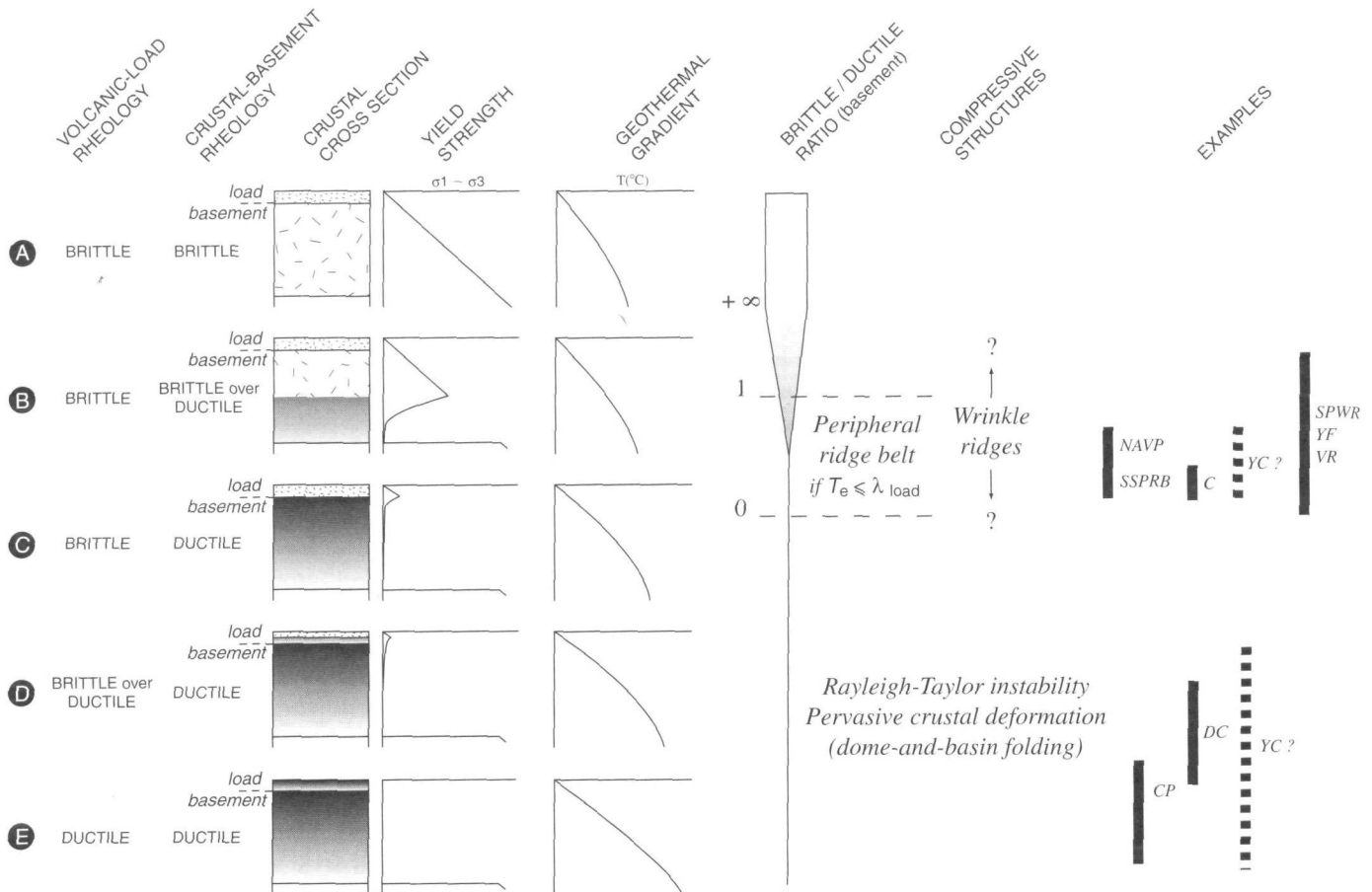
Figure 19. Rheologic requirements for contractional structures to form at the surface in response to plume impact, and rough estimates of ranges of rheologic conditions prevailing while the contractional structures discussed in the text were being formed. NAVP—North Atlantic Volcanic Province, SSPRB—south Syria Planum ridge belt, C—Venusian coronae, YC—Yilgarn craton (interpreted to display either a contractional peripheral belt or dome-and-basin folding), SPWR—Syria Planum wrinkle ridges, YF—Yakima folds, VR—Venusian volcanic rises, CP—Venusian crustal plateaus, DC—Dharwar craton greenstone belts.

absent ductile crust in comparison to brittle-crust thickness and ridge burial by more recent deposits or lavas. On Mars, eruption of the Tharsis Montes-related lavas may have buried part of the South Syria Planum ridge belt.

Crustal rheology for dome-and-basin folding by Rayleigh-Taylor instability

Dome-and-basin folding can be modeled by isothermal experiments of subsidence due to Rayleigh-Taylor instability development at the interface between a dense volcanic load and a lighter crust overlying a viscous mantle. This model requires that the DBT (ductile-to-brittle transition) be located either within the volcanic load or at the surface (Chardon, 1997). If the DBT lies within the load, the brittle-ductile interface does not deform, and sagduction does not produce any deformation between this interface and the surface. Experiments in which a thermal gradient is taken into account show that the instability-amplification rate is closely dependent on the geothermal gra-

dient. Dome geometry depends on the ratio of the load to basement thicknesses (Woidt, 1978). Formation of well-developed domes requires this ratio to be at least 1 (Chardon, 1997).

Relationships between Rayleigh-Taylor instability and a plume may be of two kinds. The dense load that sinks may be a volcanic pile that erupted in response to plume impingement on the bottom of the lithosphere. Subsequently, the thermal anomaly due to the plume causes the DBT to shift upward above the basement-load boundary, resulting in sinking of the dense load. The other possibility is that a dense load at the surface, or part of the load, is older than the plume, in which case upward migration of the DBT destabilizes the older load and causes it to sink. The latter case probably corresponds to the Dharwar greenstone belts (Chardon et al., 1998). Complete removal of the impact-crater record at Venusian crustal plateaus before the beginning of the observed tectonic activity, as well as short ribbon wavelength, supports the interpretation that the DBT was close to the surface or even at the surface (Ghent and Hansen, 1999), allowing sagduction of dense magmas erupted

early in the plume history. The greenhouse effect on Venus (current surface temperature, 470 °C; atmospheric pressure, 92 bars), if already operating by that time, would have facilitated the DBT's rising to shallower depth than would have been possible from the influence of the plume alone.

Rheologic model for mantle-plume–induced contraction

A major distinction should be made between cases in which the lithosphere is strong enough to support the load of erupted magma and cases in which the lithospheric support is too weak to maintain a high topography after the initial strong thermal anomaly has waned, resulting in volcanic-load sagduction (Fig. 19). Wrinkle ridges and peripheral belts correspond to the first case, whereas dome-and-basin folding correspond to the latter case. Whether the load can be maintained is primarily governed by the thermal state of the crust and mantle, and the volume of the load depends on the heat anomaly carried by the plume as well as the size (gravity) of the planet.

B/D > 1 and DBT occurs below the volcanic load. On the basis of available examples, no major structures are expected to form as long as the brittle crust is thicker than the ductile crust (Fig. 19A).

0 < B/D < 1 and DBT occurs below the volcanic load. Decreasing *B/D* improves the likelihood of producing wrinkle ridges by topographic subsidence (Fig. 19B). Available terrestrial and extraterrestrial examples suggest that shallow and fine rheologic layering is needed for wrinkle ridges to form. Mafic lava flows interbedded with volcano-sedimentary sequences, such as observed in terrestrial flood-basalt provinces, will provide the most likely conditions for wrinkle ridges to form. However, we cannot dismiss the hypothesis that some layered sedimentary sequences may also be suitable for wrinkle-ridge formation. Because of the absence of adequate modeling at a crustal scale, uncertainty exists on the maximum *B/D* ratio that would allow wrinkle ridges to form. However, we expect that ideal conditions required for wrinkle ridges to form are met when the degree of isostatic load compensation $C = 1$, the level of compensation being set by the elastic crustal thickness and, hence, the geotherm steepness. Topographic subsidence triggering wrinkle-ridge formation thus depends on the elastic thickness, the density contrast between the crust and mantle, and the size of the volcanic load (equation 3).

Contractional peripheral belts are expected to form under similar conditions and are interpreted to result from gravitational spreading of the excess topography created by the plume in a brittle upper crust underlain by a weak layer of greater thickness. Numerical and experimental modeling indicate that if the elastic thickness wavelength of the plate supporting the load is smaller than the load wavelength, then peripheral belts will form if the ductile crust is thicker than the brittle crust. The North Atlantic volcanic province peripheral belt displays fewer contractional annuli than the South Syria Planum ridge belt, which we interpret to reflect a higher *B/D* ratio in the former.

B/D = 0 and DBT occurs at the base of the volcanic load. The geothermal gradient may increase sufficiently to raise the DBT to the boundary between the basement and the load (Fig. 19C). This scenario is interpreted to be the transition stage between cases in which the volcanic-load topography can be supported by the strength of the underlying materials and cases in which it cannot and thus will tend to sink. This transition stage does not appear to have been observed in the examples discussed in this paper. Experimental modeling firmly suggests that the volcanic load will not sink (Chardon, 1997). Models by Merle and Borgia (1996) predict that this stage should correspond to the observation of a contractional peripheral belt composed of many closely spaced compressional annuli.

B/D = 0 and DBT occurs within the volcanic load. When the geothermal gradient is high enough to shift the DBT to within the volcanic load, the tectonic style is dominated by dome-and-basin folding (Fig. 19D). Crustal-scale Rayleigh-Taylor instability at the basement-load interface induces sagduction of the ductile part of the load, whereas the surface remains mainly undisturbed. Mineralogical and geobarometric constraints suggest that the Archean geotherm at the Dharwar craton was high. The DBT during dome-and-basin folding, as deduced from metamorphism, would have been at a depth equivalent to ~200 MPa, i.e., probably 5 km or more (Moyen, 2000).

B/D = 0 and DBT occurs at or close to the surface. Under these conditions, the surface expression of sagduction is structures having variable orientations that are functions of parameters such as distance to the locus of maximum subsidence, mechanical heterogeneities in the crust at the surface, and remote stress trajectories (Fig. 19E). Observation of pervasive deformation on the crustal plateaus of Venus (which have undergone very little erosion since their formation) argues in favor of a very shallow DBT on that planet.

GUIDE TO USING CONTRACTIONAL STRUCTURES TO LOCATE PALEO-MANTLE PLUMES ON EARTH

Identifying plume-related contractional structures

Wrinkle ridges and peripheral belts have been found in post-Archean terrains, whereas dome-and-basin folding is observed at some greenstone belts. Conditions suitable to wrinkle-ridge and peripheral-belt development appear thus to have been dominantly met after the Archean, whereas the absence of greenstone belts in Proterozoic terrains suggests that Rayleigh-Taylor instability-induced plume tectonics was probably restricted to the Archean. This does not preclude that deformation at some Archean cratons may also result from lithospheric mechanisms akin to plate tectonics (e.g., de Witt, 1998). Furthermore, the small number of examples discussed in the present study does not disallow the possibility of wrinkle-ridge and peripheral-belt occurrences in Archean terrains. Although structural analysis of contractional structures may be helpful in de-

termining the location of past plume centers, the involvement of a plume should be supported by independent evidence, such as flood-basalt geochemistry and fanning dike swarms of similar age.

Guidelines to interpreting and using wrinkle ridges and contractional peripheral belts to locate paleo-mantle plumes

Clue to past occurrences. The dilatancy due to injection of dikes of the Mackenzie swarm seems to require formation of contractional peripheral belts in order to avoid an anomalously high domal uplift. Because radiating-dike swarms are likely associated with most plumes and have been clearly identified for nearly 30 years (Ernst and Buchan, 1997), then contractional peripheral belts are predicted to be quite common unless the geodynamic context is unfavorable. For instance, passive rifting approximately normal to the main dike trend may produce enough room in the crust to accommodate the total dike dilation.

Geometry of structures. When seeking evidence of past plumes, contractional tectonic structures that must be considered include thrust faults and folds. The suspected wrinkle ridges or peripheral belts should be oriented perpendicular to radiating-dike swarms of similar age. Wrinkle ridges and peripheral belts are expected to surround the initial plume center because both kinds of structures are initiated at the beginning of plume activity. Nevertheless, perfect concentric geometry is not expected in most cases, because tectonic stress resulting from plate motions deviates the stress trajectories generated by the plume (Muller and Pollard, 1977; McKenzie et al., 1992). Structural analysis and comparison to the structural style at the Yakima fold-and-thrust belt, as described in detail by various authors (see references in the first section of this paper), should help in evaluating similarities with wrinkle ridges.

Lithologic requirements. The planetary record tends to demonstrate that stratified flood basalts provide the preferred, if not the only possible lithology in which structures akin to wrinkle ridges form. This argument may be important to consider for distinguishing between ancient wrinkle ridges and contractional peripheral belts. A peripheral belt would be expected instead of wrinkle ridges if the structures indifferently affect both lava flows and basement. A further constraint is that annulus diameter for a peripheral belt must be large enough to circumscribe the entire initial hotspot-uplifted topography, whereas wrinkle-ridge occurrence is independent of slope angle.

Factors clouding the contractional record. Factors determining the existence or absence of wrinkle ridges or peripheral belts include the following: (1) The previously imposed structural grain of the crust is expected to guide the geometry of subsequent deformations, similar to the influence of the Cle Elum–Wallula topographic lineament on Yakima ridge orientation at the Columbia Plateau. (2) Subsequent deformation events may overprint the contractional features. In order to retrieve past ridge geometry, subsequent deformation must be subtracted by some appropriate means such as unfolding balanced cross sections or closing rift borders after accounting for a rift shoulder effect. (3) There may not have been a thin brittle crust at the time of plume activity. In terrestrial environments similar to the present Earth, formation of wrinkle ridges or a peripheral belt at hotspots requires a thin brittle crust or a brittle crust that is thin compared to the thickness of the ductile crust. These requirements are most likely to be met (a) when the crust is oceanic, (b) when the crust has already been tectonically thinned, (c) when the crust is being thinned (e.g., by rifting), or (d) when the hotspot thermal anomaly is high enough to shift the DBT significantly upward.

If a rifting event predates, or is contemporaneous with, flood-basalt volcanism, another constraint is that crustal stretching should not exceed a threshold value. Beyond this threshold, the buoyant low-density mantle from which the melt has been extracted will induce permanent uplift instead of subsidence. Subsidence and subsequent wrinkle-ridge formation are possible only if there is no rifting associated with plume activity, if rifting is aborted, or if most stretching postdates flood-basalt emplacement. Details in regard to the stretching threshold can be found in White and McKenzie (1989; Fig. 7). Aborted rifting will probably enhance subsidence by trapping magma beneath the thinned lithosphere (Thompson and Gibson, 1991), which upon cooling will exert downward traction of the lithosphere, generating further compression at the surface.

To give an example, this model explains why the Yellowstone plume was involved in tectonic contraction, whereas the Ethiopian plume was not. Formation of the Yakima fold-and-thrust belt on the Columbia River flood basalts occurred after the underlying crust was significantly thinned earlier, during the Eocene, but the stretching factor never exceeded 1.5 during the rifting event or during Columbia River basalt emplacement, which would have marked the transition from subsidence to uplift. Conversely, in western Ethiopia, eruption of the Abyssinian flood basalts, probably above the plume center (Korme, 1997), occurred between 31 Ma and 29 Ma (Hofmann et al., 1997) in a thick Precambrian basement, while extension in Afar had not yet begun (Menzies et al., 1997; Courtillot et al., 1999). That the crustal basement underlying the flood basalts was not thinned by rifting may explain why no contractional structures associated with the plume have been observed in the flood basalts (Korme, 1997; Chorowicz et al., 1998).

In addition, at least two specific geodynamic conditions can affect wrinkle-ridge and peripheral-belt formation.

1. Wrinkle ridges can be influenced by the magnitude of the ambient stress field. Although the magnitude of compressive stress generated by the plume may be sufficient to produce wrinkle ridges, the extraterrestrial record, especially in impact craters and basins, suggests that the ambient stress field is also important and that the orientation of ridges will be a combination of the plume-related stresses and the regional ambient stresses. It cannot be dismissed that in some instances, contractional structures would have formed anyway even in the ab-

sence of a mantle plume, provided that a thick sequence of stratified lava flows loaded a thin brittle crust. In such a case, their geometry and orientation would have been fully determined by the geometry of the ambient stress field.

2. Peripheral belts can be influenced by lateral variations in mechanical properties of the crust (e.g., crystalline crust vs. sedimentary crust; oceanic crust vs. continental crust). (a) As a first example, plume uplift at a small distance from a plate boundary may tend to relax at the boundaries instead of forming a peripheral belt. However, if the plate boundary is at a larger distance from the topographic uplift edge, it will probably not impede peripheral-belt formation, as illustrated in the next example. (b) In example 2, peripheral-belt development needs lateral free boundaries at some distance from the plume edge in order to induce ductile creep in the lower crust (Merle and Borgia, 1996). Thus, plume impingement beneath a huge intracontinental basin is thought to provide appropriate conditions for the formation of a peripheral belt, because the boundary conditions may be considered as moving freely. Distribution of the contractional features will be determined by the movements in the creeping lower crust instead of by plate boundaries. (c) As a third example, peripheral-belt development may be impeded near the edge of a passive margin because of the thinning of the continental lower crust toward the oceanic margin, which will make upper-crustal contraction by folding and thrusting impossible.

Conversely, plate-boundary stresses are thought to only have a minor effect on wrinkle-ridge formation. Plume-related subsidence exerts vertical stress on a well-defined part of the crust that will relax in situ. Thus the stress that forms wrinkle ridges is not transmitted to plate boundaries where they would relax.

Most post-Archean plumes, provided that these conditions have been filled, are candidates to have induced compressional tectonics. As seen in the case histories discussed herein, even when compressional features are recognized in association with a mantle plume, they are usually attributed to plate tectonics rather than plume tectonics. Therefore, we suggest that any contractional features of the types that are spatially and temporally associated with mantle plumes should be reevaluated for possible plume linkage.

Guidelines to interpreting and using Rayleigh-Taylor instability-driven structures

Although Rayleigh-Taylor instability-driven plume tectonics has been identified in greenstone belts, it provides only one of several possible mechanisms of greenstone-belt formation. Detailed structural mapping helps in assessing Rayleigh-Taylor instability as a mechanism for greenstone belts. Detailed study of the geometry of contacts between the basement and volcanic units and detailed structural mapping of fold axes and crenulation lineations, such as at the Dharwar greenstone belts (Chardon, 1997; Chardon et al., 1996, 1998), have been demonstrated

to provide strong constraints for evaluating this mechanism. Remote-sensing techniques have proven to be another efficient means of mapping and interpreting structures associated with volcanic-load sinking above plumes (Ghent and Hansen, 1999). Both concentric and radiating fold and microfold axes are expected to form in that context. Concentric fold axes would suggest the outer part of the sinking load, whereas radiating fold axes are expected to indicate closer proximity to the plume center. Fold axes with various orientations and anastomosing patterns would be interpreted to indicate the locus of maximum subsidence, and the most intense deformation is anticipated in such areas. Crosscutting relationships are expected to emphasize polyphase deformation. Dome geometry gives a clue to the volcanic-load thickness to basement thickness ratio.

Greenstone belts displaying such features provide constraints on the depth of the DBT and, hence, help reveal the existing geotherm at the time of deformation. It should be noted, however, that the locus of maximum subsidence, which is mainly dependent on structural heterogeneities and volcanic-load shape, may not coincide with the plume center.

ACKNOWLEDGMENTS

APPENDIX 1. ANALYSIS OF PROPOSED RELATIONSHIPS BETWEEN THE YAKIMA FOLD-AND-THRUST BELT AND CASCADIA SUBDUCTION

The influence of subduction on stress on land may be of two kinds (Uyeda and Kanamori, 1979), depending on the subduction dip angle: either compressional perpendicular to the trench (gentle dip) or tensile perpendicular to the trench (steep dip), in which case extension tends

to produce backarc spreading. Most subduction zones are consistent with this model.

The present Cascadia subduction dip angle is within the range 4°–20° from the western deformation front eastward (Crosson and Owens, 1987; Hyndman and Wang, 1995), in agreement with the current compressive state of stress at the Columbia Plateau. The stress orientation that would be predicted by subduction is, however, at odds with the orientation of the Yakima fold-and-thrust belt. At compressive margins, the direction of compression is normal to the trench if the obliquity of the subducting plate's slip vector relative to the trench is either null or greater than a critical angle, partly depending on local conditions (McCaffrey, 1992). Obliquity of the Juan de Fuca plate's slip vector is on the order of 45° offshore Oregon and the southern half of Washington. Comparison with other subduction zones suggests that if the compression at the Columbia Plateau was a consequence of this subduction, the maximum-principal-stress trajectory would have to be east-west to north-northeast–south-southwest, meaning that the Yakima fold axes would have to be more or less normal to their observed trend (Suppe et al., 1975; Zoback et al., 1990).

Alternatively, it may be suggested that at the time of Yakima fold-and-thrust belt initiation, the state of stress was extensional and produced the Columbia Plateau subsidence in a backarc rifting environment (Reidel et al., 1989a; Saltus, 1993). Early Tertiary crustal stretching actually took place in the Yakima area. First, however, it almost stopped before flood-basalt eruption, which is the reverse of what would be expected if subsidence was a consequence of backarc spreading. Second, backarc extension requires a much steeper subduction dip angle than currently exists. Given that the Juan de Fuca plate has almost entirely been subducted now and that slab dip angle is expected to increase as a function of the age of the subducting plate (Uyeda and Kanamori, 1979), the driving mechanism for an initially high subduction dip angle (allowing for the Columbia Plateau area stretching and subsidence, which would have then dramatically decreased to its present value) remains to be found. Third, Columbia Plateau subsidence in response to subduction-related stress would probably oppose the development of large-scale compressive structures such as the Yakima folds, in agreement with the absence of reported fold-and-thrust belts, to our knowledge, in the other backarc settings throughout the world (e.g., Von Huene et al., 1989, regarding subduction at Peru).

The inconsistencies between the Columbia Plateau case and the predictions from Uyeda and Kanamori's (1979) subduction model may be explained by the superposition of a regional stress source that dominates over subduction-related stress. For instance, the state of stress at the Altiplano-Puna high plateau (Andes), where extension is observed to be parallel to the trench (Zoback, 1992), has been explained by gravitational spreading of the high topography (Sébrier et al., 1985; Froidevaux and Ricard, 1987). The state of stress on the upper part of the subducting Cocos plate, at the Middle America Trench, includes areas where compression is parallel to the trench, similar to the situation of the western Columbia Plateau. The high complexity of the state of stress in this region has been attributed to the nearby triple junction where the North American, Cocos, and Caribbean plates meet (Guzmán Speziale et al., 1989). At the Indo-Burma accretionary prism, between the Burma arc and the Red River fault, the state of stress is also compressional parallel to the trench and has been explained by clockwise rotation of the South China block in response to the development of the Eastern Himalayan syntaxis produced by the indentation of India in the Eurasian plate (Holt et al., 1991; Holt and Haines, 1993).

Retro-foreland basins (i.e. basins in the foreland on the side of the mountain belt opposite to the subduction) undergoing compression not only have principal stress trajectories perpendicular to the state of stress in the Yakima fold-and-thrust belt area, they also have a different structural style. For instance, the Subandean zone displays thrusts verging toward the South American plate edge, and both focal mechanisms and inversion of fault data sets emphasize that the maximum principal stress is perpendicular to the trench, as predicted by Uyeda and Kanamori's (1979) model. The Subandean thrusts are connected to deeper fault planes dipping toward the Andean cordilleras (e.g., Sébrier et al., 1985; Roeder, 1988). Similar observations have been reported at the Pyrenean mountains. Subduction of the Iberian continental lithosphere beneath the European plate has induced folding and thrusting in the Aquitaine retro-foreland basin, and the thrusts are connected at depth to a major thrust dipping toward the Pyrenean axial zone (Vergés et al., 1995). In both the Andean and Pyrenean examples, the direction of shortening is directly due to plate convergence. The Columbia Plateau regional tectonic setting is similar to that of these retro-foreland basins, and if the Yakima fold-and-thrust belt had formed in response to subduction processes, then seismic refraction profiling should have imaged at least one large, deep, thrust plane connecting the ridges at depth and dipping westward, but no such fault was imaged (Catchings and Mooney, 1988). Absence of such a structure is in agreement with the absence of any large thrust fault or other type of fracture in the sedimentary layers underlying the Columbia River Basalt Group that would connect the overlying anticlines to deep Cascadian structures to the west (Jarchow et al., 1994). Although Lutter et al. (1994) interpreted the basalt-sediment interface as a décollement level, no reflection has been observed on wide-angle seismic profiles to mark this interface, either because of seismic reverberations in the flood basalts or merely because it does not exist (Jarchow et al., 1994).

From the foregoing, it follows that the Cascade Ranges and the Columbia Plateau are distinct geodynamic units, implying that the Yakima ridges appear to be currently growing independently from the stress prevailing in the Cascades. The failure to follow Uyeda and Kanamori's (1979) model of subduction-generated stress implies overprinting by another regional stress source. The subsurface structure of the Yakima fold-and-thrust belt is also atypical of subsurface structures in retro-foreland basins. We conclude that subduction-related stress may have contributed to the stress producing the Yakima ridges, but the primary stress source for the deviatoric stress to exceed rock strength and trigger ridge growth parallel to the trench should be of another type. Other stress sources are evaluated in the main body of the paper.

REFERENCES CITED

Abbott, D., 1996, Plumes and hotspots as sources of greenstone belts: Lithos, v. 37, p. 113–127.

Acuña, M.H., Connerney, J.E.P., Wasilewski, P.J., Ness, N.F., Reme, H., Mazelle, C., Vignes, D., Lin, R.P., Mitchell, D.L., and Cloutier, P.A., 1999, Global distribution of crustal magnetization discovered by the Mars Global Surveyor MAG/ER experiment: Science, v. 284, p. 790–793.

Allemand, P., and Thomas, P.G., 1992, Modèle fragile des rides martiennes contraint par la géométrie de surface: Comptes Rendus de l'Académie des Sciences, Sér. II, v. 315, p. 1397–1402.

Arndt, N.T., Albarède, F., and Nisbet, E.G., 1997, Mafic and ultramafic magmatism, in de Wit, M.J., and Ashwal, L.D., eds., Greenstone belts: Oxford Monographs on Geology and Geophysics, v. 35, p. 233–254.

Assumpção, M., 1992, The regional intraplate stress field in South America: Journal of Geophysical Research, v. 97, p. 11889–11903.

Atwater, T., 1970, Implications of plate tectonics for the Cenozoic tectonic evolution of western North America: Geological Society of America Bulletin, v. 81, p. 3513–3536.

Banerdt, W.B., Golombek, M.P., and Tanaka, K.L., 1992, Stress and tectonics on Mars, in Kiefer, W.S., et al., eds., Mars: Tucson, Arizona, University of Arizona Press, p. 249–297.

Banerdt, W.B., Phillips, R.J., Sleep, N.H., and Saunders, R.S., 1982, Thick shell tectonics on one-plate planets: Applications to Mars: Journal of Geophysical Research, v. 87, p. 9723–9733.

Banks, B.K., and Hansen, V.L., 1999, Intratessera flood-lava basins (ITBs) constrain timing of crustal plateau structures: Houston, Texas, Lunar and Planetary Institute, Lunar and Planetary Science Conference 30, CD-ROM, 2053.pdf.

Baragar, W.R.A., Ernst, R.E., Hulbert, L., and Peterson, T., 1996, Longitudinal petrochemical variation in the Mackenzie dyke swarm, northwestern Canadian Shield: Journal of Petrology, v. 37, p. 317–359.

Barley, M.E., Pickard, A.L., and Sylvester, P.J., 1997, Emplacement of a large igneous province as a possible cause of banded iron formation 2.45 billion years ago: Nature, v. 385, p. 55–58.

Barley, M.E., Krapez, B., Groves, D.I., and Kerich, B., 1998, The Late Archean bonanza: Metallogenic and environmental consequences of the interaction between mantle plumes, lithospheric tectonics and global cyclicity: Precambrian Research, v. 91, p. 65–90.

Basilevsky, A.T., 1994, Concentric wrinkle ridge pattern around Sif and Gula Montes, Houston, Texas, Lunar and Planetary Institute, Lunar and Planetary Science Conference 25, p. 63–64.

Basilevsky, A.T., Head, J.W., III, Ivanov, M.A., and Kryuchkov, V.P., 1999, Impact craters on geologic units of northern Venus: Implications for the duration of the transition from tesserae to regional plains: Geophysical Research Letters, v. 26, p. 2593–2596.

Battistini, R., 1984, L'utilisation des cratères météoritiques à ejecta fluidisés comme moyen d'étude spatiale et chronologique de l'eau profonde (hydrolithosphère) de Mars: Revue de Geomorphologie Dynamique, v. 33, p. 25–41.

Beck, M.E., 1978, Summary of tectonic models for the origin of the Columbia River Plateau, *in* Tectonics and seismicity of the Columbia Plateau Workshop, Basalt Waste Isolation Program: Seattle, Washington, Battelle Conference Facilities, 9 p.

Bentley, R.D., 1977, Stratigraphy of the Yakima basalts and structural evolution of the Yakima Ridges in the western Columbia Plateau: Geologic excursions in the Pacific Northwest, *in* Brown, E.H., and Ellis, R.C., eds., Geological Society of America Annual Meeting, Seattle, Washington: Bellingham, Washington, Western Washington Press, Guidebook, p. 339–389.

Bijwaard, H., and Spakman, W., 1999, Tomographic evidence for a narrow mantle plume below Iceland: Earth and Planetary Science Letters, v. 166, p. 121–126.

Bilotti, F., and Suppe, J., 1999, The global distribution of wrinkle ridges on Venus: Icarus, v. 139, p. 137–157.

Bindschadler, D.L., Schubert, G., and Kaula, W.K., 1992a, Coldspots and hotspots: Global tectonics and mantle dynamics of Venus: Journal of Geophysical Research, v. 97, p. 13495–13532.

Bindschadler, D.L., DeCharon, A., Beratan, K.K., Smrekar, S.E., and Head, J.W., 1992b, Magellan observations of Alpha Regio: Implications for formation of complex ridged terrains on Venus: Journal of Geophysical Research, v. 97, p. 13563–13577.

Boldreel, L.O., and Andersen, M.S., 1993, Late Paleocene to Miocene compression in the Faeroe-Rockall area, *in* Parker, J.R., ed., Petroleum geology of northwest Europe: London, England, Geological Society, Proceedings of the 4th Conference, p. 1025–1034.

Boldreel, L.O., and Andersen, M.S., 1998, Tertiary compressional structures on the Faeroe-Rockall Plateau in relation to northeast Atlantic ridge-push and alpine foreland stresses: Tectonophysics, v. 300, p. 13–28.

Borgia, A., 1994, Dynamic basis of volcanic spreading: Journal of Geophysical Research, v. 99, p. 17791–17804.

Borgia, A., Burr, J., Montero, W., Morales, L.D., and Alvarado, G.E., 1990, Fault propagation folds induced by gravitational failure and slumping of the central Costa Rica volcanic range: Implications for large terrestrial and Martian volcanic edifices: Journal of Geophysical Research, v. 95, p. 14357–14382.

Borgia, A., Ferrari, L., and Pasquarè, G., 1992, Importance of gravitational spreading in the tectonic and volcanic evolution of Mount Etna: Nature, v. 357, p. 231–235.

Borgia, A., Koenig, E., and Fink, J.F., 2000, A planetary perspective of gravitational spreading from small volcanic cones to large crustal plates: Houston, Texas, Lunar and Planetary Institute, Lunar and Planetary Science Conference 31, CD-ROM, 1896.pdf.

Bouhallier, H., Chardon, D., and Choukroune, P., 1995, Strain patterns in Archean dome and basin structures: The Dharwar craton (Karnataka, South India): Earth and Planetary Science Letters, v. 135, p. 57–75.

Bourgeois, O., 2000, L'exhumation des marges passives: Rennes, France, Centre Nationale de la Recherche Scientifique Research Project, 18 p.

Breuer, D., Spohn, T., and Wullner, U., 1993, Mantle differentiation and the crustal dichotomy of Mars: Planetary and Space Science, v. 41, p. 269–293.

Brodie, J., and White, N., 1995, The link between basin inversion and igneous underplating, *in* Buchanan, J.G., and Buchanan, P.G., eds., Basin inversion: Geological Society [London] Special Publication 88, p. 21–38.

Burchfiel, B.C., Cowan, D.S., and Davis, G.A., 1992, Tectonic overview of the Cordilleran orogen in the western United States, *in* Burchfiel, B.C., Lipman, P.W., and Zoback, M.L., eds., The Cordilleran orogen: Conterminous U.S.: Boulder, Colorado, Geological Society of America, Geology of North America, v. G-3, p. 407–479.

Camp, V.E., 1995, Mid-Miocene propagation of the Yellowstone mantle plume head beneath the Columbia River basalt source region: Geology, v. 23, p. 435–438.

Camp, V.E., and Hooper, P.R., 1981, Geologic studies of the Columbia Plateau: Part I. Late Cenozoic evolution of the southeast part of the Columbia River Basalt province: Geological Society of America Bulletin, v. 92, p. 659–668.

Campbell, I.H., and Hill, R.I., 1988, A two-stage model for the formation of the granite-greenstone terrains of the Kalgoorlie-Norseman area, Western Australia: Earth and Planetary Science Letters, v. 90, p. 11–25.

Campbell, N.P., 1989, Structural and stratigraphic interpretation of rocks under the Yakima fold belt, Columbia Basin, based on recent surface mapping and well data, *in* Reidel, S.P., and Hooper, P.R., eds., Volcanism and tectonism in the Columbia River flood-basalt province: Geological Society of America Special Paper 239, p. 209–222.

Campbell, N.P., and Bentley, R.D., 1981, Late Quaternary deformation of Toppenish Ridge uplift in south-central Washington: Geology, v. 9, p. 519–524.

Carlson, R.W., and Hart, W.K., 1987, Crustal genesis on the Oregon plateau: Journal of Geophysical Research, v. 92, p. 6191–6206.

Catchings, R.D., and Mooney, W.D., 1988, Crustal structure of the Columbia Plateau: Evidence for continental rifting: Journal of Geophysical Research, v. 93, p. 459–474.

Chadwick, B., Ramakrishnan, M., and Viswanatha, M.N., 1985, A comparative study of tectonic fabrics and deformation in Dharwar grits and phyllites and Sargur quartzites on the West of the Chitradurga supracrustal belt, Karnataka: Journal of the Geological Society of India, v. 26, p. 526–546.

Chadwick, B., Vasudev, V.N., and Hegde, G.V., 2000, The Dharwar craton, southern India, interpreted as the result of Late Archean oblique convergence: Precambrian Research, v. 99, p. 91–111.

Chardon, D., 1997, Les déformations continentales archéennes [Ph.D. thesis]: Mémoire de Géosciences-Rennes, v. 74, Rennes, France, Université de Rennes II, 257 p.

Chardon, D., Choukroune, P., and Jayananda, M., 1996, Strain patterns, décollement and incipient sagducted greenstone terrains in the Archaean Dharwar craton (south India): Journal of Structural Geology, v. 18, p. 991–1004.

Chardon, D., Choukroune, P., and Jayananda, M., 1998, Sinking of the Dharwar basin (South India): Implications for Archean tectonics: Precambrian Research, v. 91, p. 15–39.

Chorowicz, J., Collet, B., Bonavia, F.F., Mohr, P., Parrot, J.-F., and Korme, T., 1998, The Tana basin, Ethiopia: Intra-plateau uplift, rifting and subsidence: Tectonophysics, v. 295, p. 351–367.

Choukroune, P., Bouhallier, H., and Arndt, N.T., 1995, Soft lithosphere during periods of Archean crustal growth or crustal reworking, in Coward, M.P., and Ries, A.C., eds., Early Precambrian processes: Geological Society [London] Special Publication, 95, p. 67–86.

Choukroune, P., Ludden, J.N., Chardon, D., Calvert, A.J., and Bouhallier, H., 1997, Archean crustal growth and tectonic processes: A comparison of the Superior province, Canada and the Dharwar craton, India, in Burg, J.-P., and Ford, M., eds., Orogeny through time: Geological Society [London] Special Publication, 121, p. 63–98.

Connerney, J.E.P., Acuña, M.H., Wasilewski, P.J., Ness, N.F., Reme, H., Mazelle, C., Vignes, D., Lin, R.P., Mitchell, D.L., and Cloutier, P.A., 1999, Magnetic lineations in the ancient crust of Mars: Science, v. 284, p. 794–798.

Costard, F., 1990, Distribution et caractéristiques du pergélisol sur Mars: Son influence sur certains traits de la géomorphologie [Ph.D. thesis]: Paris, Université Panthéon-Sorbonne, 327 p.

Costard, F., 1993, Martian permafrost: International Journal of Refrigeration, v. 16, p. 91–100.

Courtillot, V., Jaupart, C., Manighetti, I., Tapponier, P., and Besse, J., 1999, On causal links between flood basalts and continental breakup: Earth and Planetary Science Letters, v. 166, p. 177–195.

Crosson, R.S., and Owens, T.J., 1987, Slab geometry of the Cascadia subduction zone beneath Washington from earthquake hypocenters and teleseismic converted waves: Geophysical Research Letters, v. 14, p. 824–827.

Cummings, M.L., Evans, J.G., Ferns, M.L., and Lees, K.R., 2000, Stratigraphic and structural evolution of the middle Miocene synvolcanic Oregon-Idaho graben: Geological Society of America Bulletin, v. 112, p. 668–682.

Davies, G.F., 1993, Conjectures on the thermal and tectonic evolution of the earth: Lithos, v. 30, p. 281–289.

de Witt, M.J., 1998, On Archean granite, greenstones, cratons and tectonics: Does the evidence demand a verdict?: Precambrian Research, v. 91, p. 181–226.

Dikau, R., Brunsden, D., Schrott, L., and Ibsen, M.-L., eds., 1996, Landslide recognition: Identification, movement and causes: New York, John Wiley and Sons, 251 p.

Dixon, J.M., and Summers, J.M., 1983, Patterns of total incremental strain in subsiding troughs: Experimental centrifuged models of inter-diapir synclines: Canadian Journal of Earth Sciences, v. 20, p. 1843–1861.

Dragert, H., and Hyndman, R.D., 1995, Continuous GPS monitoring of elastic strain in the northern Cascadia subduction zone: Geophysical Research Letters, v. 22, p. 755–758.

Dragert, H., Hyndman, R.D., Rogers, G.C., and Wang, K., 1994, Current deformation and the width of the seismogenic zone of the northern Cascadia subduction thrust: Journal of Geophysical Research, v. 99, p. 653–668.

Duncan, R.A., 1982, A captured island chain in the Coast Range of Oregon and Washington: Journal of Geophysical Research, v. 87, p. 10827–10837.

Ernst, R.E., and Buchan, K.L., 1997, Giant radiating dyke swarms: Their use in identifying pre-Mesozoic large igneous provinces and mantle plumes, in Mahoney, J.J., and Coffin, M.F., eds., Large igneous provinces: Continental, oceanic, and planetary flood volcanism: American Geophysical Union Geophysical Monograph 100, p. 297–333.

Ernst, R.E., and Buchan, K.L., 1998, Arcuate dyke swarms associated with mantle plumes on Earth: Implications for Venusian coronae: Houston, Texas, Lunar and Planetary Institute, Lunar and Planetary Science Conference 29, CD-ROM, 1021.pdf.

Fleitout, L., and Froidevaux, C., 1982, Tectonics and topography for a lithosphere containing density heterogeneities: Tectonics, v. 1, p. 21–56.

Frey, H.V., 1979, Thaumasia: A fossilized early forming Tharsis uplift: Journal of Geophysical Research, v. 84, p. 1009–1023.

Frey, H.V., Bills, B.G., Nerem, R.S., and Roark, J.H., 1996, The isostatic state

of Martian topography—Revisited: Geophysical Research Letters, v. 23, p. 721–724.

Froidevaux, C., and Ricard, Y., 1987, Tectonic evolution of high plateaus: Tectonophysics, v. 134, p. 227–238.

Geist, D., and Richards, M., 1993, Origin of the Columbia Plateau and Snake River Plain: Deflection of the Yellowstone plume: Geology, v. 21, p. 789–792.

Geoffroy, L., Angelier J., and Bergerat, F., 1993, Sur l'évolution tectonique cassante tertiaire des Iles Féroé, Atlantique Nord: La compression féringienne: Comptes Rendus de l'Académie des Sciences, Sér. II, v. 316, p. 975–982.

Geoffroy, L., Bergerat, F., and Angelier, J., 1994, Tectonic evolution of the Greenland-Scotland Ridge during the Paleogene: New constraints: Geology, v. 22, p. 653–656.

Ghent, R., and Hansen, V.L., 1999, Structural and kinematic analysis of eastern Ovda Regio, Venus: Implications for crustal plateau formation: Icarus, v. 139, p. 116–136.

Gilmore, M.S., Ivanov, M.A., Head, J.W., III, and Basilevsky, A.T., 1997, Duration of tessera deformation on Venus: Journal of Geophysical Research, v. 102, p. 13357–13368.

Golombek, M.P., Anderson, F.S., and Zuber, M.T., 2000, Martian wrinkle ridge topography: Evidence for subsurface faults from MOLA: Houston, Texas, Lunar and Planetary Institute, Lunar and Planetary Conference 31, CD-ROM, 1294.pdf.

Golombek, M.P., Plescia, J.B., and Franklin, B.J., 1991, Faulting and folding in the formation of planetary wrinkle ridges in Proceedings, Lunar and Planetary Science Conference, 21st: Houston, Texas, Lunar and Planetary Institute, p. 679–693.

Gorman, B.E., Pearce, T.H., and Birkett, T.C., 1978, On the structure of Archean greenstone belts: Precambrian Research, v. 6, p. 23–41.

Griffiths, R.W., and Campbell, I.H., 1991, Interaction of mantle plume heads with the Earth's surface and onset of small-scale convection: Journal of Geophysical Research, v. 96, p. 18295–18310.

Grimm, R.E., 2000, Magnetic lineations on Mars: Formation by Noachian crustal accretion or depletion?: Houston, Texas, Lunar and Planetary Institute, Lunar and Planetary Science Conference 31, CD-ROM, 2056.pdf.

Grosfils, E.B., and Head, J.W., 1994, The global distribution of giant radiating dike swarms on Venus: Implications for the global stress state: Geophysical Research Letters, v. 21, p. 701–704.

Guzmán Speziale, M., Pennington, W.D., and Matumoto, T., 1989, The triple junction of the North America, Cocos, and Caribbean plates: Seismicity and tectonics: Tectonics, v. 8, p. 981–997.

Hagood, M.A., 1986, Structure and evolution of the Horse Heaven Hills, south-central Washington: Richland, Washington, Rockwell Hanford Operations Report RHO-BW-SA-344 P, 176 p.

Hagstrum, J.T., Swanson, D.A., and Evarts, R.C., 1999, Paleomagnetism of an east-west transect across the Cascade arc in southern Washington: Implications for regional tectonism: Journal of Geophysical Research, v. 104, p. 12853–12863.

Hamilton, W.B., 1998, Archean magmatism and deformation were not products of plate tectonics: Precambrian Research, v. 91, p. 143–179.

Hansen, V.L., Banks, B.K., and Ghent, R.R., 1999, Tessera terrain and crustal plateaus, Venus: Geology, v. 27, p. 1071–1074.

Hansen, V.L., and Willis, J.J., 1998, Ribbon terrain formation, southwestern Fortuna Tessera, Venus: Implications for lithosphere evolution: Icarus, v. 132, p. 321–343.

Hartmann, W.K., 1973, Martian surface and crust: Review and synthesis: Icarus, v. 19, p. 550–575.

Head, J.W., Crumpler, L.S., Aubele, J.C., Guest, J.E., and Saunders, R.S., 1992, Venus volcanism: Classification of volcanic features and structures, associations, and global distribution from Magellan data: Journal of Geophysical Research, v. 97, p. 13153–13197.

Head, J.W., Kreslavsky, M., Hiesinger, H., Ivanov, M., Smith, D.A., and Zuber, M.T., 1998, Oceans in the past history of Mars: Tests for their presence

using Mars Orbiter Laser Altimeter (MOLA) data: Geophysical Research Letters, v. 24, p. 4401–4404.

Head, J.W., Ivanoc, M., Hiesinger, H., Kreslavsky, M., Thomson, B., and Pratt, S., 2000, Oceans in the past history of Mars?: Evidence for recession and timing from MOLA data: Houston, Texas, Lunar and Planetary Institute, Lunar and Planetary Science Conference 31, CD-ROM, 1750.pdf.

Head, J.W., and Wilson, L., 1992, Magma reservoirs and neutral buoyancy zones on Venus: Implications for the formation and evolution of volcanic landforms: Journal of Geophysical Research, v. 97, p. 3877–3903.

Hemphill-Haley, M.A., and Humphreys, E.D., 1997, Role of the Cascadia subduction zone and Pacific Northwest pull-apart in dilation of the western United' States: American Geophysical Union Meeting, poster, http://darkwing.uoregon.edu/~markhh/index.html.

Herrick, R.R., and Phillips, R.J., 1992, Geological correlations with the interior density structure of Venus: Journal of Geophysical Research, v. 97, p. 16017–16034.

Hill, R.I., 1991, Starting plumes and continental break-up: Earth and Planetary Science Letters, v. 104, p. 398–416.

Hiller, K.H., Janle, P., Neukum, G.P.O., Guest, J.E., and Lopes, R.M.C., 1982, Mars: Stratigraphy and gravimetry of Olympus Mons and its aureole: Journal of Geophysical Research, v. 87, p. 9905–9915.

Hofmann, C., Courtillot, V., Féraud, G., Rochette, P., Yirgu, G., Ketefo, E., and Pik, R., 1997, Timing of the Ethiopian flood basalt event and implications for plume birth and global change: Nature, v. 389, p. 838–841.

Holt, W.E., Ni, J.F., Wallace, T.C., and Haines, A.J., 1991, The active tectonics of the Eastern Himalayan syntaxis and surrounding regions: Journal of Geophysical Research, v. 96, p. 14595–14632.

Holt, W.E., and Haines, A.J., 1993, Velocity fields in deforming Asia from the inversion of earthquake-released strains: Tectonics, v. 12, p. 1–20.

Hooper, P.R., 1997, The Columbia River flood basalt province: Current status, *in* Mahoney, J. J., and Coffin, M. F., eds., Large igneous provinces: Continental, oceanic, and planetary flood volcanism: American Geophysical Union Geophysical Monograph 100, p. 1–27.

Hooper, P.R., and Conrey, R.M., 1989, A model for the tectonic setting of the Columbia River basalt eruptions, *in* Reidel, S.P., and Hooper, P.R., eds., Volcanism and tectonism in the Columbia River flood-basalt province: Geological Society of America Special Paper 239, p. 293–306.

Hooper, P.R., and Hawkesworth, C.J., 1993, Isotopic and geochemical constraints on the origin and evolution of the Columbia River Basalt: Journal of Petrology, v. 34, p. 1203–1246.

Houseman, G., and England P., 1986, A dynamical model of lithosphere extension and sedimentary basin formation: Journal of Geophysical Research, v. 91, p. 719–729.

Hyndman, R.D., and Wang, K., 1995, The rupture zone of Cascadia great earthquakes from current deformation on the thermal regime: Journal of Geophysical Research, v. 100, p. 22133–22154.

Hyndman, R.D., Yorath, C.J., Clowes, R.M., and Davis, E.E., 1990, The northern Cascadia subduction zone at Vancouver Island: Seismic structure and tectonic history: Canadian Journal of Earth Sciences, v. 27, p. 313–329.

Ivanov, M., and Head, J.W., 2000, Stratigraphy of ridges and ribbons in tessera terrain, Venus: Houston, Texas, Lunar and Planetary Institute, Lunar and Planetary Conference 31, CD-ROM, 1233.pdf.

Jaeger, W.L., 2000, A new model for corona formation on Venus: Houston, Texas, Lunar and Planetary Institute, Lunar and Planetary Conference 31, CD-ROM, 1079.pdf.

Janes, D.M., Squyres, S.W., Bindschadler, D.L., Baer, G., Schubert, G., Sharpton, V.L., and Stofan, E.R., 1992, Geophysical models for the formation and evolution of coronae on Venus: Journal of Geophysical Research, v. 97, p. 16055–16067.

Jarchow, C.M., Catchings, R.D., and Lutter, W.J., 1994, Large-explosive source, wide-recording aperture, seismic profiling on the Columbia Plateau, Washington: Geophysics, v. 59, p. 259–271.

Jayananda, M., Moyen, J.-F., Martin, H., Peucat, J.-J., Auvray, B., and Mahabaleswar, B., 2000, Late Archean (2550-2520 Ma) juvenile magmatism in the Eastern Dharwar craton, southern India: Constraints from geochronology, Nd-Sr isotopes and whole rock geochemistry: Precambrian Research, v. 99, p. 225–254.

Kent, R.W., Hardarson, B.S., Saunders, A.D., and Storey, M., 1996, Plateaux ancient and modern: Geochemical and sedimentological perspectives on Archaean oceanic magmatism: Lithos, v. 37, p. 129–142.

Kerr, R.A., 1997, Why the West stands tall: Science, v. 275, p. 1564–1565.

Kletetschka, G., Wasilewski, P.J., Borosio, A., and Taylor, P.T., 2000, Origin of magnetic linear pattern on Mars: Houston, Texas, Lunar and Planetary Institute, Lunar and Planetary Conference 31, CD-ROM, 1348.pdf.

Koch, D.M., and Manga, M., 1996, Neutral buoyant diapirs: A model for Venus coronae: Geophysical Research Letters, v. 23, p. 225–228.

Korme, T., 1997, Etude des relations géométriques entre la tectonique et le volcanisme en Ethiopie à l'aide de données spatiales [Ph.D. thesis]: Paris, France, Université Pierre et Marie Curie, 165 p.

Krassilnikov, A.S., 2000, Formation of coronae on Venus: Tectonophysical modelling using self-deforming gravity models: Houston, Texas, Lunar and Planetary Institute, Lunar and Planetary Conference 31, CD-ROM, 1336.pdf.

Lawver, L.A., and Müller, R.D., 1994, Iceland hotspot track: Geology, v. 22, p. 311–314.

Lutter, W.J., Catchings, R.D., and Jarchow, C.M., 1994, An image of the Columbia Plateau from inversion of high-resolution seismic data: Geophysics, v. 59, p. 1278–1289.

McCaffrey, R., 1992, Oblique plate convergence, slip vectors, and forearc deformation: Journal of Geophysical Research, v. 97, p. 8905–8915.

McEwen, A.S., Malin, M.C., Carr, M.H., and Hartmann, W.K., 1999, Voluminous volcanism on early Mars revealed in Valles Marineris: Nature, v. 397, p. 584–586.

McGill, G.E., 1998, Central Eistla Regio: Origin and relative age of topographic rise: Journal of Geophysical Research, v. 103, p. 5889–5896.

McGill, G.E., and Squyres, S.W., 1991, Origin of Martian crustal dichotomy: Evaluating hypotheses: Icarus, v. 93, p. 386–393.

McGovern, P.J., and Solomon, S.C., 1993, State of stress, faulting, and eruption characteristics of large volcanoes on Mars: Journal of Geophysical Research, v. 98, p. 23553–23579.

McGovern, P.J., and Solomon, S.C., 1998, Growth of large volcanoes on Venus: Mechanical models and implications for structural evolution: Journal of Geophysical Research, v. 103, p. 11071–11101.

McKenzie, D., 1994, The relationship between topography and gravity on Earth and Venus: Icarus, v. 112, p. 55–88.

McKenzie, D., McKenzie, J.M., and Saunders, R.S., 1992, Dike emplacement on Venus and on Earth: Journal of Geophysical Research, v. 97, p. 15977–15990.

Magee-Roberts, K.P., and Head, J.W., 1993, Large-scale volcanism associated with coronae on Venus: Implications for formation and evolution: Geophysical Research Letters, v. 20, p. 1111–1114.

Malin, M.C., and Edgett, K.S., 1999, Oceans or seas in the martian northern lowlands: High resolution imaging tests of proposed coastlines, Geophysical Research Letters, v. 26, p. 3049–3052.

Malone, S.D., 1978, A review of eastern Washington seismicity: Tectonics and Seismicity of the Columbia Plateau Workshop, Basalt Waste Isolation Program: Seattle, Washington, Battelle Conference Facilities, 6 p.

Mangold, N., 1997, Rhéologie du pergélisol de Mars: Applications géomorphologiques et structurales: Conséquences sur l'origine des contraintes compressives [Ph.D. thesis]: Grenoble, France, Université Joseph Fourier, 248 p.

Mangold, N., Allemand, P., and Thomas, P., 1999, Datation of compressional deformation on Mars: Evidence for a single and global origin: Houston, Texas, Lunar and Planetary Institute, Lunar and Planetary Conference 30, CD-ROM, 1017.pdf.

Mann, G.M., and Meyer, C.E., 1993, Late Cenozoic structure and correlations to seismicity along the Olympic-Wallowa lineament, northwestern United States: Geological Society of America Bulletin, v. 105, p. 853–871.

Martin, B.S., 1984, Paleomagnetism of basalts in northeastern Oregon and north-central Idaho: Geological Society of America Abstracts with Programs, v. 16, p. 247.

Masson, P., 1980, Contribution to the structural interpretation of the Valles Marineris–Noctis Labyrinthus–Claritas Fossae regions of Mars: The Moon and the Planets, v. 22, p. 211–219.

Mège, D., 1994, Aspects structuraux du complexe magmato-tectonique de Tharsis sur Mars [Ph.D. thesis]: Orsay, France, Université Paris-Sud, 384 p.

Mège, D., 1999a, A stress history consistent with the volcanic and tectonic history, of the early Tharsis flood basalt province on Mars: Houston, Texas, Lunar and Planetary Institute, Lunar and Planetary Conference 30, CD-ROM, 2065.pdf.

Mège, D., 1999b, Surface shortening at the Coprates ridged plain, Syria Planum flood basalt province, Mars: Houston, Texas, Lunar and Planetary Institute, Lunar and Planetary Conference 30, CD-ROM, 1876.pdf.

Mège, D., Chardon, D., and Hansen, V.L., 2000, Rayleigh-Taylor instability-driven plume tectonics and the evolution of the Archean, Venusian, and Martian crusts: Houston, Texas, Lunar and Planetary Institute, Lunar and Planetary Science Conference 31, CD-ROM, 1998.pdf.

Mège, D., and Masson, P., 1996, A plume tectonics model for the Tharsis province, Mars: Planetary and Space Science, v. 44, p. 1,499–1,546.

Mège, D., and Reidel, S.P., 2000, Two-dimensional shortening at planetary wrinkle ridges: Houston, Texas, Lunar and Planetary Institute, Lunar and Planetary Science Conference 31, CD-ROM, 1570.pdf.

Melosh, H.J., 1978, The tectonics of mascon loading, *in* Proceedings, Lunar and Planetary Science, 9th: Geochimica et Cosmochimica Acta, Supplement 10, p. 3513–3525.

Menzies, M., Gallagher, K., Yelland, A., and Hurford, A., 1997, Volcanic and nonvolcanic rifted margins of the Red Sea and Gulf of Aden: Crustal cooling and margin evolution in Yemen: Geochimica et Cosmochimica Acta, v. 61, p. 2511–2527.

Merle, O., and Borgia, A., 1996, Scaled experiments of volcanic spreading: Journal of Geophysical Research, v. 101, p. 13805–13817.

MOLA Science Team, 2000, MOLA 0.125° shade map: http://ltpwww.gsfc.nasa.gov/tharsis/shademap.html.

Moyen, J.-F., 2000, Le magmatisme granitique à la transition archéen-protérozoique: L'exemple du craton de Dharwar, Inde du Sud (granite de Closepet et intrusions associées) [Ph.D. thesis]: Clermont-Ferrand, France, Université Blaise Pascal, 350 p.

Moyen, J.-F., Martin, H., Jayananda, M., Peucat, J.-J., and Auvray, B., 1997, Time-space evolution of the late Archaean magmatism in the Dharwar craton (Karnataka, South India): European Union of Geosciences Meeting, 9th Annual Meeting, Strasbourg, France, Abstracts, p. 169.

Morgan, W.J., 1971, Convection plumes in the lower mantle: Nature, v. 230, p. 41–42.

Muller, O.H., and Pollard, D.D., 1977, The stress state near Spanish Peaks, Colorado, determined from a dike pattern: Pure and Applied Geophysics, v. 115, p. 69–86.

Myers, J.S., and Swagers, C., 1997, The Yilgarn craton, *in* de Wit, M.J., and Ashwal, L.D., eds., Greenstone belts: Oxford Monographs on Geology and Geophysics, v. 35, p. 640–656.

Nadin, P.A., Kusznir, N.J., and Toth, J., 1995, Transient regional uplift in the early Tertiary of the northern North Sea and the development of the Iceland plume: Geological Society [London] Journal, v. 152, p. 953–958.

Nimmo, F., 2000, Dike intrusion as a possible cause of linear Martian magnetic anomalies: Geology, v. 28, p. 391–394.

Olson, P., 1994, Mechanics of flood basalt magmatism, *in* Ryan, M.P., ed., Magmatic systems: San Diego, California, Academic Press, p. 1–18.

Parker, T.J., Gorsline, D.S., Saunders, R.S., Pieri, D.C., and Schneeberger, D.M. 1993, Coastal geomorphology of the Martian northern plains: Journal of Geophysical Research, v. 98, p. 11061–11078.

Passchier, C.W., 1995, Precambrian orogenesis: Was it really different?: Geologie en Mijnbouw, v. 74, p. 141–150.

Passchier, C.W., 1998, The late Archaean and early Proterozoic: What happened next?: Geologie en Mijnbouw, v. 76, p. 357–360.

Peulvast, J.P., and Masson, P.L., 1993, Erosion and tectonics in central Valles Marineris (Mars): A new morphostructural model: Earth, Moon and Planets, v. 61, p. 191–217.

Peulvast, J.-P., Mège, D., Chiciak, J., Costard, F., and Masson, P., 2001, Morphology, evolution, and tectonics of Valles Marineris wallslopes (Mars): Geomorphology (in press).

Pierce, K.L., and Morgan, L.A., 1992, The track of the Yellowstone hot spot: Volcanism, faulting, and uplift, *in* Link, P.K., Kuntz, M.A., and Platt, L.B., eds., Regional geology of eastern Idaho and western Wyoming: Geological Society of America Memoir 179, p. 1–53.

Phillips, R.J., and Hansen, V.L., 1998, Geological evolution of Venus: Rises, plains, plumes, and plateaus: Science, v. 279, p. 1492–1497.

Phillips, R.J., Sleep, N.H., and Banerdt, W.B., 1990, Permanent uplift in magmatic systems with application to the Tharsis region of Mars: Journal of Geophysical Research, v. 95, p. 5089–5100.

Plescia, J.B., 1991, Wrinkle ridges in Lunae Planum, Mars: Implications for shortening and strain: Geophysical Research Letters, v. 18, p. 913–916.

Plescia, J.B., and Golombek, M.P., 1986, Origin of planetary wrinkle ridges based on the study of terrestrial analogs: Geological Society of America Bulletin, v. 97, p. 1289–1299.

Plescia, J.B., and Saunders, R.S., 1982, Tectonic history of the Tharsis region, Mars: Journal of Geophysical Research, v. 87, p. 9775–9791.

Pollard, D.D., and Johnson, A.M., 1973, Mechanics of growth of some laccolithic intrusions in the Henry Mountains, Utah. II: Bending and failure of overburden layers and sill formation: Tectonophysics, v. 18, p. 311–354.

Price, E.H., and Watkinson, A.J., 1989, Structural geometry and strain distribution within eastern Umtanum fold ridge, south-central Washington, *in* Reidel, S.P., and Hooper, P.R., eds., Volcanism and tectonism in the Columbia River flood-basalt province: Geological Society of America Special Paper 239, p. 265–281.

Pruis, M.J., and Tanaka, K.L., 1995, The Martian northern plains did not result from plate tectonics: Houston, Texas, Lunar and Planetary Institute, Lunar and Planetary Science Conference 26, p. 1147–1148.

Reidel, S.P., 1984, The Saddle Mountains: The evolution of an anticline in the Yakima fold belt: American Journal of Science, v. 284, p. 942–978.

Reidel, S.P., Scott, G.R., Bazard, D.R., Cross, R.W., and Dick, B., 1984, Post-12 million year clockwise rotation in the central Columbia Plateau, Washington: Tectonics, v. 3, p. 251–273.

Reidel, S.P., Fecht, K.R., Hagood, M.C., and Tolan, T.L., 1989a, The geologic evolution of the central Columbia Plateau, *in* Reidel, S.P., and Hooper, P.R., eds., Volcanism and tectonism in the Columbia River flood-basalt province: Geological Society of America Special Paper 239, p. 247–264.

Reidel, S.P., Hooper, P.R., Beeson, M.H., Fecht, K.R., Bentley, R.D., and Anderson, J.L., 1989b, The Grande Ronde basalt, Columbia River Basalt Group; Stratigraphic descriptions and correlations in Washington, Oregon, and Idaho, *in* Reidel, S.P., and Hooper, P.R., eds., Volcanism and tectonism in the Columbia River flood-basalt province: Geological Society of America Special Paper 239, p. 21–53.

Reidel, S.P., Campbell, N.P., Fecht, K.R., and Lindsey, K.A., 1994, Late Cenozoic structure and stratigraphy of south-central Washington: Washington Division of Geology and Earth Resources Bulletin, v. 80, p. 159–180.

Reidel, S.P., and Tolan, T.L., 1994, Late Cenozoic structure and correlation to seismicity along the Olympic-Wallowa lineament, northwestern United States: Discussion: Geological Society of America Bulletin, v. 106, p. 1634–1638.

Reymer, A., and Schubert, G., 1986, Rapid growth of some major segments of continental crust: Geology, v. 14, p. 299–302.

Richards, M.A., Duncan, R.A., and Courtillot, V.E., 1989, Flood basalts and hot-spot tracks: Plume heads and tails: Science, v. 246, p. 103–107.

Roeder, D., 1988, Andean-age structure of Eastern cordillera (province of La Paz, Bolivia): Tectonics, v. 7, p. 23–39.

Rosenblatt, P., Head, J.W., Pinet, P.C., Ivanov, M.A., and Collins, G., 1997, Topographic and stratigraphic analysis of two Venusian volcanic rises: Western Eistla and Bell regiones: Houston, Texas, Lunar and Planetary Institute, Lunar and Planetary Science Conference 28, CD-ROM, 1066.pdf.

Rosenblatt P., Barriot, J.-P., and Pinet, P.C., 1998, Regional analysis of topography, gravimetry and geology at two Venusian hot spots: Western Eistla and Bell regiones, and their peripheries: Houston, Texas, Lunar and Planetary Institute, Lunar and Planetary Science Conference 29, CD-ROM, 1798.pdf.

Ruzicka, A., 2000, Magnetic lineations on Mars: Evidence for plate tectonics or for magnetic aeolian deposits?: Houston, Texas, Lunar and Planetary Institute, Lunar and Planetary Conference 31, CD-ROM, 1575.pdf.

Saltus, R.W., 1993, Upper-crustal structure beneath the Columbia River Basalt Group, Washington: Gravity interpretation controlled by borehole and seismic studies: Geological Society of America Bulletin, v. 105, p. 1247–1259.

Sandwell, D.T., Johnson, C.L., Bilotti, F., and Suppe, J., 1997, Driving forces for limited tectonics on Venus: Icarus, v. 129, p. 232–244.

Sandwell, D.T., and Schubert, G., 1992, Evidence for retrograde lithospheric subduction in Venus: Science, v. 257, p. 766–770.

Saunders, A.D., Storey, M., Kent, R.W., and Norry, M.J., 1992, Consequences of plume-lithosphere interactions, *in* Storey, B.C., et al., eds., Magmatism and the cause of continental break-up: Geological Society [London] Special Publication 68, p. 41–60.

Saunders, A.D., Tarney, J., Kerr, A.C., and Kent, R.W., 1996, The formation and fate of large oceanic igneous provinces: Lithos, v. 37, p. 81–95.

Savage, J.C., Lisowski, M., and Prescott, W.H., 1991, Strain accumulation in western Washington: Journal of Geophysical Research, v. 96, p. 14493–14507.

Schubert, G., Solomon, S.C., Turcotte, D.L., Drake, M.J., and Sleep, N.H., 1992, Origin and thermal evolution of Mars, *in* Kiefer, W.S., et al., eds., Mars: Tucson, Arizona, University of Arizona Press, p. 147–183.

Schultz, R.A., 1989, Strike-slip faulting of ridged plains near Valles Marineris, Mars: Nature, v. 341, p. 424–426.

Schultz, R.A., 2000, Localization of bedding-plane slip and backthrust faults above blind thrust fault: Keys to wrinkle ridge structure: Journal of Geophysical Research, v. 105, E5, p. 12035–12052.

Schultz, R.A., and Tanaka, K.L., 1994, Lithospheric-scale buckling and thrust structures on Mars: The Coprates rise and south Tharsis ridge belt: Journal of Geophysical Research, v. 99, p. 8371–8385.

Schultz, R.A., and Watters, T.R., 1995, Elastic buckling of fractured basalt on the Columbia Plateau, Washington State, *in* Daemen, J.J.K., and Schultz, R.A., eds., Proceedings of the 35th U.S. Rock Mechanics Symposium: Rotterdam, Balkema, p. 855–860.

Scott, D.H., and Dohm, J.M., 1990, Chronology and global distribution of fault and ridge systems on Mars, *in* Proceedings, Lunar and Planetary Science Conference, 20th: Houston: Texas, Lunar and Planetary Institute, p. 487–501.

Scott, D.H., and Tanaka, K.L., 1986, Geologic map of the western equatorial region of Mars: U.S. Geological Survey Miscellaneous Investigation Series Map I-1802-A, scale 1:15 000 000, 1 sheet.

Sébrier, M., Mercier, J.-L., Mégard, F., Laubacher, G., and Carey-Gailhardis, 1985, Quaternary normal and reverse faulting and the state of stress in the central Andes of south Peru: Tectonics, v. 4, p. 739–780.

Self, S., Thordarson, T., and Keszthelyi, L., 1997, Emplacement of continental flood basalt lava flows, *in* Mahoney, J.J., and Coffin, M.F., eds., Large igneous provinces: Continental, oceanic, and planetary flood volcanism: American Geophysical Union Geophysical Monograph 100, p. 381–410.

Senske, D.A., and Plaut, J.J., 2000, The Tellus region of Venus: Processes in the formation and modification of tessera terrain: Houston, Texas, Lunar and Planetary Institute, Lunar and Planetary Science Conference 31, CD-ROM, 1496.pdf.

Shen-Tu, B., Holt, W.E., and Haines, A.J., 1999, Deformation kinematics in the western United States determined from Quaternary fault slip rates and recent geodetic data: Journal of Geophysical Research, v. 104, p. 28927–28955.

Sheriff, S.D., 1984, Paleomagnetic evidence for spatially distributed post-Miocene rotation of western Washington and Oregon: Tectonics, v. 3, p. 397–408.

Sleep, N.H., 1994, Martian plate tectonics: Journal of Geophysical Research, v. 99, p. 5639–5655.

Sleep, N.H., and Phillips, R.J., 1979, An isostatic model for the Tharsis province, Mars: Geophysical Research Letters, v. 6, p. 803–806.

Sleep, N.H., and Phillips, R.J., 1985, Gravity and lithospheric stress on the terrestrial planets with reference to the Tharsis region of Mars: Journal of Geophysical Research, v. 90, p. 4469–4489.

Smrekar, S.E., and Raymond, C., 1999, Constraints on the Martian plate tectonic hypothesis from gravity and topography data: Houston, Texas, Lunar and Planetary Institute, Fifth International Conference on Mars, CD-ROM, 6172.pdf.

Smrekar, S.E., and Stofan, E.R., 1997, Corona formation and heat loss on Venus by coupled upwelling and delamination: Science, v. 277, p. 1289–1294.

Solomon, S.C., Smrekar, S.E., Bindschadler, D.L., Grimm, R.E., Kaula, W.M., McGill, G.E., Phillips, R.J., Saunders, R.S., Schubert, G., Squyres, S.W., and Stofan, E.R., 1992, Venus tectonics: An overview of Magellan observations: Journal of Geophysical Research, v. 97, p. 13199–13255.

Sprenke, K.F., and Baker, L.L., 2000, Polar wandering on Mars?: Houston, Texas, Lunar and Planetary Institute, Lunar and Planetary Science Conference 31, CD-ROM, 1930.pdf.

Squyres, S.W., Clifford, S.M., Kusmin, R.O., Zimbelman, J.R., and Costard, F.M., 1992a, Ice in the Martian regolith, *in* Kiefer, W.S., et al., eds., Mars: Tucson, Arizona, University of Arizona Press, p. 523–554.

Squyres, S.W., Janes, D.M., Baer, G., Bindschadler, D.L., Schubert, G., Sharpton, V.L., and Stofan, E.R., 1992b, The morphology and evolution of coronae on Venus: Journal of Geophysical Research, v. 97, p. 13611–13634.

Stofan, E.R., and Head, J.W., III, 1990, Coronae of Mnemosyne Regio: Morphology and origin: Icarus, v. 83, p. 216–243.

Stofan, E.R., Sharpton, V.L., Schubert, G., Baer, G., Bindschadler, D.L., Janes, D.M., and Squyres, S.W., 1992, Global distribution of coronae and related features on Venus: Implications for origin and relation to mantle processes: Journal of Geophysical Research, v. 97, p. 13347–13378.

Stofan, E.R., Smrekar, S.E., Bindschadler, D.L., and Senske, D.A., 1995, Large topographic rises on Venus: Implications for mantle upwelling: Journal of Geophysical Research, v. 100, p. 23317–23327.

Storey, M., Mahoney, J.J., Kroenke, L.W., and Saunders, A.D., 1991, Are oceanic plateaus of komatiite formation?: Geology, v. 19, p. 376–379.

Suppe, J., and Narr, W., 1989, Fault-related folding on the Earth with application to wrinkle ridges on Mars and the moon, *in* Watters, T.R., and Golombek, M.P., eds., MEVTV Workshop on Tectonic Features on Mars: Houston, Texas, Lunar and Planetary Institute Technical Report 89-06, p. 55–56.

Suppe, J., Powell, C., and Berry, R., 1975, Regional topography, seismicity, Quaternary volcanism, and the present-day tectonics of the western United States: American Journal of Science, v. 275-A, p. 397–436.

Swanson, D.A., Anderson, J.L., Camp, V.E., Hooper, P.R., Taubeneck, W.H., and Wright, T.L., 1981, Reconnaissance geologic map of the Columbia River Basalt Group, northern Oregon and western Idaho: U.S. Geological Survey Open-File Report 81-797, scale 1:250 000.

Takahashi, E., Nakajima, K., and Wright, T.L., 1998, Origin of the Columbia River basalts: Melting model of a heterogeneous plume head: Earth and Planetary Science Letters, v. 162, p. 63–80.

Tanaka, K.L., 1986, The stratigraphy of Mars: Journal of Geophysical Research, v. 91, p. E139–E158.

Tanaka, K.L., and Davis, P.A., 1988, Tectonic history of the Syria Planum province of Mars: Journal of Geophysical Research, v. 93, p. 14893–14917.

Tanaka, K.L., Golombek, M.P., and Banerdt, W.B., 1991, Reconciliation of stress and structural histories of the Tharsis region of Mars: Journal of Geophysical Research, v. 96, p. 15617–15633.

Tanaka, K.L., and Schultz, R.A., 1991, Late Noachian development of the Coprates rise, Mars: NASA Technical Memorandum 4300, p. 70–72.

Thelin, G.P., and Pike, R.J., 1991, Landforms of the conterminous United States—A digital shaded-relief portrayal: U.S. Geological Survey Miscellaneous Investigations Map 2206, scale 1:3 500 000.

Thomas, P., and Allemand, P., 1993, Quantitative analysis of the extensional tectonics of Tharsis bulge, Mars: Geodynamic implications: Journal of Geophysical Research, v. 98, p. 13097–13108.

Thompson, R.N., and Gibson, S.A., 1991, Subcontinental mantle plumes, hotspots and pre-existing thinspots: Geological Society [London] Journal, v. 148, p. 973–977.

Tolan, T.L., and Reidel, S.P., 1989, Structure map of a portion of the Columbia River flood-basalt province, in Reidel, S.P., and Hooper, P.R., eds., Volcanism and tectonism in the Columbia River flood-basalt province: Geological Society of America Special Paper 239, scale 1:550 000, 1 sheet.

Tolan, T.L., Reidel, S.P., Beeson, M.H., Anderson, J.L., Fecht, K.R., and Swanson, D.A., 1989, Revisions to the estimates of the areal extent and volume of the Columbia River Basalt Group, in Reidel, S.P., and Hooper, P.R., eds., Volcanism and tectonism in the Columbia River flood-basalt province: Geological Society of America Special Paper 239, p. 1–20.

Turcotte, D.L., and Schubert, G., 1982, Geodynamics: Applications of continuum physics to geological problems: New York, John Wiley and Sons, 450 p.

Underwood, J.R., 1992, Geologic mapping, Claritas Fossae region, Mars: Progress report: Lunar and Planetary Science Conference 23 [Abstracts]: Houston, Texas, Lunar and Planetary Institute, p. 1459–1460.

Uyeda, S., and Kanamori, H., 1979, Back-arc opening and the mode of subduction: Journal of Geophysical Research, v. 84, p. 1049–1061.

Vågnes, E., Gabrielsen, R.H., and Haremo, P., 1998, Late Cretaceous-Cenozoic intraplate contractional deformation at the Norwegian continental shelf: Timing, magnitude and regional implications: Tectonophysics, v. 300, p. 29–46.

VanDecar, J.C., James, D.E., and Assumpçao, M., 1995, Seismic evidence for a fossil mantle plume beneath South America and implications for plate driving forces: Nature, v. 378, p. 25–31.

Van Wyk de Vries, B., Kerle, N., and Petley, D., 2000, Sector collapse forming at Casita volcano, Nicaragua: Geology, v. 28, p. 167–170.

Vergés, J., Millán, H., Roca, E., Muñoz, J.A., Marzo, M., Cirés, J., Den Bezemer, T., Zoetemeijer, R., and Cloetingh, S., 1995, Eastern Pyrenees and related foreland basins: Pre-, syn- and post-collisional crustal-scale cross-sections: Marine and Petroleum Geology, v. 12, p. 893–915.

Von Huene, R., Bourgois, J., Miller, J., and Pautot, G., 1989, A large-scale tsunamigenic landslide and debris flow along the Peru Trench: Journal of Geophysical Research, v. 94, p. 1703–1714.

Watters, T.R., 1988, Wrinkle ridge assemblages on the terrestrial planets: Journal of Geophysical Research, v. 93, p. 10236–10254.

Watters, T.R., 1989, Periodically spaced anticlines of the Columbia Plateau, in Reidel, S.P., and Hooper, P.R., eds., Volcanism and tectonism in the Columbia River flood-basalt province: Geological Society of America Special Paper 239, p. 283–292.

Watters, T.R., 1991, The origin of periodically spaced wrinkled ridges on the Tharsis plateau of Mars: Journal of Geophysical Research, v. 96, p. 15599–15616. Correction: Watters, T.R., 1991, Journal of Geophysical Research, v. 96, p. 22829–22832.

Watters, T.R., 1992, System of tectonic features common to Earth, Mars, and Venus: Geology, v. 20, p. 609–612.

Watters, T.R., 1993, Compressional tectonism on Mars: Journal of Geophysical Research, v. 98, p. 17049–17060.

Watters, T.R., and Maxwell, T.A., 1983, Crosscutting relations and relative ages of ridges and faults in the Tharsis region of Mars: Icarus, v. 56, p. 278–298.

Watters, T.R., and Robinson, M., 1997, Radar and photoclinometric studies of wrinkle ridges on Mars: Journal of Geophysical Research, v. 102, p. 10889–10903.

Watters, T.R., and Schultz, R.A., 1995, Rock mass strength criterion applied to ridged plains on Mars: Implications for elastic buckling [Abstracts]: Houston, Texas, Lunar and Planetary Institute, Lunar and Planetary Science Conference 31, p. 1471–1472.

West, M.W., Ashland, F.X., Busacca, A.J., Berger, G.W., and Shaffer, M.E., 1996, Late Quaternary deformation, Saddle Mountains anticline, south-central Washington: Geology, v. 24, 1123–1126.

White, R.S., 1992, Initiation of the Iceland plume and opening of the North Atlantic, in Tonkard, A.J., and Balkwill, H.R., eds., Extensional tectonics and stratigraphy of the North Atlantic margin: American Association of Petroleum Geologists Bulletin, v. 46, p. 149–154.

White, R.S., Smallwood, J.R., Staples, R.K., and Richardson, K.R., 1997, Anatomy of the Iceland plume: From early Tertiary continental breakup to the present day: Geological Society of America Abstracts with Programs, v. 29, no. 7, p. A167.

White, R.S., and McKenzie, D., 1989, Magmatism at rift zones: The generation of volcanic continental margins and flood basalts: Journal of Geophysical Research, v. 94, p. 7685–7729.

White, R.S., and McKenzie, D., 1995, Mantle plumes and flood basalts: Journal of Geophysical Research, v. 100, p. 17543–17585.

Wilson, L., and Head, J.W., 2000, Tharsis-radial graben systems as the surface manisfestation of plume-related dike intrusion complexes: Models and implications: Houston, Texas, Lunar and Planetary Institute, Lunar and Planetary Science Conference 31, CD-ROM, 1371.pdf.

Woidt, W., 1978, Finite element calculations applied to salt dome analysis: Tectonophysics, v. 50, 369–386.

Zoback, M.L., 1992, First- and second-order patterns of stress in the lithosphere: The World Stress Map Project: Journal of Geophysical Research, v. 97, p. 11703–11728.

Zoback, M.L., and Richardson, R.M., 1996, Stress perturbation and intraplate seismicity associated with ancient continental rifts: Journal of Geophysical Research, v. 101, p. 5459–5475.

Zoback, M.L., and Thompson, G.A., 1978, Basin and Range rifting in northern Nevada: Clues from a mid-Miocene rift and its subsequent offsets: Geology, v. 6, p. 111–116.

Zoback, M.L., Zoback, M.D., Adams, J., Bell, S., Suter, M., Suarez, G., Jacob, K., and Estabrook, C., 1990, Stress map of North America: Boulder, Colorado, Geological Society of America, Continent-scale map-005, scale 1:5 000 000, 4 sheets.

Zoback, M.L., McKee, E.H., Blakely, R.J., and Thompson, G.A., 1994, The northern Nevada rift: Regional tectono-magmatic relations and middle Miocene stress direction: Geological Society of America Bulletin, v. 106, p. 371–382.

Zuber, M.T., 1995, Wrinkle ridges, reverse faulting, and the depth penetration of lithospheric strain in Lunae Planum, Mars: Icarus, v. 114, p. 80–92.

Zuber, M.T., and Aist, L.L., 1990, The shallow structure of the Martian lithosphere in the vicinity of the ridged plains: Journal of Geophysical Research, v. 95, p. 14215–14230.

Zuber, M.T., Solomon, S.C., Phillips, R.J., Smith, D.E., Tyler, G.L., Aharonson, O., Balmino, G., Banerdt, W.B., Head, J.W., Johnson, C.L., Lemoine, F.G., McGovern, P.J., Neumann, G.A., Rowlands, D.D., and Zhong, S., 2000, Internal structure and early thermal evolution of Mars from Mars Global Surveyor topography and gravity: Science, v. 287, p. 1788–1793.